2019-12

BAJA EXPRESS: THE EMERGENCE OF CONVERGENT BOUNDARY ATMOSPHERIC RIVERS AND THEIR EFFECTS IN SOUTH CENTRAL UNITED STATES

Sexson, Jeremy W.

Monterey, CA; Naval Postgraduate School

NAVAL POSTGRADUATE SCHOOL

MONTEREY, CALIFORNIA

THESIS

BAJA EXPRESS: THE EMERGENCE OF CONVERGENT BOUNDARY ATMOSPHERIC RIVERS AND THEIR EFFECTS IN SOUTH CENTRAL UNITED STATES

by

Jeremy W. Sexson

December 2019

Thesis Advisor:	Wendell A. Nuss
Second Reader:	Joel W. Feldmeier

THIS PAGE INTENTIONALLY LEFT BLANK

REPORT DOCUMENTATION PAGE	*Form Approved OMB No. 0704-0188*

1. AGENCY USE ONLY *(Leave blank)*	**2. REPORT DATE** December 2019	**3. REPORT TYPE AND DATES COVERED** Master's thesis

4. TITLE AND SUBTITLE
BAJA EXPRESS: THE EMERGENCE OF CONVERGENT BOUNDARY ATMOSPHERIC RIVERS AND THEIR EFFECTS IN SOUTH CENTRAL UNITED STATES

5. FUNDING NUMBERS

6. AUTHOR(S) Jeremy W. Sexson

7. PERFORMING ORGANIZATION NAME(S) AND ADDRESS(ES)
Naval Postgraduate School
Monterey, CA 93943-5000

8. PERFORMING ORGANIZATION REPORT NUMBER

9. SPONSORING / MONITORING AGENCY NAME(S) AND ADDRESS(ES)
N/A

10. SPONSORING / MONITORING AGENCY REPORT NUMBER

11. SUPPLEMENTARY NOTES The views expressed in this thesis are those of the author and do not reflect the official policy or position of the Department of Defense or the U.S. Government.

12a. DISTRIBUTION / AVAILABILITY STATEMENT	**12b. DISTRIBUTION CODE**
Approved for public release. Distribution is unlimited.	A

13. ABSTRACT (maximum 200 words)

Scientists have studied atmospheric rivers (ARs) vigorously since the early 1990s. They are more commonly known to be associated with the warm conveyor belt of extratropical cyclones, pulling moisture from the tropics. However, there is a type of AR, originating from convergent boundaries, with characteristics that differ from the more commonly studied ARs, hereby labeled convergent boundary atmospheric rivers, or CBARs. Four cases were analyzed in order to define these CBARs. This study found that 1) CBARs form as a result of the associated convergent boundary; 2) CBARs form and evolve independent of extratropical cyclones; and 3) CBARs have a significant impact on inland weather, including fog and restricted visibility, freezing rain, and severe weather. This study also found that, in all four cases, there was a convergence of two AR systems, and that convergence may have been the primary method for extracting precipitation from the ARs.

14. SUBJECT TERMS	**15. NUMBER OF PAGES**
atmospheric rivers, ITCZ, convergent boundary, moisture transport, forecasting	103
	16. PRICE CODE

17. SECURITY CLASSIFICATION OF REPORT	**18. SECURITY CLASSIFICATION OF THIS PAGE**	**19. SECURITY CLASSIFICATION OF ABSTRACT**	**20. LIMITATION OF ABSTRACT**
Unclassified	Unclassified	Unclassified	UU

NSN 7540-01-280-5500

Standard Form 298 (Rev. 2-89)
Prescribed by ANSI Std. 239-18

THIS PAGE INTENTIONALLY LEFT BLANK

Approved for public release. Distribution is unlimited.

BAJA EXPRESS: THE EMERGENCE OF CONVERGENT BOUNDARY ATMOSPHERIC RIVERS AND THEIR EFFECTS IN SOUTH CENTRAL UNITED STATES

Jeremy W. Sexson
Lieutenant Commander, United States Navy
BS, Texas A & M University, 2003
MEd, Texas A & M University, 2007

Submitted in partial fulfillment of the
requirements for the degree of

MASTER OF SCIENCE IN METEOROLOGY AND PHYSICAL OCEANOGRAPHY

from the

NAVAL POSTGRADUATE SCHOOL
December 2019

Approved by: Wendell A. Nuss
Advisor

Joel W. Feldmeier
Second Reader

Wendell A. Nuss
Chair, Department of Meteorology

THIS PAGE INTENTIONALLY LEFT BLANK

ABSTRACT

Scientists have studied atmospheric rivers (ARs) vigorously since the early 1990s. They are more commonly known to be associated with the warm conveyor belt of extratropical cyclones, pulling moisture from the tropics. However, there is a type of AR, originating from convergent boundaries, with characteristics that differ from the more commonly studied ARs, hereby labeled convergent boundary atmospheric rivers, or CBARs. Four cases were analyzed in order to define these CBARs. This study found that 1) CBARs form as a result of the associated convergent boundary; 2) CBARs form and evolve independent of extratropical cyclones; and 3) CBARs have a significant impact on inland weather, including fog and restricted visibility, freezing rain, and severe weather. This study also found that, in all four cases, there was a convergence of two AR systems, and that convergence may have been the primary method for extracting precipitation from the ARs.

THIS PAGE INTENTIONALLY LEFT BLANK

TABLE OF CONTENTS

THIS PAGE INTENTIONALLY LEFT BLANK

LIST OF FIGURES

THIS PAGE INTENTIONALLY LEFT BLANK

LIST OF TABLES

THIS PAGE INTENTIONALLY LEFT BLANK

LIST OF ACRONYMS AND ABBREVIATIONS

AMS	American Meteorological Society
AR	atmospheric river
CBAR	convergent boundary atmospheric river
CFS	climate forecast system
CFSR	climate forecast system reanalysis
CO	carbon monoxide
DFW	Dallas-Fort Worth, Texas
GOES	Geostationary Operational Environmental Satellite
GPT	geopotential height
IR	infrared
ITCZ	intertropical convergence zone
IVT	vertically integrated water vapor transport
MF	vertically integrated moisture flux
NCEP	National Centers for Environmental Prediction
NWS	National Weather Service
QV	mixing ratio
SAT	San Antonio, Texas
THE	theta (potential temperature)
TME	tropical moisture export
WCB	warm conveyor belt
WV	water vapor
XXW	cross cross-section winds

THIS PAGE INTENTIONALLY LEFT BLANK

ACKNOWLEDGMENTS

I would like to thank the following groups and individuals: Professor Wendell Nuss for advising this project and for his encouragement in studying this topic; CDR Joel Feldmeier for reviewing the content and structure of the thesis; Dr. Carolyn Reynolds for sharing research topics on atmospheric rivers; the Naval Postgraduate School Graduate Writing Center for coaching assistance throughout this process; Alex Garcia for the knowledge he shared and the opportunity he gave me during my internship at KABB TV; CDR Paula Travis for her guidance and leadership during my time at the Naval Postgraduate School; and my cohort and the Meteorology/Oceanography community for their support. I also am grateful to my wife, Denise, and our children for their ongoing support and encouragement.

THIS PAGE INTENTIONALLY LEFT BLANK

I. INTRODUCTION

A. MOTIVATION AND HYPOTHESES

Atmospheric rivers (ARs) are poleward water vapor transports whose lengths are greater than their widths. ARs have been studied in depth and are known to be associated with extratropical cyclones. These ARs typically pull moisture in from the tropics near Hawaii (Pineapple Express) or the Caribbean (Maya Express). However, satellite observations suggest that ARs emerge from another prominent area around the globe near the equator. In the East Pacific, just north of the equator, winds from the northeast and southeast converge forming an area of low-pressure, resulting in thunderstorms. This convergent boundary encircles the globe and is known as the Intertropical Convergence Zone (ITCZ). Viewed from satellite imagery, AR formation takes place in North America from January through March at this convergent boundary. These ARs appear to pull moisture from the convergent boundary and transport it through Mexico into the United States and out into the western Atlantic. These convergent boundary atmospheric rivers, henceforth denoted as CBARs, are a primary source of winter precipitation for U.S. inland areas such as Texas. Since CBARs have not traditionally been the focus of AR studies, not much has been discussed about their formation and contribution to hydrology and meteorology. This study serves to fill in the AR gap by taking a deeper look into CBARs and their effects on local populations and military operations.

Three hypotheses are brought forth: 1) CBARs form as a result of an associated convergent boundary (in this study, the ITCZ); 2) CBARs form and evolve independent of extratropical cyclones; and 3) CBARs have a significant impact on inland weather.

B. BACKGROUND

Scientists have studied ARs vigorously since the early 1990s (Ralph et al. 2017). In a pilot study conducted in 1992, R.E. Newell and his team sought out to analyze why carbon monoxide (CO) levels were especially elevated in areas where it did not originate. They found high values of CO “well removed from potential sources and in regions where neither vertical transport into the free troposphere from the boundary layer or horizontal

transport by the prevailing wind provided a straightforward explanation." The group decided to observe water vapor transport from the tropics to see if this would shed some light on the movement of CO. As a result of the desire to study the CO transport problem, the ongoing study of these phenomenon emerged. Termed "atmospheric rivers," Zhu and Newell (1994) found that these water vapor transports "can carry as much water as the Amazon River."

The *Glossary of Meteorology* from the American Meteorological Society (AMS) defines an AR as such:

> An atmospheric river is a long, narrow, and transient corridor of strong horizontal water vapor transport that is typically associated with a low-level jet stream ahead of the cold front of an extratropical cyclone. The water vapor in atmospheric rivers is supplied by tropical and/or extratropical moisture sources. Atmospheric rivers frequently lead to heavy precipitation where they are forced upward, for example, by mountains or by ascent in the warm conveyor belt. Horizontal water vapor transport in the midlatitudes occurs primarily in atmospheric rivers and is focused in the lower troposphere. Atmospheric rivers are the largest 'rivers' of fresh water on Earth, transporting on average more than double the flow of the Amazon River. (AMS 2019)

The complexity of these water vapor transports has called into question the very definition the AR. With the purpose of taking a deeper look into the AR problem, over 100 experts in several different fields came together, including meteorology, hydrology, oceanography, polar science, ecology, water management, and civil engineering. Their goal was to determine where the science of ARs lies, and to assess whether it needs to be updated (Ralph et al. 2017). An AR is typically described as a filament where the along-stream dimension is often up to five times larger than the across stream dimension (Newell et al. 1992). ARs are known to have a length greater than 2,000 km, a width of less than 1,000 km, and a length-width ratio greater than two (Guan and Waliser 2015; Zhou et al. 2018). Other research shows that rather than an AR being a river of moisture exported from the subtropics, it is a footprint left behind by poleward traveling storms (Dacre et al. 2015). It is possible that ARs, warm conveyor belts (WCBs), and tropical moisture exports (TMEs) are the same phenomenon (Ralph et al. 2017). The definition in the AMS *Glossary of Meteorology* shows the horizontal structure of an AR that may be related to the WCB,

found in Figure 1a. However, many studies of the midlatitude atmosphere indicate that these phenomena are related but distinct (Ralph et al. 2017). The result of the aforementioned meeting was the above definition from the *AMS Glossary*. Though a standard for the vertical structure has not been found in the literature, Figure 1b shows the vertical structure of an AR, according to the *AMS Glossary*. The AR shown in the vertical structure has an upward extent of about 4 km (approximately 616 mb).

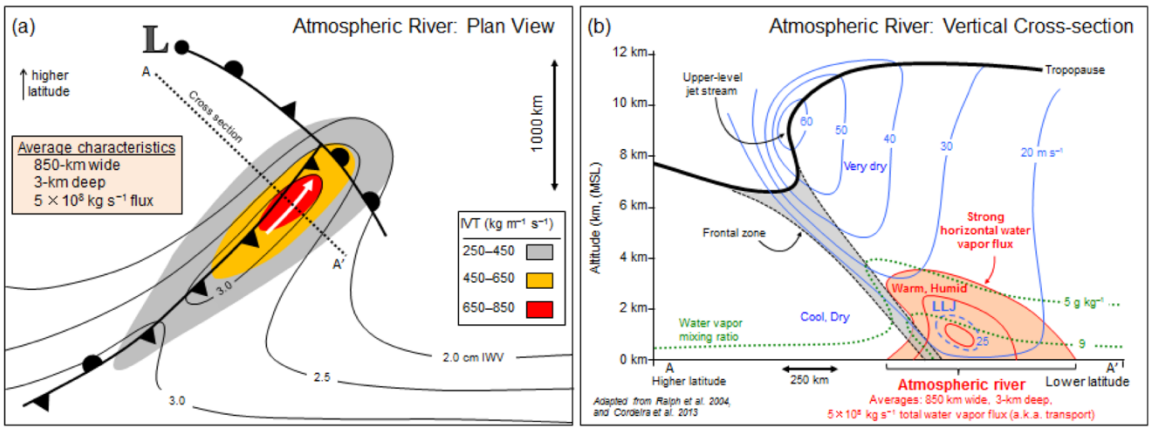

(a) AR horizontal structure. (b) AR vertical structure

Figure 1. Structure of an Atmospheric River. Source: AMS (2019).

According to Paltan et al. (2017), "the presence or absence of ARs significantly drives global hydrological variability." ARs cover approximately 10% of Earth's circumference in the midlatitudes. However, they make up over 90% of total poleward water vapor transport (Guan and Waliser 2015). On average, 11 ARs exist globally at any given time, and the global AR cycle is stronger in the Northern Hemisphere. ARs also play important roles in the global water cycle, including in regional weather and hydrology (Guan and Waliser 2015). In another study, Guan and Waliser (2017) show that they account for the majority of the total meridional vertically integrated water vapor transport (IVT) in the midlatitudes while occupying only a small fraction of the zonal circumference. According to Guan and Waliser (2015), a typical AR may carry the equivalent water content of 7–15 times the Mississippi River. A study by Zhu and Newell (1998) shows that 3–5 ARs exist in each hemisphere at any given time. ARs also "account for 84% of the

total meridional IVT and 8% of the zonal circumference between 30°–50° N." (Guan and Waliser 2015)

Rutz et al. (2015) found that high impact weather in western North America, such as heavy precipitation, might be the result of ARs. They show that ARs are linked to heavy flooding events over western Europe and the eastern United States. Their data shows that 20–50% of cool-season precipitation happens the day of or the day after AR landfall between 32.5° and 52.5° latitude, corresponding to 15–40% for ARs that cross the Baja peninsula at 24°–32.5° latitude.

Since the study of ARs began, several types have been analyzed. One, termed the Pineapple Express, emerges from the northeast Pacific between 20°–35° N and 140°–160° W, and affects the California coast (Zhou et al. 2018). Zhou et al. also note that this as well as other ARs form due to large moisture content at low latitudes. They found that cyclonic activity in these areas might cause this formation pattern Payne and Magnusdottir (2016). found that warm, heavy precipitation anomalies and intense moisture transport characterize the coastline, where atmospheric moisture rises 48 hours prior to landfall.

A second prominent AR emerges from the Caribbean or Gulf of Mexico and is called the Maya Express. The Maya Express is the cause of many flood cases in the Midwest (Hedstrom 2014). Hedstrom (2014) also notes that whereas rainfall from Pineapple Express events is extracted from terrain, Maya Express events are more dynamic due to upper potential vorticity anomalies and an increase of moisture flux across the northern Gulf Coast.

The study by Hedstrom (2014) reveals that ARs appear to be associated with the WCB of extratropical cyclones, where strong wind and abundant water vapor exist at low latitudes. This study also shows that the AR is drawn up into the cyclone and dissipates as the cyclone decays. The water vapor removed from the tropical belt of high moisture at about 15°–20° latitude often exists in filamentary form for several days before becoming associated directly with a low-pressure system (Zhu and Newell 1994).

A study by Dacre et al. (2015) shows that ARs may be footprints left behind by extratropical cyclones and are negligible to the enhancement of these cyclones, as "water

vapor convergence into and out of the system is negligible and even negative during the most rapidly intensifying stage of the cyclone evolution showing that water vapor is actually exported from the system." This study shows ARs are almost always associated with extratropical cyclones, as with many of these transports, evaporation of water vapor from the sea surface occurs behind the cold front. Dacre et al. (2015) also note that this evaporation is the primary contributor of the total cyclone water vapor content. They show that high total column water vapor and strong low-level winds in the pre-cold frontal region of a cyclone lead to intense poleward moisture transport. This may also explain the latent heat liberation found in Newell and Zhu's study (1994), where this latent heat allows the cyclone's pressure to fall when the water vapor transport penetrates the cyclone.

On the contrary, formation of ARs may originate apart from extratropical cyclones, and cyclonic activity may contribute to their development (Newell and Zhu 1998). In fact, extratropical cyclones over the oceans often track toward the head of the ARs where water vapor convergence is greatest (Zhu and Newell 1998). The moisture shown in the satellite images comes from water vapor already existing in the ITCZ, then travels northeastward (Newell et al. 1992), usually with the dominant 250 mb jet stream pattern. The trade winds and abundance of moisture over warm waters reflects this enhanced equatorial IVT (Guan and Waliser 2015). They can persist for many days while moving through the atmosphere. A month's worth of data shows the presence of ARs, moving and developing in a coherent fashion throughout a 12-hour period (Newell et al. 1992).

C. OBJECTIVE

Scientists have studied ARs such as the Pineapple Express and Maya Express extensively. These ARs tend to coincide with baroclinic cyclones and may be associated with the WCB of extratropical cyclones (Hedstrom 2014). However, other AR types may exist that have not often been studied. Formation of ARs may actually originate apart from the genesis and development of these extratropical cyclones (Newell and Zhu 1998). Newell and Zhu (1998) note that cyclonic activity may affect the development of the rivers themselves, as the ARs may emerge from convergent boundaries such as the ITCZ. The goal of this research is to characterize these types of ARs (labeled CBARs) and analyze

their dynamics and possible interactions with another AR, specifically the Maya Express. This study will also look into the meteorological effects of CBARs.

II. DATA AND METHODS

This background serves to show the methods used to identify unique characteristics of CBARS and points out certain criteria used to classify them. This section discusses the specific surface and upper-level features used for this research to give a deeper understanding of CBARs as well as the data sets and computer program used to analyze four unique case studies.

Climate Forecast System Reanalysis (CFSR) data from the National Centers for Environmental Prediction (NCEP) was used to study four separate atmospheric river cases. The CFSR uses the Climate Forecast System (CFS), which is defined by the National Centers for Environmental Information (NCEI 2019) as "a model representing the global interaction between Earth's oceans, land, and atmosphere. ...The model offers hourly data with a horizontal resolution down to one-half of a degree (approximately 56 km)." The CFS assimilates surface, upper air balloon, aircraft, and satellite observations (NCEI 2019). The "CFSR was designed and executed as a global, high resolution, coupled atmospheric-ocean-land surface-sea ice system to provide the best estimate of the state of these coupled domains over a 32-year period of record from January 1979 to March 2011." (NCEI 2019)

Archived geostationary satellite imagery from the National Oceanographic and Atmospheric Administration (NOAA) Geostationary Operational Environmental Satellite (GOES) series was used. Four separate case studies were chosen which showed convergent boundary atmospheric rivers (CBARs) emerging from the Pacific near or at the ITCZ and propagating through the southern U.S. to the East Coast. The case studies are listed as follows: Case 1: 2126 February 2015; Case 2: 1519 January 2017; Case 3: 2529 March 2018; and Case 4: 813 February 2019. Each case was chosen using typical characteristics of ARs: satellite imagery showed a stream of water vapor transport that was longer than its width; IVT, diagnosed as discussed below, was elevated in the area in conjunction with the satellite signature; the moisture signature began in the Pacific near or at the ITCZ, and the transport flowed through Texas, then out through the East Coast of the United States. Note: Imagery from GOES-13/16 (East) is 15 minutes behind the imagery from GOES-15

(West). For example, a GOES-15 image taken at 1800 UTC will have a corresponding GOES-13/15 image taken at 1745 UTC.

Data analysis was conducted using a computer program called VISUAL which is a meteorological diagnostic and display program developed by Dr. Wendell Nuss and Steve Drake (1990) at the Naval Postgraduate School that uses "graphic kernel system (GKS) primitives and National Center for Atmospheric Research (NCAR) Graphics routines to examine meteorological grids and observations." GKS offers users a standardized system for displaying two-dimensional images. The NCAR Graphics routines organize large amounts of data and provide a visual representation of that data. VISUAL allows the user to make a variety of diagnostic computations in order to manipulate the data on the plot to generate the desired output. The program "uses the GKS plot segmentation and graphical input capabilities and is primarily intended to be used interactively to explore data on the workstation screen and generate hardcopy output when appropriate." (Nuss and Drake 1990) VISUAL was used to plot atmospheric data including sea-level pressure (SLP), 850 mb wind, 850 mb temperature, 700 mb geopotential height, 500 mb geopotential height, 250 mb wind, IVT, latent heat flux, potential vorticity, and 6-hour precipitation.

Several methods have been used to identify a water vapor transport as an atmospheric river. In the most prevalent method, ARs are typically described as having a length greater than 2,000 km, a width less than 1,000 km, and a length-width ratio greater than two (Guan and Waliser 2015; Zhou et al. 2018). Each case study shows a satellite signature of water vapor transport with these features. Case 1 has a length of 5,100 km and a width of 985 km. Case 2 has a length of 6,550 km and a width of 655 km. Case 3 has a length of 4,550 km and a width of 750 km. Case 4 has a length of 7,565 km and a width of 805 km. All four cases can therefore be described by this criterion as ARs. As GOES imagery shows these ARs emerging from the ITCZ (a convergent boundary), the ARs in these four cases are classified as CBARs.

Vertically integrated water vapor transport (IVT) is typically used to calculate the water vapor transport in the x (zonal) and y (meridional) directions across a specified area (in this case, from the Pacific near the ITCZ to the East Coast of the U.S.). IVT was calculated as:

$$IVT_x = -\frac{1}{g} \int uqdp$$

$$IVT_y = -\frac{1}{g} \int vqdp$$

"where g is the gravitational acceleration, u (v) is the zonal (meridional) wind, q is the specific humidity, and p is the pressure." (Guan and Waliser 2017) IVT levels were calculated and plotted in VISUAL, with areas of elevated IVT (proposed atmospheric rivers) clearly visible and identified.

Vertically integrated moisture flux (MF) was calculated in a box around the Gulf of Mexico through Texas at specific longitude (λ) and latitude (ϕ) locations (Zhu and Newell 1998) to evaluate the source of the moisture associated with the AR. The moisture flux is calculated as:

$$MF = -\frac{1}{\rho} \int_{ps}^{pt} q\,|\boldsymbol{V}|\,\mathrm{dp}$$

where ρ is density, *ps* is surface pressure, *pt* is pressure at the top of the troposphere, q is specific humidity (g kg^{-1}), and $|\boldsymbol{V}|$ is the magnitude of the horizontal wind velocity.

The 700 mb geopotential height (GPT) surface was analyzed to look for synoptic scale features that may be associated with the formation of CBARS. The 500 mb GPT surface was analyzed to look for connections to upper-level CBAR propagation.

The 250 mb winds were analyzed to locate the subtropical jet. It appeared, initially, that once the CBAR was generated near the ITCZ, that the transport followed the upper-air flow patterns. The upper-level jet stream was analyzed to identify a possible link to the long distance and the deep inland penetration of the CBAR.

The 850 mb winds were used to look for vertical wind shear and signatures of a low-level jet. Dynamically, Case 3, which showed a similar pattern to the other cases, produced severe weather in central Texas, which may have been enhanced by vertical wind shear. ARs have also been shown to be associated with a low-level jet, so the low-level winds were analyzed to identify any indication of a low-level jet.

According to the definition from the AMS *Glossary of Meteorology* (2019), ARs are typically associated with the warm conveyor belt of extratropical cyclones. The 850

mb temperature and associated sea-level pressure were used to identify any fronts associated with the specific CBAR.

The vertical structure of the CBAR was analyzed at specific points for each case. A time was chosen where the IVT levels were more elevated in the CBAR area than the surrounding areas. Specific points were chosen along the elevated IVT path to show CBAR continuity across the path, specifically the CBAR origin, the CBAR landfall, the area of inland penetration (usually in Texas to show CBAR strength and continuity), and the eastern head of the CBAR. Elements analyzed were mixing ratio, potential temperature (theta), and cross cross-section winds (XXW). The mixing ratio was analyzed in accordance with criterion typically used to describe an AR (usually 5 g kg^{-1}). Theta was used to identify any frontal patterns. XXW was used to identify any shift in wind patterns and to identify any existing low-level jets.

The VISUAL program has the ability to plot backward trajectories of air parcels. A parcel trajectory was conducted at 850 mb and 700 mb to assess the movement of air along the CBAR path. These trajectories were also used to confirm the origin of the moisture flux at both lower and upper levels in order to identify the CBARs' location and origin.

The methods outlined in this section are used to develop a deeper understanding of CBARs as their own AR type. These methods aid in identifying characteristics that may separate CBARs from typical ARs such as the Maya Express and Pineapple Express. In the following sections, Chapter III outlines the characteristics of each of the four case studies, Chapter IV shows specific results determined by the analysis, and Chapter V summarizes the study and its findings.

III. CASE STUDIES

A lack of research regarding the influence of Pacific moisture on inland winter precipitation provided the motivation for this study. Specifically, Texas receives the majority of its winter precipitation from these Pacific moisture plumes. As such, four cases were chosen for this data analysis. These case studies were originally identified by satellite signatures exhibiting characteristics of ARs. Precipitation for all cases is highlighted in Texas, as part of this study evaluates the effects of deep inland penetration of CBARs (hypothesis 3). Specifically, precipitation reports are taken from the San Antonio (SAT) International Airport and the Dallas-Fort Worth (DFW) International Airport by way of the National Weather Service (NWS) Forecast Office for each city.

All four cases show CBARs emerging from a convergent boundary, namely the ITCZ. They all exceed the length-width ratio of two, and they seem to follow the 250 mb subtropical jet stream pattern. The case studies also suggest a convergence of two AR systems.

As few studies have been done on these Pacific moisture plumes and they have not officially been classified, these cases were chosen in order to further understand their characteristics and their effects on inland weather. As a result, an official classification for these plumes as CBARs has been made.

A. CASE 1

Case 1 took place from 21–26 February 2015. This case is unique in the fact that this CBAR brought freezing rain into Texas. On 1800 UTC 22 February, this CBAR had a length of 5,100 km, a width of 985 km, and a length-width ratio greater than five, as seen in Figure 2. Satellite infrared (IR) imagery shows the CBAR coming from the ITCZ just north of the Equator, about 1,550 km southwest of the Baja Peninsula, extending to Virginia. The water vapor (WV) imagery shows an abundance of water vapor along this same path, shown in Figure 3. Cool colors indicate high water vapor content, whereas warm colors indicate low water vapor content. Figure 4 shows IVT at this time is stronger along the path of the satellite signature. Red arrows indicate the direction of IVT, and the length

of the arrows correspond to the amount of IVT at that point (i.e., longer arrows indicate higher IVT). The IVT plot also shows an area of moisture coming up from the Gulf of Mexico as seen by the IVT vectors over the Gulf, and this transport is converging with the Pacific moisture near the Texas coast. This may explain why this particular event brought freezing rain. The fog recorded may be from the cooler Pacific moisture overrunning the warmer Gulf moisture. This event also appears to show two ARs, the Pacific CBAR and the Maya Express AR, converging.

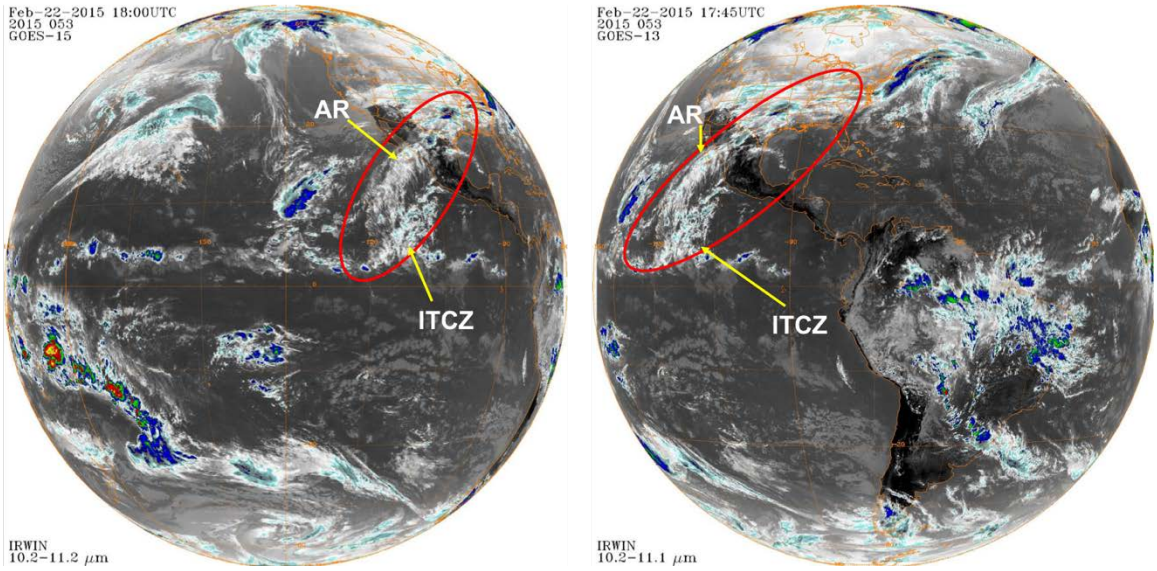

Left: GOES-15 (West) 1800 UTC 22 February 2015; right: GOES-13 (East) 1745 UTC 22 February 2015.

Figure 2. Case 1 GOES IR Imagery. Source: Knapp (2008).

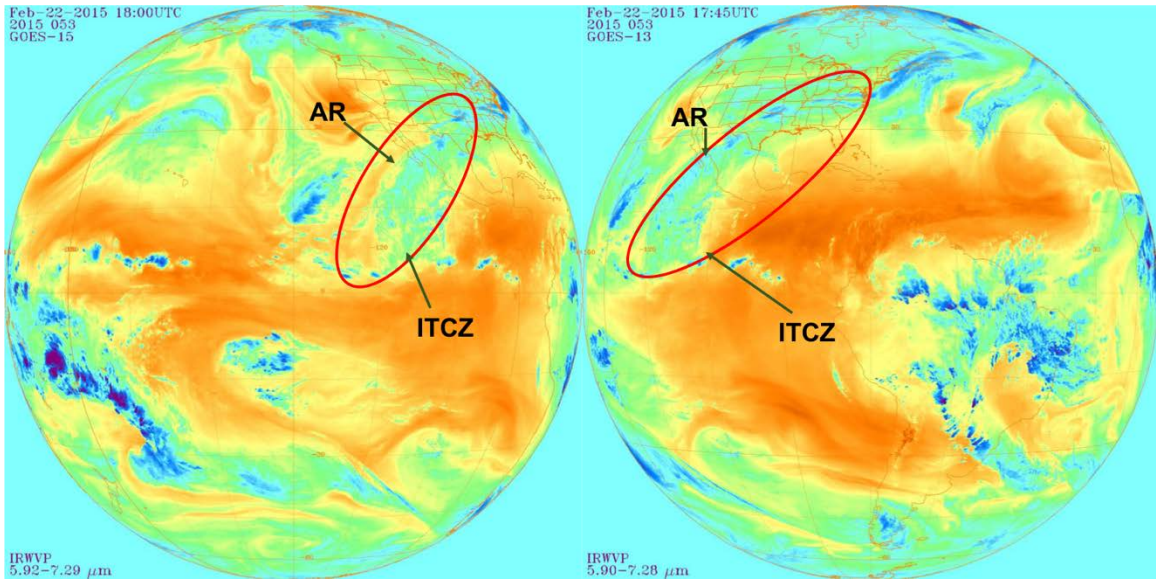

Left: GOES-15 (West) 1800 UTC 22 February 2015; right: GOES-13 East 1745 UTC 22 February 2015.

Figure 3. Case 1 GOES WV Imagery. Source: Knapp (2008).

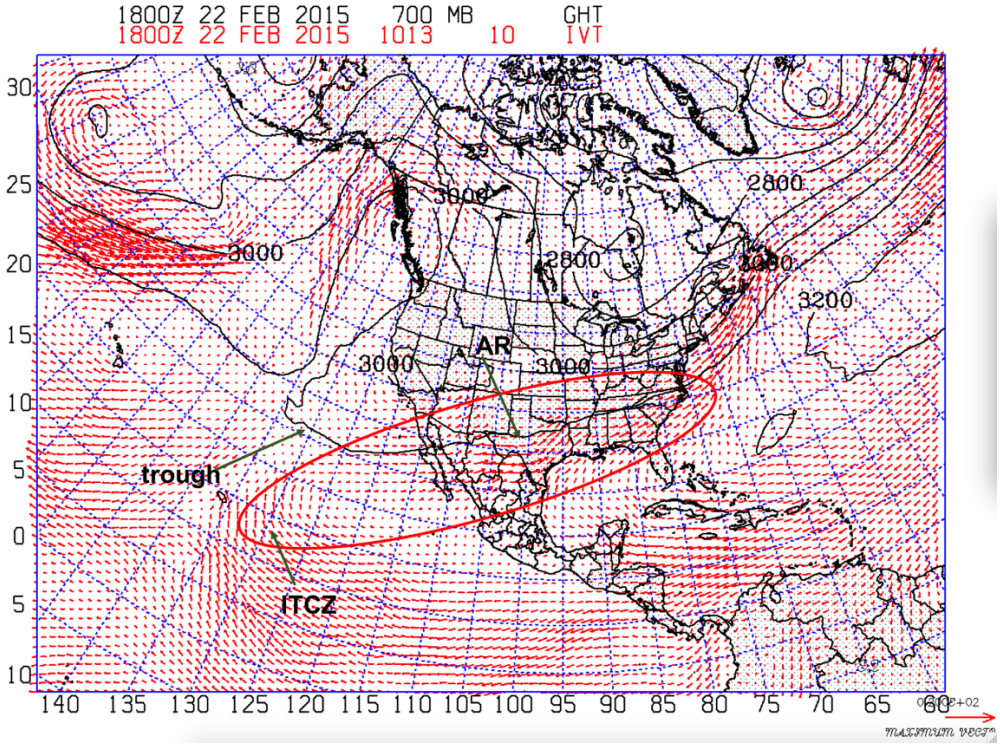

IVT plot for 1800 UTC 22 February 2015. Strong IVT signature begins west of Baja and travels through the southern U.S. and up along the East Coast.

Figure 4. Case 1 IVT Plot.

The CBAR pattern for Case 1 follows the 250 mb subtropical jet, which extends from Baja across the southern U.S., and the 5,800 m contour on the 500 mb geopotential height (GPT) chart seen in Figure 5. The wind fields at 850 mb and 250 mb, shown in Figure 6, indicate vertical shear at the Texas Gulf Coast, where the Gulf moisture and Pacific moisture converge.

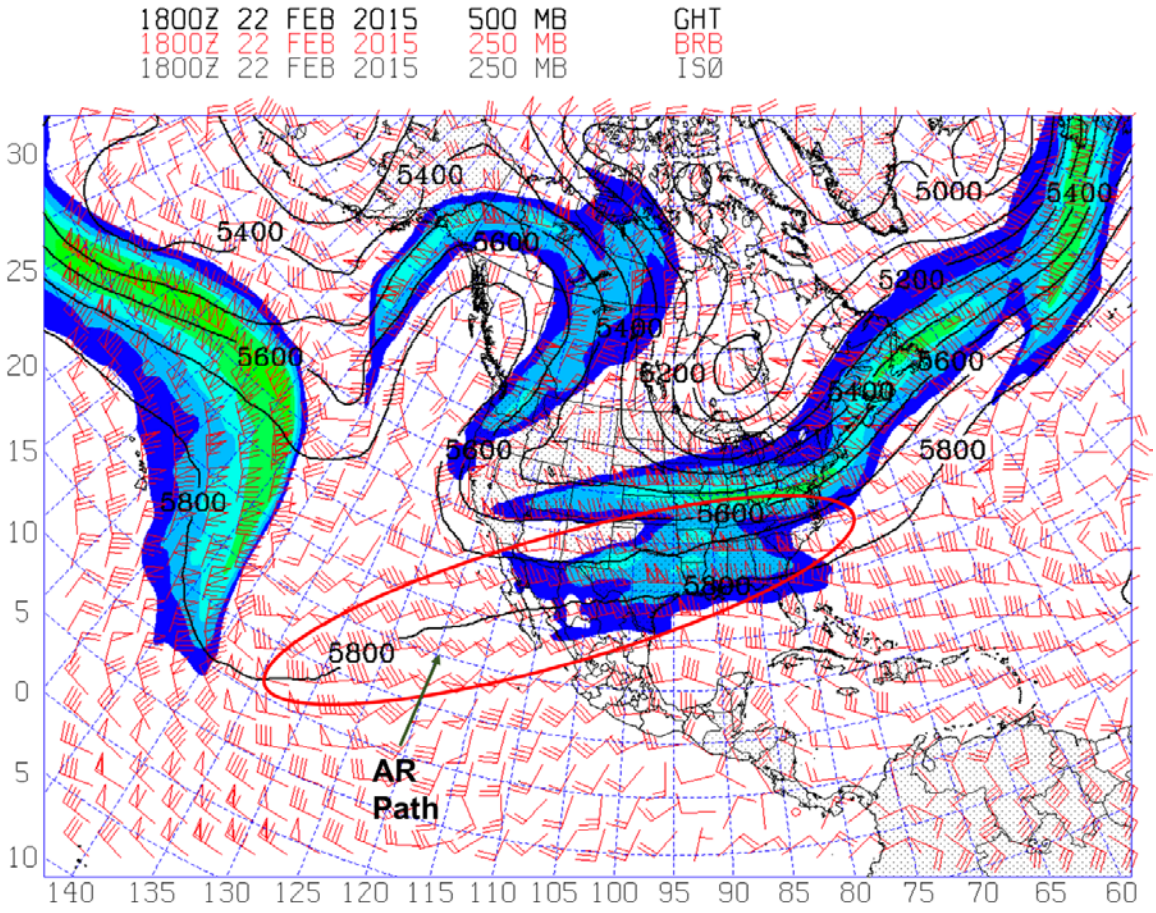

The 500 mb Geopotential Height contours are shown in black, the 250 mb jet stream is shown with the color fill, and the 250 mb wind is shown with red barbs, 1800 UTC 22 February 2015.

Figure 5. Case 1 Upper-Air Chart.

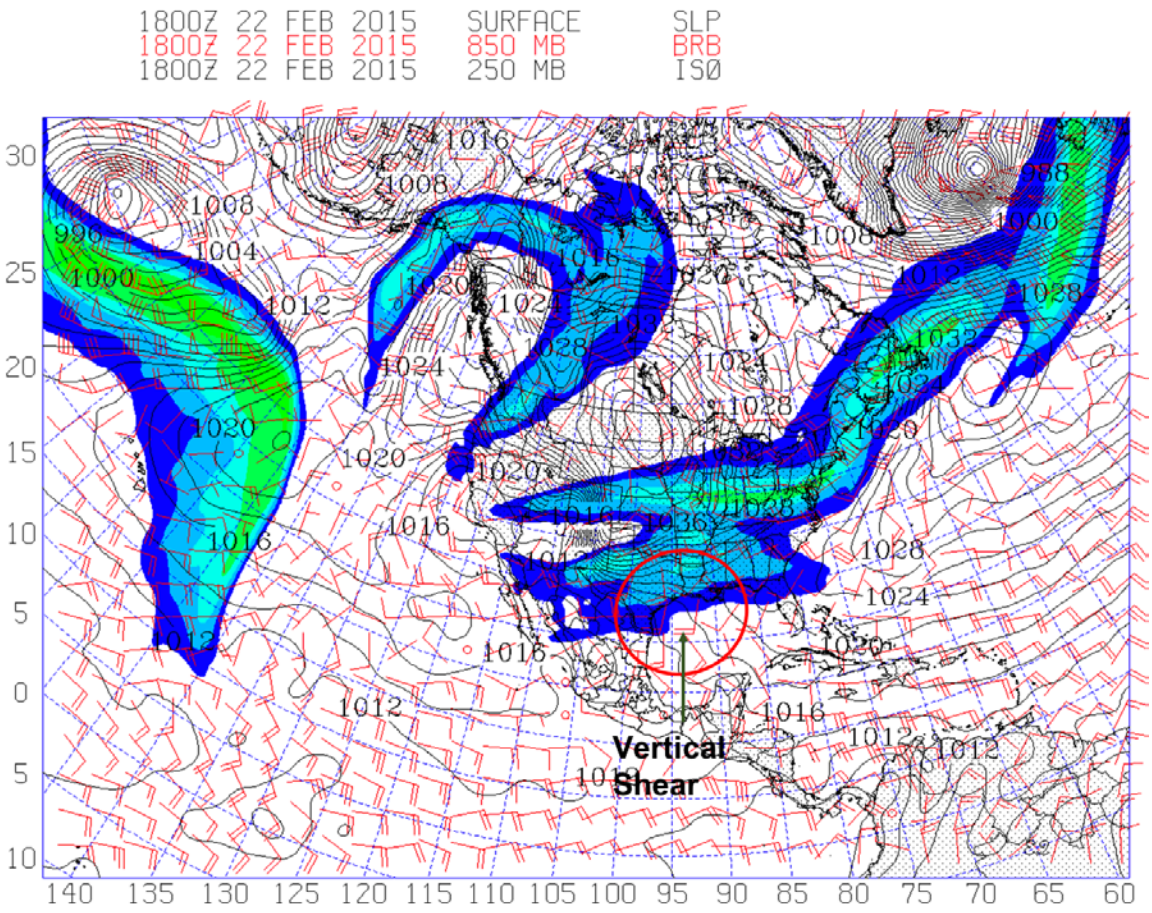

Sea-level pressure is shown in black contours, 850 mb wind with red barbs, and 250 mb jet stream with a color fill, 1800 UTC 22 February 2015.

Figure 6. Case 1 Surface and Upper-Air Chart.

The Dallas-Fort Worth (DFW) Forecast Office recorded 2.13 in. of precipitation and 0.3 in. of snow throughout the Case 1 time period. Figure 7 shows the report for February 2015. Observed weather was recorded as fog or mist, thunder, ice pellets, and freezing rain or drizzle. The San Antonio (SAT) Forecast Office reported only a trace of precipitation, shown in the report in Figure 8. However, observed weather included fog or mist, smoke or haze, and freezing rain or drizzle.

WFO Monthly/Daily Climate Data

```
000
CXUS54 KFWD 081319
CF6DFW
PRELIMINARY LOCAL CLIMATOLOGICAL DATA (WS FORM: F-6)

                                        STATION:   DALLAS FORT WORTH
                                        MONTH:     FEBRUARY
                                        YEAR:      2015
                                        LATITUDE:   32 54 N
                                        LONGITUDE:  97  2 W

  TEMPERATURE IN F:       :PCPN:    SNOW:  WIND      :SUNSHINE: SKY     :PK WND
==========================================================================
1   2   3   4   5  6A  6B    7    8   9   10  11  12  13   14  15   16   17  18
                                    12Z  AVG MX 2MIN
DY MAX MIN AVG DEP HDD CDD  WTR  SNW DPTH SPD SPD DIR MIN PSBL S-S WX    SPD DR
==========================================================================

 1  58  34  46  -1  19   0 0.10  0.0    0 15.6 31 340   M    M   7 1      36 330
 2  42  24  33 -14  32   0 0.00  0.0    0 10.4 25 350   M    M   4        31 330
 3  54  31  43  -5  22   0 0.00  0.0    0  9.9 18 160   M    M   9        22 160
 4  57  37  47  -1  18   0    T  0.0    0 12.3 26 350   M    M   9 18     32 340
 5  37  29  33 -15  32   0    T  0.0    0  9.4 23 360   M    M  10 16     27 360
 6  58  32  45  -3  20   0 0.00  0.0    0  9.9 17 170   M    M   6 8      23 160
 7  69  42  56   8   9   0 0.00  0.0    0 17.9 29 190   M    M   1 1      35 180
 8  73  51  62  14   3   0 0.00  0.0    0  8.6 23 190   M    M   1 1      28 190
 9  75  46  61  12   4   0 0.00  0.0    0  8.6 16  10   M    M   1        20  10
10  75  45  60  11   5   0 0.00  0.0    0  9.9 22 170   M    M   1        26 160
11  67  45  56   7   9   0 0.00  0.0    0 12.6 25  10   M    M   3        32  10
12  55  36  46  -3  19   0 0.00  0.0    0 10.9 23  20   M    M   3        30  30
13  67  35  51   2  14   0 0.00  0.0    0  7.1 18 200   M    M   2        23 210
14  78  40  59   9   6   0 0.00  0.0    0  6.7 14 220   M    M   1        17 210
15  73  50  62  12   3   0    T  0.0    0 12.5 28 190   M    M   8        33 190
16  62  29  46  -4  19   0 0.22    T    0 17.9 29 350   M    M   9 1      37 330
17  54  28  41  -9  24   0 0.05  0.0    0  8.2 32 320   M    M   7 13     41 330
18  57  30  44  -6  21   0 0.00  0.0    0  4.6 15  60   M    M   1        20  50
19  60  32  46  -5  19   0 0.00  0.0    0 11.9 22 130   M    M   4        25 140
20  70  46  58   7   7   0    T  0.0    0 17.9 36 190   M    M   8 1      42 180
21  67  46  57   6   8   0 0.00  0.0    0 14.7 30 200   M    M   8        39 200
22  50  29  40 -12  25   0 1.30    T    0 16.6 29  20   M    M  10 1346   35  20
23  30  26  28 -24  37   0 0.17  0.2    T 15.7 30  30   M    M  10 146    36  30
24  37  25  31 -21  34   0    T  0.0    T  5.9 14 340   M    M  10 16     17 340
25  52  32  42 -10  23   0 0.66  0.1    0  4.1 12 140   M    M   6 148    14 140
26  38  30  34 -19  31   0    T    T    0 15.7 28 360   M    M   8 18     34 360
27  30  24  27 -26  38   0 0.26  2.0    0 11.5 20  30   M    M  10 146    25  40
28  32  26  29 -24  36   0 0.20    T    2  6.9 12  40   M    M  10 146    13  40
==========================================================================
SM 1577  980       537   0  2.96     2.3 313.9          M      167
==========================================================================
AV 56.3 35.0                            11.2 FASTST   M    M   6    MAX(MPH)
                                 MISC ----->  # 36 190              # 42  180
==========================================================================
NOTES:
# LAST OF SEVERAL OCCURRENCES

COLUMN 17 PEAK WIND IN M.P.H.

PRELIMINARY LOCAL CLIMATOLOGICAL DATA (WS FORM: F-6) , PAGE 2

                                        STATION:  DALLAS FORT WORTH
                                        MONTH:    FEBRUARY
                                        YEAR:     2015
                                        LATITUDE:   32 54 N
                                        LONGITUDE:  97  2 W

[TEMPERATURE DATA]      [PRECIPITATION DATA]       SYMBOLS USED IN COLUMN 16

AVERAGE MONTHLY: 45.7   TOTAL FOR MONTH:   2.96    1 = FOG OR MIST
DPTR FM NORMAL:  -4.2   DPTR FM NORMAL:    0.30    2 = FOG REDUCING VISIBILITY
HIGHEST:     78 ON 14   GRTST 24HR  1.46 ON 22-23      TO 1/4 MILE OR LESS
LOWEST:      24 ON 27, 2                            3 = THUNDER
                        SNOW, ICE PELLETS, HAIL     4 = ICE PELLETS
                        TOTAL MONTH:   2.3 INCHES   5 = HAIL
                        GRTST 24HR   2.0 ON 27-27   6 = FREEZING RAIN OR DRIZZLE
                        GRTST DEPTH:   2 ON 28      7 = DUSTSTORM OR SANDSTORM:
                                                        VSBY 1/2 MILE OR LESS
                                                    8 = SMOKE OR HAZE
[NO. OF DAYS WITH]      [WEATHER - DAYS WITH]       9 = BLOWING SNOW
                                                    X = TORNADO
```

Figure 7. NWS Forecast Office Report for Dallas-Fort Worth, February 2015. Source: NWS Dallas-Fort Worth (2014).

WFO Monthly/Daily Climate Data

```
000
CXUS54 KEWX 030106
CF6SAT
PRELIMINARY LOCAL CLIMATOLOGICAL DATA (WS FORM: F-6)

                                        STATION:   SAN ANTONIO
                                        MONTH:     FEBRUARY
                                        YEAR:      2015
                                        LATITUDE:   29 31 N
                                        LONGITUDE:  98 28 W

  TEMPERATURE IN F:       :PCPN:    SNOW:  WIND      :SUNSHINE: SKY     :PK WND
=================================================================================
1   2   3   4   5  6A  6B    7    8   9   10  11  12  13   14  15   16   17  18
                                     12Z  AVG MX 2MIN
DY MAX MIN AVG DEP HDD CDD  WTR  SNW DPTH SPD SPD DIR MIN PSBL S-S WX    SPD DR
=================================================================================

 1  77  48  63  10   2   0 0.00  0.0    0 10.4 26 360   M    M   8 12     36 360
 2  52  38  45  -8  20   0 0.00  0.0    0  8.8 22  20   M    M   7        31  10
 3  45  41  43 -10  22   0 0.28  0.0    0  3.5  9 160   M    M  10 18     10 110
 4  53  44  49  -5  16   0 0.02  0.0    0  4.0 10 230   M    M   8 18     14 220
 5  53  42  48  -6  17   0    T  0.0    0  9.7 21 360   M    M  10 1      27 340
 6  56  43  50  -4  15   0 0.00  0.0    0  3.8 12 210   M    M   8        16 200
 7  68  49  59   5   6   0 0.00  0.0    0  9.1 18 220   M    M   6        24 210
 8  74  52  63   9   2   0    T  0.0    0  8.6 16 230   M    M   6 128    20 230
 9  84  50  67  13   0   2 0.00  0.0    0  3.6 14  20   M    M   0        19  10
10  80  46  63   8   2   0 0.00  0.0    0  7.2 15 200   M    M   0        23 210
11  76  47  62   7   3   0 0.00  0.0    0  6.3 20 150   M    M   2        26 130
12  65  48  57   2   8   0 0.00  0.0    0 10.6 21  10   M    M   5        32  50
13  69  47  58   3   7   0 0.00  0.0    0  4.3 13 200   M    M   6        17 230
14  74  48  61   6   4   0 0.00  0.0    0  6.1 13 230   M    M   6 18     16 220
15  70  61  66  10   0   1 0.06  0.0    0  8.4 17 160   M    M   9 18     22 160
16  65  40  53  -3  12   0 0.02  0.0    0 11.9 30 350   M    M   9 1      37 350
17  56  36  46 -10  19   0    T    T    0  8.6 23 350   M    M   6 4      29 340
18  64  32  48  -8  17   0 0.00  0.0    0  7.3 17 180   M    M   0        23 180
19  70  38  54  -2  11   0 0.00  0.0    0 10.2 23 160   M    M   1        30 160
20  79  58  69  12   0   4 0.00  0.0    0 14.3 22 160   M    M   8        28 150
21  79  62  71  14   0   6 0.00  0.0    0  9.1 16 170   M    M   7        21 180
22  66  40  53  -4  12   0    T  0.0    0 11.4 28  20   M    M  10 18     37  20
23  41  32  37 -20  28   0    T  0.0    0 14.1 24  10   M    M  10 6      32  30
24  42  32  37 -21  28   0    T  0.0    0  6.8 12 110   M    M  10 168    14  10
25  67  36  52  -6  13   0 0.01  0.0    0  6.5 20 340   M    M   3 1      26 320
26  62  36  49  -9  16   0 0.00  0.0    0 10.3 23  20   M    M   3        29  50
27  38  33  36 -22  29   0 0.02  0.0    0 11.1 18  30   M    M  10 18     26  40
28  39  34  37 -21  28   0 0.12  0.0    0  9.1 14  10   M    M  10 1      19  60
=================================================================================
SM 1764 1213       337  13  0.53    T    235.1          M       178
=================================================================================
AV 63.0 43.3                                8.4 FASTST   M    M   6    MAX(MPH)
                                  MISC ----> # 30 350                # 37  350
=================================================================================
NOTES:
# LAST OF SEVERAL OCCURRENCES

COLUMN 17 PEAK WIND IN M.P.H.

PRELIMINARY LOCAL CLIMATOLOGICAL DATA (WS FORM: F-6) , PAGE 2

                                        STATION:  SAN ANTONIO
                                        MONTH:    FEBRUARY
                                        YEAR:     2015
                                        LATITUDE:   29 31 N
                                        LONGITUDE:  98 28 W

[TEMPERATURE DATA]      [PRECIPITATION DATA]       SYMBOLS USED IN COLUMN 16

AVERAGE MONTHLY: 53.2   TOTAL FOR MONTH:   0.53    1 = FOG OR MIST
DPTR FM NORMAL:  -2.4   DPTR FM NORMAL:   -1.26    2 = FOG REDUCING VISIBILITY
HIGHEST:     84 ON  9   GRTST 24HR  0.30 ON  3- 4      TO 1/4 MILE OR LESS
LOWEST:      32 ON 24,23                           3 = THUNDER
                        SNOW, ICE PELLETS, HAIL    4 = ICE PELLETS
                        TOTAL MONTH:    T          5 = HAIL
                        GRTST 24HR    T  ON 17-17  6 = FREEZING RAIN OR DRIZZLE
                        GRTST DEPTH:   0           7 = DUSTSTORM OR SANDSTORM:
                                                       VSBY 1/2 MILE OR LESS
                                                   8 = SMOKE OR HAZE
[NO. OF DAYS WITH]      [WEATHER - DAYS WITH]      9 = BLOWING SNOW
                                                   X = TORNADO
```

Figure 8. NWS Forecast Office Report for San Antonio, February 2015. Source: NWS Austin-San Antonio (2014).

B. CASE 2

Case 2 took place from 15–19 January 2017. This case is a more typical scenario in that it brought fog and drizzle into Texas, representative of Texas winter weather influenced by Pacific moisture. On 1200 UTC 19 January, the CBAR had a length of 6,550 km, a width of 655 km, and a length-width ratio of ten. In Figure 9, IR satellite imagery shows the CBAR coming from the Pacific, about 2,450 km southeast of Hawaii extending to Virginia. The WV imagery moisture signature confirms this pattern and path seen in Figure 10. The IVT plot shows higher IVT from the Pacific along the CBAR path. However, Figure 11 shows a strong IVT signature coming up from the Gulf of Mexico, converging with the Pacific moisture along the Texas Coast, as in Case 1. Once again, this looks like it may be a case of overrunning as well as a case of converging ARs.

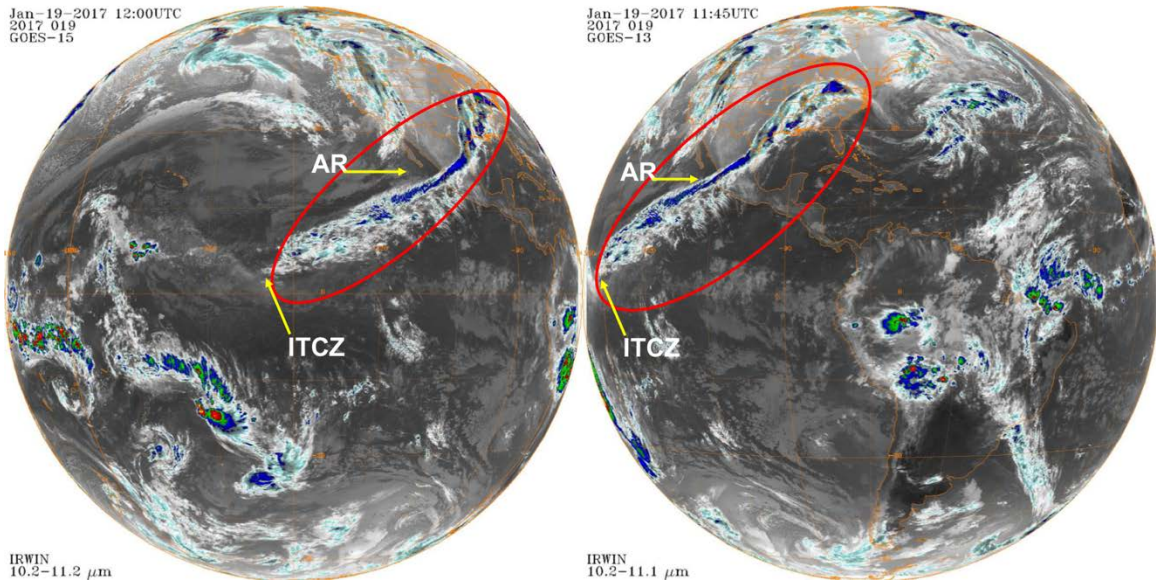

Left: GOES-15 (West) 1200 UTC 19 January 2017; right: GOES-13 (East) 1145 UTC 19 January 2017.

Figure 9. Case 2 GOES IR Imagery. Source: Knapp (2008).

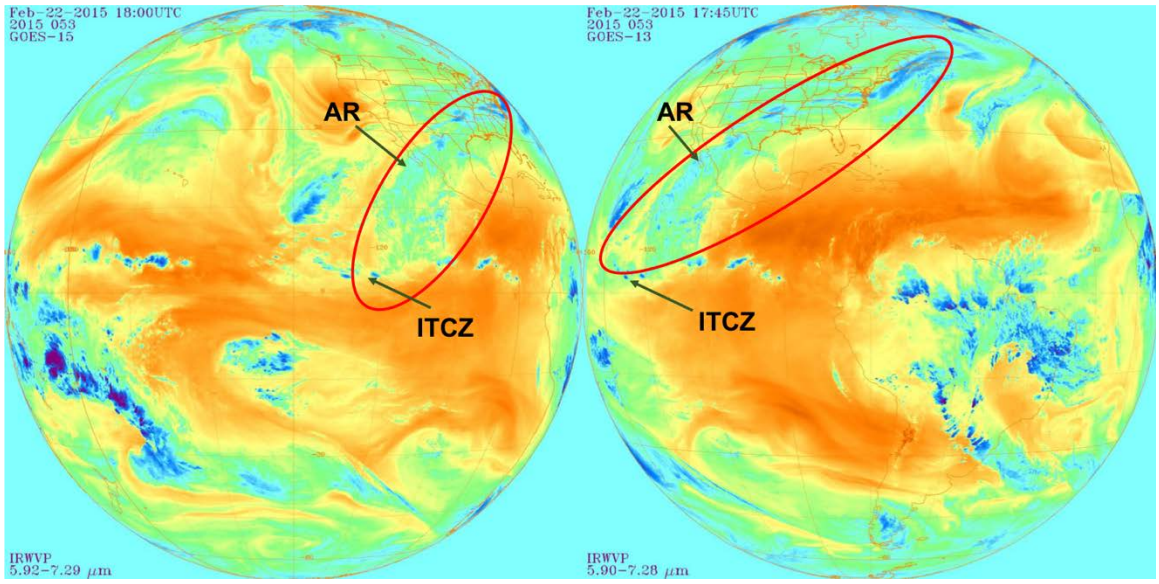

Left: GOES-15 (West) 1200 UTC 19 January 2017; right: GOES-13 (East) 1145 UTC 19 January 2017.

Figure 10. Case 2 GOES WV Imagery. Source: Knapp (2008).

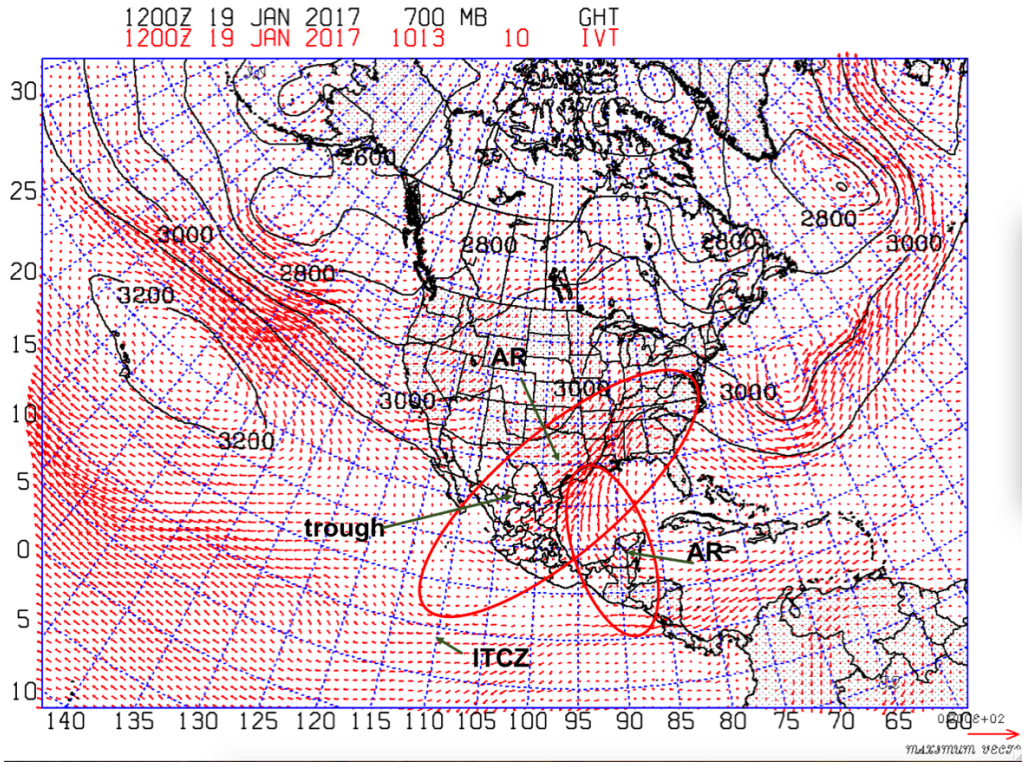

IVT plot for 1200 UTC 19 January 2017. Strong IVT signature begins west of Mexico and continues into Virginia.

Figure 11. Case 2 IVT Plot.

The CBAR pattern for Case 2 also seemed to take the shape of the subtropical jet as it flowed through Mexico and Texas over into Virginia. As in case 1, this seems to follow the 5800 m geopotential height contour in Figure 12. Though the IVT plot shows moisture convergence along the Texas coast, the 850 mb and 250 mb wind fields did not show much vertical shear in Figure 13.

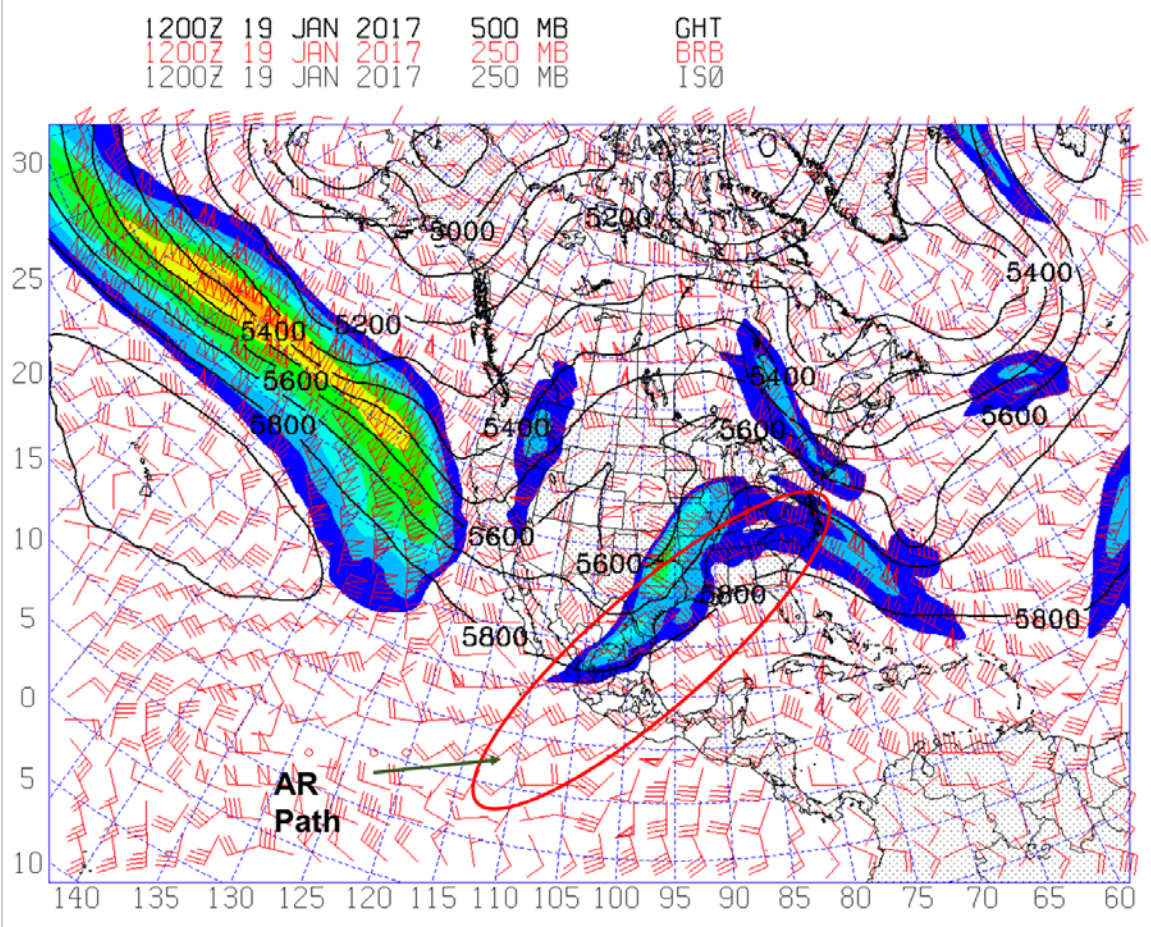

The 500 mb Geopotential Height contours are shown in black, the 250 mb jet stream is shown with the color fill, and the 250 mb wind is shown with red barbs, 1200 UTC 19 January 2017.

Figure 12. Case 2 Upper-Air Chart.

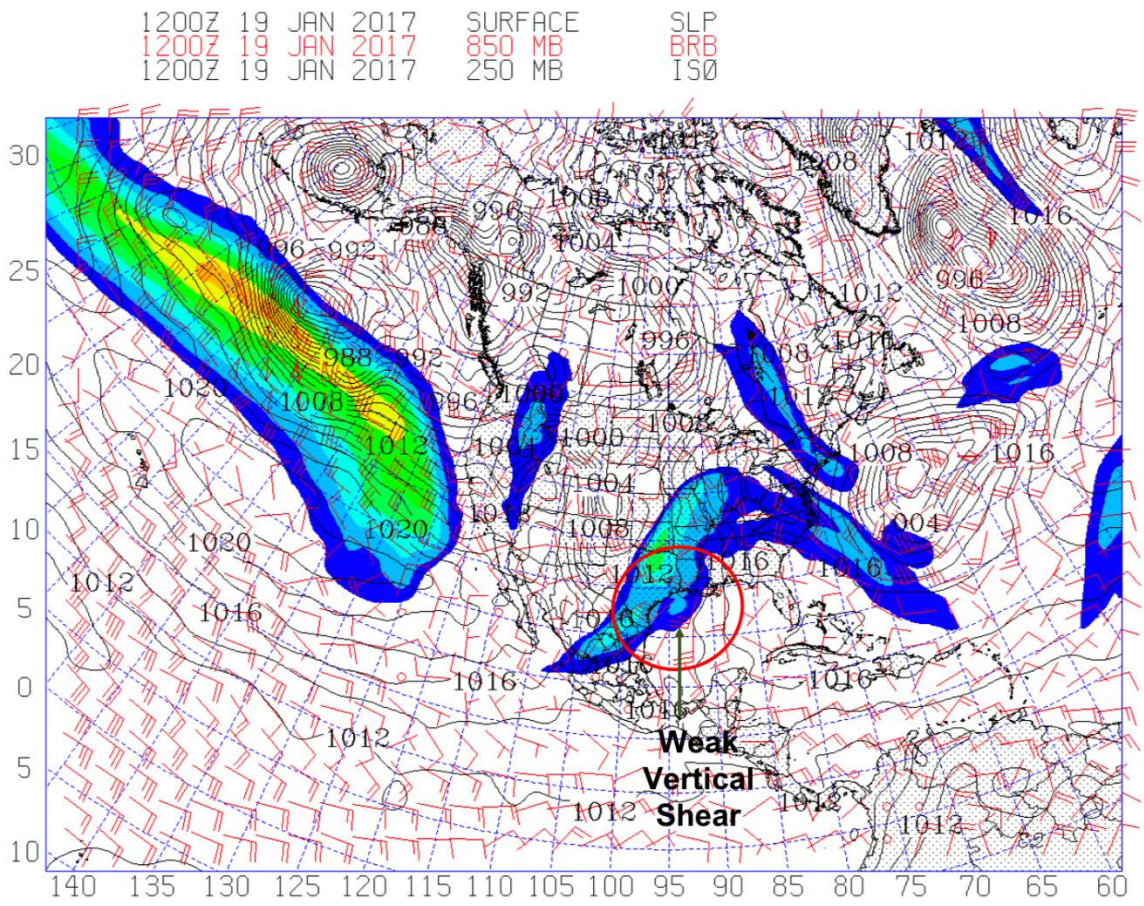

Sea-level pressure is shown in black contours, 850 mb wind with red barbs, and 250 mb jet stream with a color fill, 1200 UTC 19 January 2017.

Figure 13. Case 2 Surface and Upper-Air Chart.

Precipitation amounts were light, mostly in the form of light rain, drizzle, and fog. The DFW Forecast Office report in Figure 14 shows only 0.42 in. of precipitation recorded, and the office reported fog or mist with fog reducing visibility to 0.25 miles or less and thunder throughout the case period. The SAT Forecast Office reported 1 in. of precipitation and fog or mist with thunder, shown in Figure 15. The 3.16 in. of precipitation reported by DFW and the 1.62 in. of precipitation reported by SAT on 15 February was from the system moving through prior to the CBAR associated with this case study.

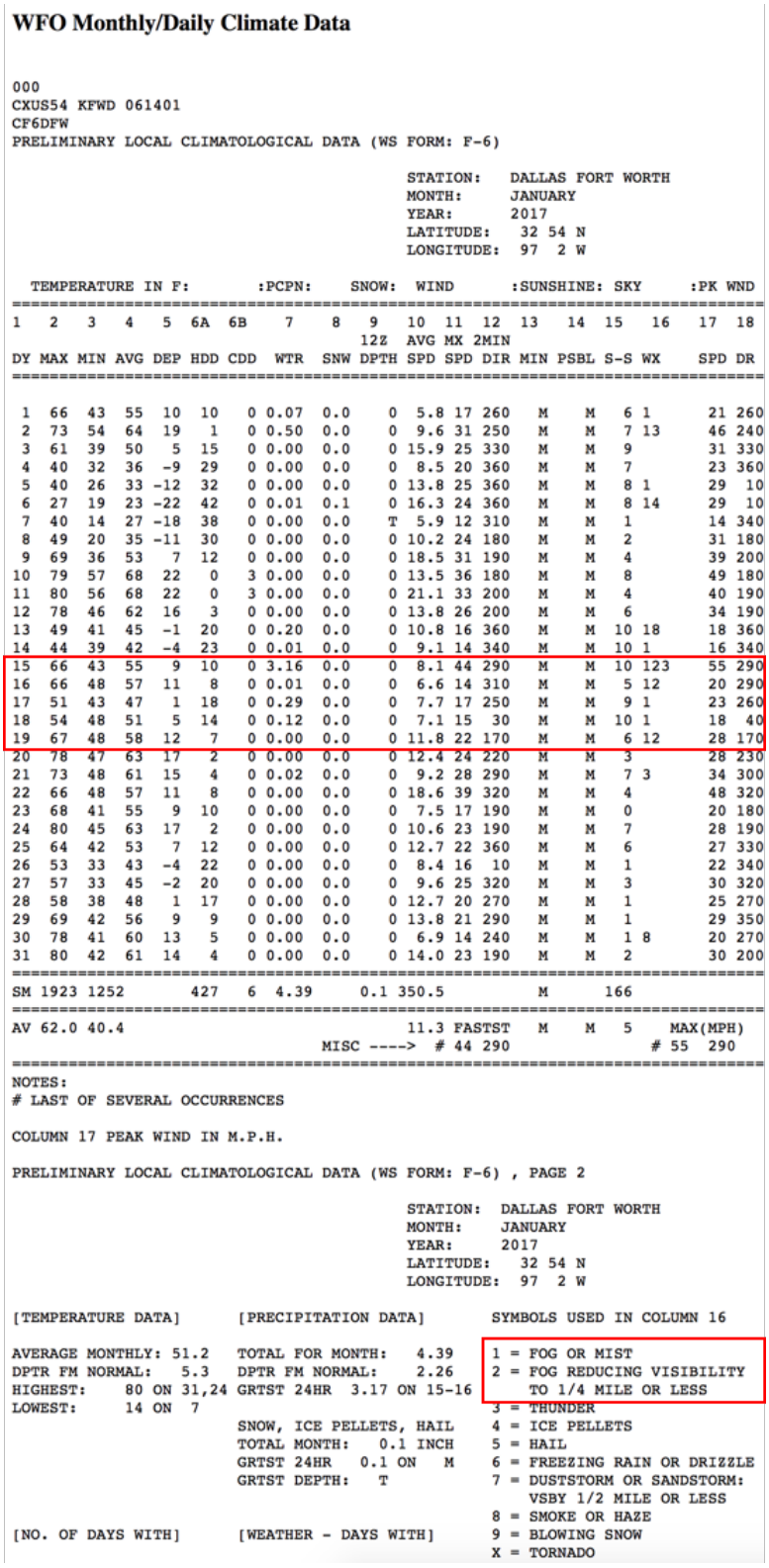

WFO Monthly/Daily Climate Data

000
CXUS54 KFWD 061401
CF6DFW
PRELIMINARY LOCAL CLIMATOLOGICAL DATA (WS FORM: F-6)

STATION: DALLAS FORT WORTH
MONTH: JANUARY
YEAR: 2017
LATITUDE: 32 54 N
LONGITUDE: 97 2 W

TEMPERATURE IN F:							:PCPN:		SNOW:	WIND			:SUNSHINE:		SKY		:PK WND	
1	2	3	4	5	6A	6B	7	8	9	10	11	12	13	14	15	16	17	18
									12Z	AVG	MX	2MIN						
DY	MAX	MIN	AVG	DEP	HDD	CDD	WTR	SNW	DPTH	SPD	SPD	DIR	MIN	PSBL	S-S	WX	SPD	DR
1	66	43	55	10	10	0	0.07	0.0	0	5.8	17	260	M	M	6	1	21	260
2	73	54	64	19	1	0	0.50	0.0	0	9.6	31	250	M	M	7	13	46	240
3	61	39	50	5	15	0	0.00	0.0	0	15.9	25	330	M	M	9		31	330
4	40	32	36	-9	29	0	0.00	0.0	0	8.5	20	360	M	M	7		23	360
5	40	26	33	-12	32	0	0.00	0.0	0	13.8	25	360	M	M	8	1	29	10
6	27	19	23	-22	42	0	0.01	0.1	0	16.3	24	360	M	M	8	14	29	10
7	40	14	27	-18	38	0	0.00	0.0	T	5.9	12	310	M	M	1		14	340
8	49	20	35	-11	30	0	0.00	0.0	0	10.2	24	180	M	M	2		31	180
9	69	36	53	7	12	0	0.00	0.0	0	18.5	31	190	M	M	4		39	200
10	79	57	68	22	0	3	0.00	0.0	0	13.5	36	180	M	M	8		49	180
11	80	56	68	22	0	3	0.00	0.0	0	21.1	33	200	M	M	4		40	190
12	78	46	62	16	3	0	0.00	0.0	0	13.8	26	200	M	M	6		34	190
13	49	41	45	-1	20	0	0.20	0.0	0	10.8	16	360	M	M	10	18	18	360
14	44	39	42	-4	23	0	0.01	0.0	0	9.1	14	340	M	M	10	1	16	340
15	66	43	55	9	10	0	3.16	0.0	0	8.1	44	290	M	M	10	123	55	290
16	66	48	57	11	8	0	0.01	0.0	0	6.6	14	310	M	M	5	12	20	290
17	51	43	47	1	18	0	0.29	0.0	0	7.7	17	250	M	M	9	1	23	260
18	54	48	51	5	14	0	0.12	0.0	0	7.1	15	30	M	M	10	1	18	40
19	67	48	58	12	7	0	0.00	0.0	0	11.8	22	170	M	M	6	12	28	170
20	78	47	63	17	2	0	0.00	0.0	0	12.4	24	220	M	M	3		28	230
21	73	48	61	15	4	0	0.02	0.0	0	9.2	28	290	M	M	7	3	34	300
22	66	48	57	11	8	0	0.00	0.0	0	18.6	39	320	M	M	4		48	320
23	68	41	55	9	10	0	0.00	0.0	0	7.5	17	190	M	M	0		20	180
24	80	45	63	17	2	0	0.00	0.0	0	10.6	23	190	M	M	7		28	190
25	64	42	53	7	12	0	0.00	0.0	0	12.7	22	360	M	M	6		27	330
26	53	33	43	-4	22	0	0.00	0.0	0	8.4	16	10	M	M	1		22	340
27	57	33	45	-2	20	0	0.00	0.0	0	9.6	25	320	M	M	3		30	320
28	58	38	48	1	17	0	0.00	0.0	0	12.7	20	270	M	M	1		25	270
29	69	42	56	9	9	0	0.00	0.0	0	13.8	21	290	M	M	1		29	350
30	78	41	60	13	5	0	0.00	0.0	0	6.9	14	240	M	M	1	8	20	270
31	80	42	61	14	4	0	0.00	0.0	0	14.0	23	190	M	M	2		30	200
SM	1923	1252		427	6	4.39		0.1	350.5				M		166			
AV	62.0	40.4								11.3	FASTST		M	M	5		MAX(MPH)	
									MISC ---->	#	44	290				#	55	290

NOTES:
LAST OF SEVERAL OCCURRENCES

COLUMN 17 PEAK WIND IN M.P.H.

PRELIMINARY LOCAL CLIMATOLOGICAL DATA (WS FORM: F-6) , PAGE 2

STATION: DALLAS FORT WORTH
MONTH: JANUARY
YEAR: 2017
LATITUDE: 32 54 N
LONGITUDE: 97 2 W

[TEMPERATURE DATA]

AVERAGE MONTHLY: 51.2
DPTR FM NORMAL: 5.3
HIGHEST: 80 ON 31,24
LOWEST: 14 ON 7

[PRECIPITATION DATA]

TOTAL FOR MONTH: 4.39
DPTR FM NORMAL: 2.26
GRTST 24HR 3.17 ON 15-16

SNOW, ICE PELLETS, HAIL
TOTAL MONTH: 0.1 INCH
GRTST 24HR 0.1 ON M
GRTST DEPTH: T

[NO. OF DAYS WITH]

[WEATHER - DAYS WITH]

SYMBOLS USED IN COLUMN 16

1 = FOG OR MIST
2 = FOG REDUCING VISIBILITY TO 1/4 MILE OR LESS
3 = THUNDER
4 = ICE PELLETS
5 = HAIL
6 = FREEZING RAIN OR DRIZZLE
7 = DUSTSTORM OR SANDSTORM: VSBY 1/2 MILE OR LESS
8 = SMOKE OR HAZE
9 = BLOWING SNOW
X = TORNADO

Figure 14. NWS Forecast Office Report for Dallas-Fort Worth, January 2017. Source: NWS Dallas-Fort Worth (2014).

WFO Monthly/Daily Climate Data

```
000
CXUS54 KEWX 011528
CF6SAT
PRELIMINARY LOCAL CLIMATOLOGICAL DATA (WS FORM: F-6)

                                        STATION:   SAN ANTONIO
                                        MONTH:     JANUARY
                                        YEAR:      2017
                                        LATITUDE:   29 31 N
                                        LONGITUDE:  98 28 W

  TEMPERATURE IN F:        :PCPN:    SNOW:  WIND      :SUNSHINE: SKY     :PK WND
=================================================================================
1   2   3   4   5  6A  6B    7    8   9   10  11  12  13   14  15   16   17  18
                                      12Z  AVG MX 2MIN
DY MAX MIN AVG DEP HDD CDD  WTR  SNW DPTH SPD SPD DIR MIN PSBL S-S WX    SPD DR
=================================================================================

 1  75  53  64  13   1   0 0.00  0.0    0  5.6 15 200   M    M   5 12     20 320
 2  77  49  63  12   2   0 0.02  0.0    0  7.5 22 310   M    M   5 123    26 310
 3  79  45  62  11   3   0 0.00  0.0    0  7.9 20  10   M    M   6        28  20
 4  52  41  47  -4  18   0 0.00  0.0    0  9.1 21 360   M    M   8        26  20
 5  70  38  54   3  11   0 0.00  0.0    0  9.7 25  10   M    M   9 8      34  10
 6  38  25  32 -19  33   0    T  0.0    0 16.3 23  10   M    M   8 6      32  10
 7  46  20  33 -18  32   0 0.00  0.0    0  5.9 15  10   M    M   0        19  10
 8  52  19  36 -15  29   0 0.00  0.0    0  6.4 14 200   M    M   3        20 190
 9  72  47  60   9   5   0 0.00  0.0    0  7.2 22 190   M    M   6 8      27 190
10  79  54  67  16   0   2 0.00  0.0    0  6.2 14 170   M    M   3 1      21 170
11  79  53  66  15   0   1 0.00  0.0    0 11.8 23 160   M    M   4        30 190
12  81  61  71  20   0   6 0.00  0.0    0 12.0 23 180   M    M   7        29 170
13  79  68  74  22   0   9    T  0.0    0 12.8 22 130   M    M  10        26 140
14  70  58  64  12   1   0 0.09  0.0    0  7.9 14 110   M    M  10 18     19 110
15  76  58  67  15   0   2 1.62  0.0    0 11.9 30 140   M    M  10 1238   37 140
16  70  59  65  13   0   0 0.60  0.0    0  4.9 10  10   M    M  10 13     14  60
17  62  50  56   4   9   0 0.11  0.0    0  9.9 18  30   M    M  10 1      27  30
18  65  48  57   5   8   0 0.27  0.0    0  7.6 15 360   M    M   9 13     20 360
19  71  50  61   9   4   0    T  0.0    0  6.8 17 210   M    M   6 1      23 240
20  75  47  61   9   4   0 0.00  0.0    0  3.5 17 130   M    M   6 128    21 130
21  83  49  66  14   0   1    T  0.0    0 10.9 35 300   M    M   6 12     50 300
22  72  48  60   8   5   0 0.00  0.0    0 20.3 38 310   M    M   1        50 310
23  76  42  59   7   6   0 0.00  0.0    0  5.9 18 220   M    M   0        23 250
24  82  44  63  11   2   0 0.00  0.0    0  5.8 17 160   M    M   4 8      20 170
25  72  50  61   9   4   0 0.00  0.0    0 10.5 21 350   M    M   6 1      27 350
26  61  40  51  -1  14   0 0.00  0.0    0  6.2 15  70   M    M   4        20  50
27  56  41  49  -3  16   0 0.00  0.0    0  8.8 18  80   M    M   8        24  80
28  61  38  50  -3  15   0 0.01  0.0    0  8.3 20 350   M    M   6        26 290
29  72  34  53   0  12   0 0.00  0.0    0  8.0 20 350   M    M   2        27 320
30  77  39  58   5   7   0 0.00  0.0    0  4.7 14 210   M    M   2 8      21 220
31  77  41  59   6   6   0 0.00  0.0    0  7.3 17 160   M    M   1        23 200
=================================================================================
SM 2157 1409       247  21  2.72     0.0 267.6          M      175
=================================================================================
AV 69.6 45.5                                8.6 FASTST   M    M   6    MAX(MPH)
                                  MISC ---->  # 38 310                # 50  300
=================================================================================
NOTES:
# LAST OF SEVERAL OCCURRENCES

COLUMN 17 PEAK WIND IN M.P.H.

PRELIMINARY LOCAL CLIMATOLOGICAL DATA (WS FORM: F-6) , PAGE 2

                                        STATION:  SAN ANTONIO
                                        MONTH:    JANUARY
                                        YEAR:     2017
                                        LATITUDE:   29 31 N
                                        LONGITUDE:  98 28 W

[TEMPERATURE DATA]      [PRECIPITATION DATA]       SYMBOLS USED IN COLUMN 16

AVERAGE MONTHLY: 57.5   TOTAL FOR MONTH:   2.72    1 = FOG OR MIST
DPTR FM NORMAL:   5.7   DPTR FM NORMAL:    0.96    2 = FOG REDUCING VISIBILITY
HIGHEST:    83 ON 21    GRTST 24HR  2.22 ON 15-16      TO 1/4 MILE OR LESS
LOWEST:     19 ON  8                               3 = THUNDER
                        SNOW, ICE PELLETS, HAIL    4 = ICE PELLETS
                        TOTAL MONTH:   0.0 INCH    5 = HAIL
                        GRTST 24HR     0.0         6 = FREEZING RAIN OR DRIZZLE
                        GRTST DEPTH:   0           7 = DUSTSTORM OR SANDSTORM:
                                                       VSBY 1/2 MILE OR LESS
                                                   8 = SMOKE OR HAZE
[NO. OF DAYS WITH]      [WEATHER - DAYS WITH]      9 = BLOWING SNOW
                                                   X = TORNADO
```

Figure 15. NWS Forecast Office Report for San Antonio, January 2017. Source: NWS Austin-San Antonio (2014).

C. CASE 3

Case 3 took place from 25–29 March 2018. This case is unique in that it brought thunderstorms and heavy rain into Texas. At 1200 UTC 26 March 2018, the CBAR in Figure 16 had a length of 4,550 km, a width of 750 km, and a length-width ratio of greater than six. Figure 17 shows the associated WV imagery. The IVT plot in Figure 18 shows a strong moisture signature coming from the ITCZ west of Baja stretching across the southern U.S. Also evident in Figure 18 is a strong signature coming from the Gulf of Mexico, converging with the CBAR in North Central Texas. This type of convergence in Cases 1 and 2 appeared to be overrunning events. In Case 3, however, this looks like a complete convergence of the Baja Express CBAR and the Maya Express AR.

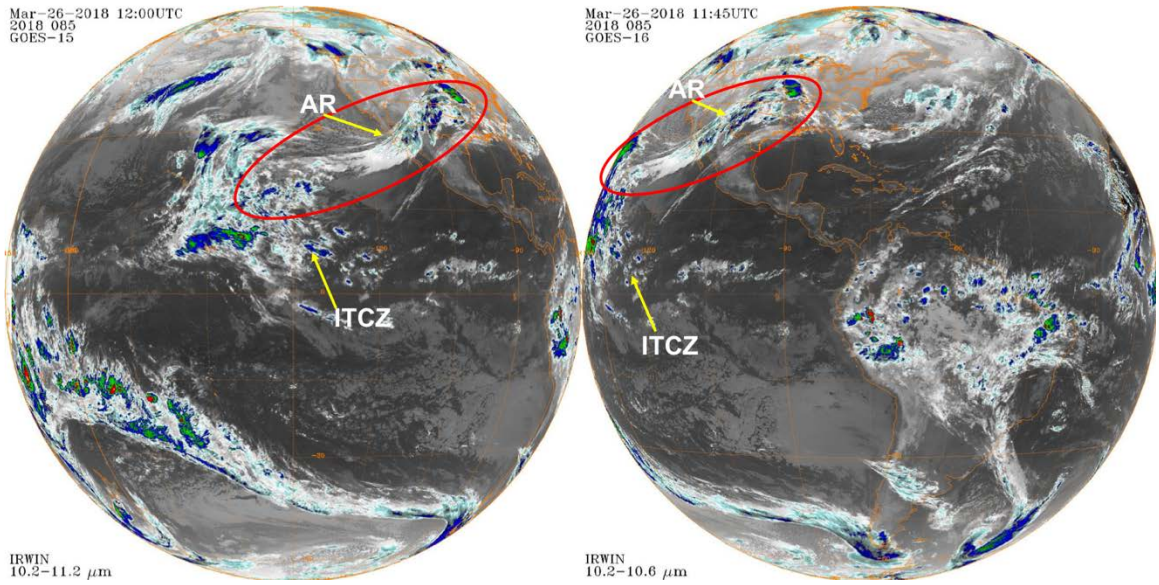

Left: GOES-15 (West) 1200 UTC 26 March 2018; right: GOES-16 (East) 1145 UTC 26 March 2018.

Figure 16. Case 3 GOES IR Imagery. Source: Knapp (2008).

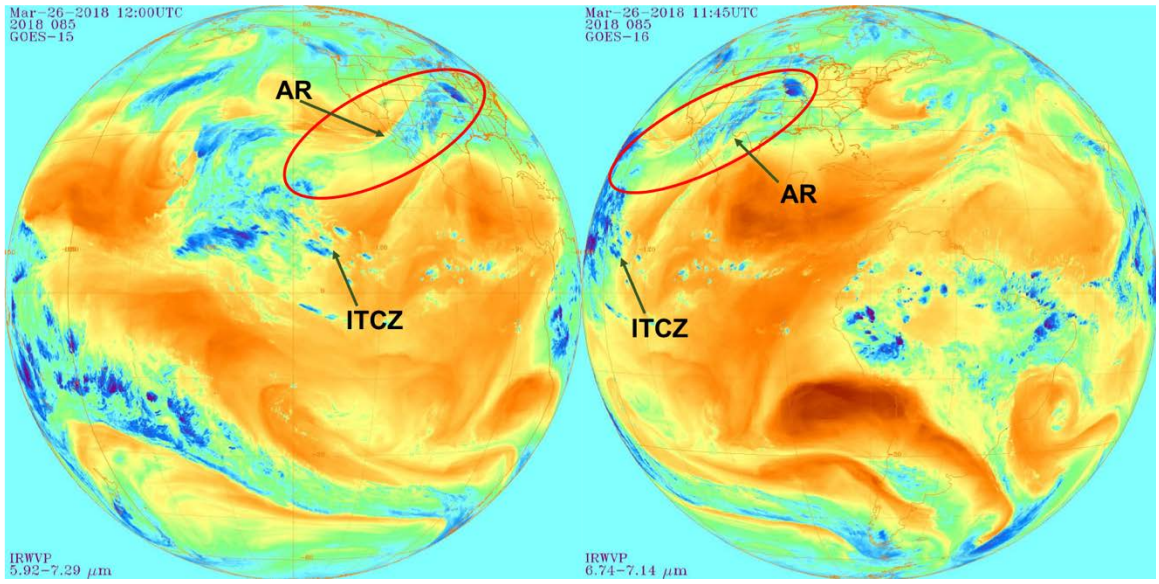

Left: GOES-15 (West) 1200 UTC 26 March 2018; Right: GOES-16 (East) 1145 UTC 26 March 2018.

Figure 17. Case 3 GOES WV Imagery. Source: Knapp (2008).

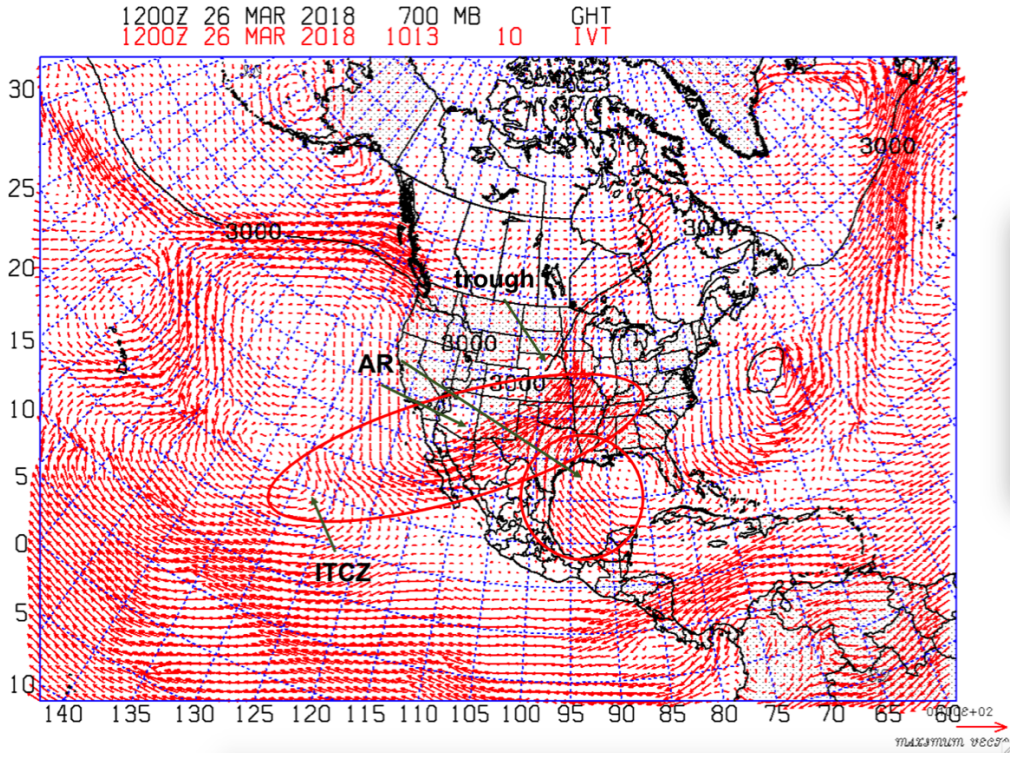

IVT plot for 1200 UTC 26 March 2018. IVT is much stronger along the CBAR path. Strong convergence can be seen in Texas.

Figure 18. Case 3 IVT Plot.

At 1200 UTC 26 March in Figure 19, when the CBAR was well- developed, it follows the subtropical jet pattern and the 5,800 m GPT. Figure 20 shows the 850 mb and 250 mb wind fields with strong vertical wind shear at the point where the two ARs converge over North Central Texas. This is where thunderstorms developed in Texas.

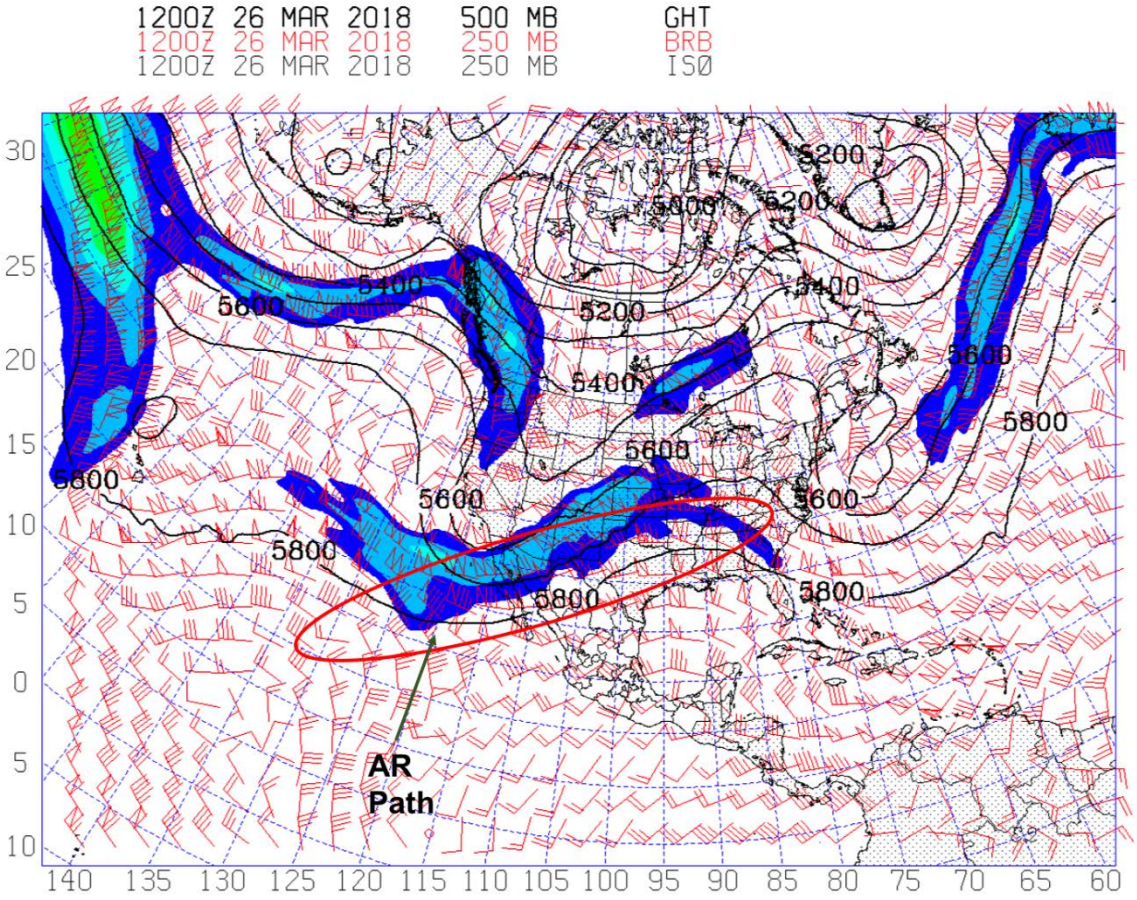

The 500 mb Geopotential Height contours are shown in black, the 250 mb jet stream is shown with the color fill, and the 250 mb wind is shown with red barbs, 1200 UTC 26 March 2018.

Figure 19. Case 3 Upper-Air Chart.

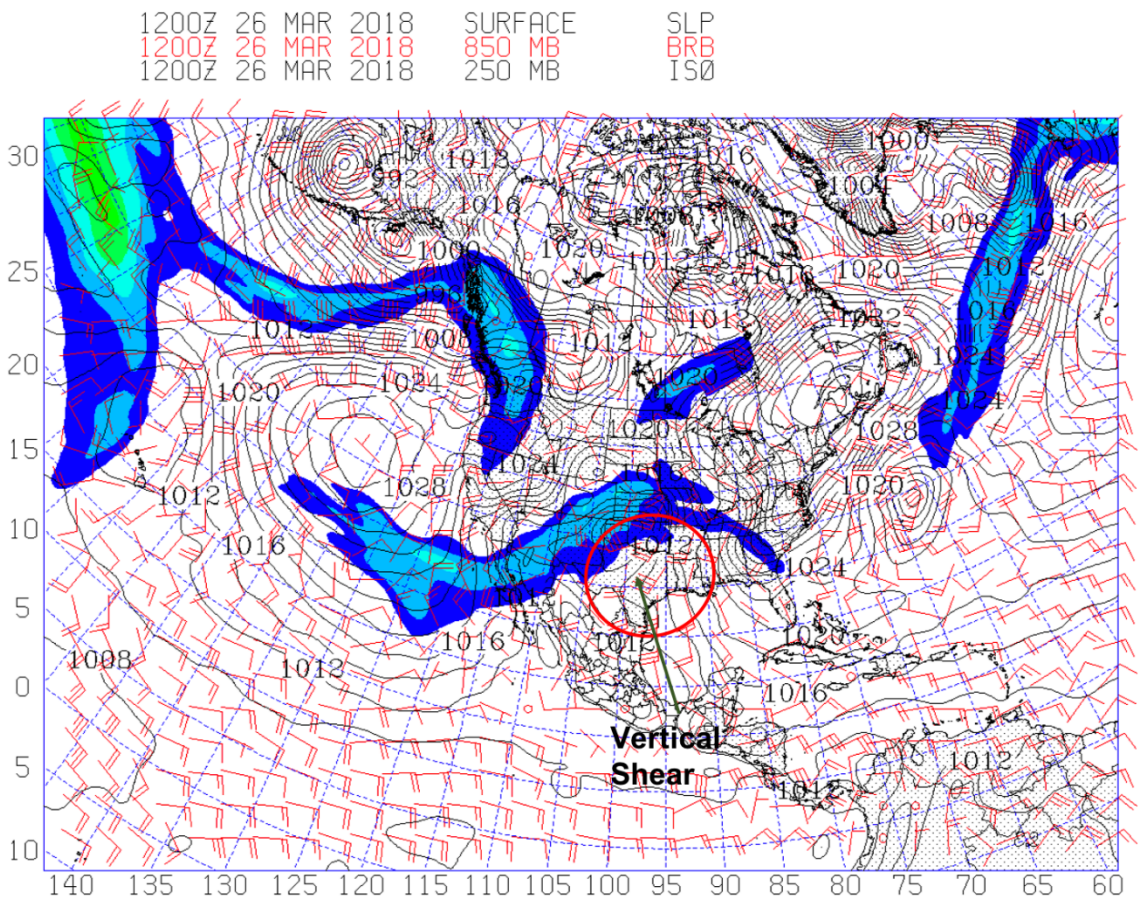

Sea-level pressure is shown in black contours, 850 mb wind with red barbs, and 250 mb jet stream with a color fill, 1200 UTC 26 March 2018.

Figure 20. Case 3 Surface and Upper-Air Chart.

The DFW Forecast Office reported 2.25 in. of precipitation throughout the Case 3 time period, shown in Figure 21. Their observed weather was fog or mist, thunder, smoke or haze and fog reducing visibility to 0.25 miles or less. Figure 22 shows the SAT Forecast Office report, showing 3.69 in. of precipitation with fog or mist and thunder as observed weather. This event recorded the strongest weather and most precipitation of the four cases.

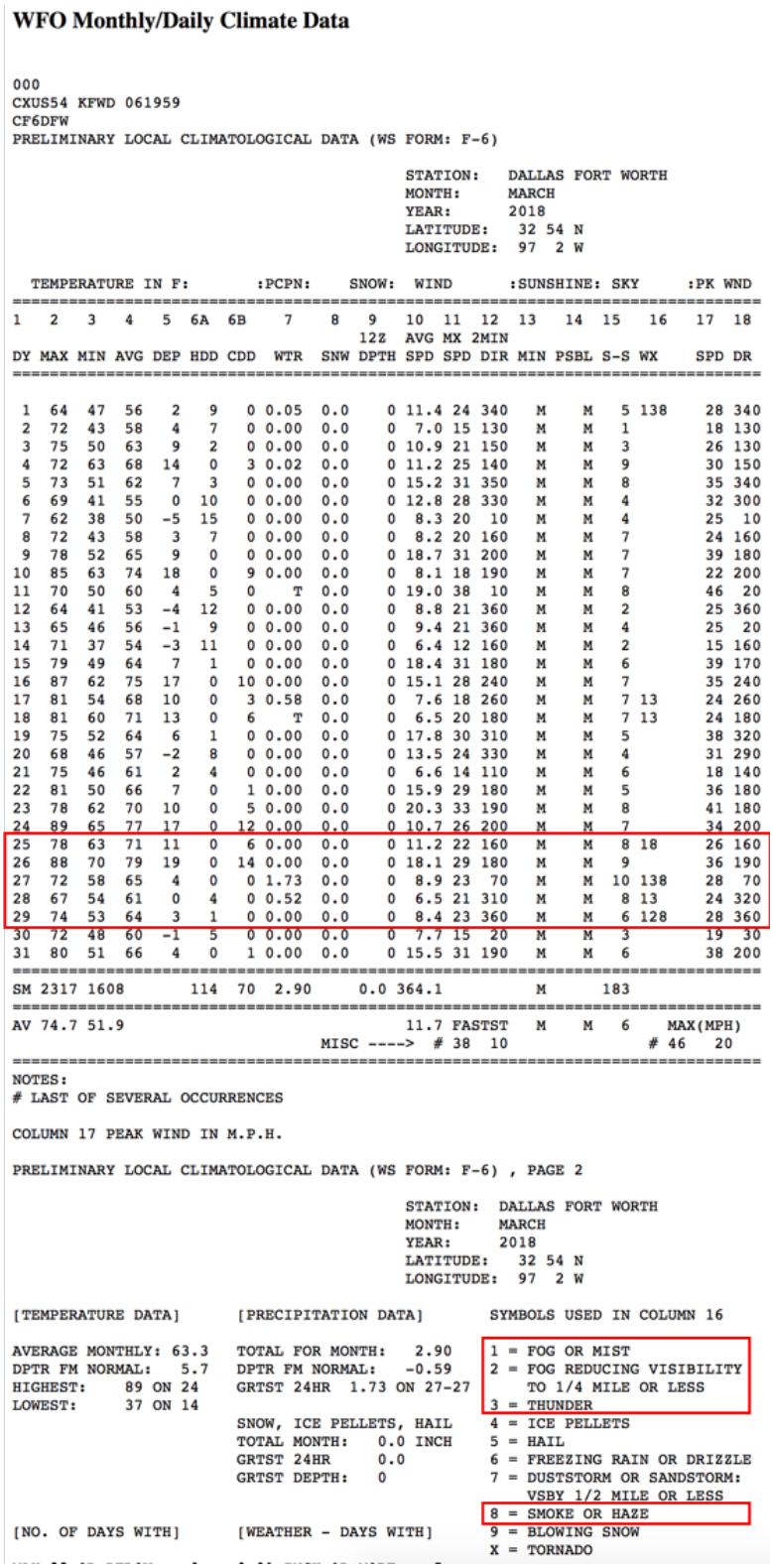

WFO Monthly/Daily Climate Data

000
CXUS54 KFWD 061959
CF6DFW
PRELIMINARY LOCAL CLIMATOLOGICAL DATA (WS FORM: F-6)

STATION: DALLAS FORT WORTH
MONTH: MARCH
YEAR: 2018
LATITUDE: 32 54 N
LONGITUDE: 97 2 W

TEMPERATURE IN F:							:PCPN:		SNOW:	WIND			:SUNSHINE:		SKY		:PK WND	
1	2	3	4	5	6A	6B	7	8	9	10	11	12	13	14	15	16	17	18
									12Z	AVG MX 2MIN								
DY	MAX	MIN	AVG	DEP	HDD	CDD	WTR	SNW	DPTH	SPD	SPD	DIR	MIN	PSBL	S-S	WX	SPD	DR
1	64	47	56	2	9	0	0.05	0.0	0	11.4	24	340	M	M	5	138	28	340
2	72	43	58	4	7	0	0.00	0.0	0	7.0	15	130	M	M	1		18	130
3	75	50	63	9	2	0	0.00	0.0	0	10.9	21	150	M	M	3		26	130
4	72	63	68	14	0	3	0.02	0.0	0	11.2	25	140	M	M	9		30	150
5	73	51	62	7	3	0	0.00	0.0	0	15.2	31	350	M	M	8		35	340
6	69	41	55	0	10	0	0.00	0.0	0	12.8	28	330	M	M	4		32	300
7	62	38	50	-5	15	0	0.00	0.0	0	8.3	20	10	M	M	4		25	10
8	72	43	58	3	7	0	0.00	0.0	0	8.2	20	160	M	M	7		24	160
9	78	52	65	9	0	0	0.00	0.0	0	18.7	31	200	M	M	7		39	180
10	85	63	74	18	0	9	0.00	0.0	0	8.1	18	190	M	M	7		22	200
11	70	50	60	4	5	0	T	0.0	0	19.0	38	10	M	M	8		46	20
12	64	41	53	-4	12	0	0.00	0.0	0	8.8	21	360	M	M	2		25	360
13	65	46	56	-1	9	0	0.00	0.0	0	9.4	21	360	M	M	4		25	20
14	71	37	54	-3	11	0	0.00	0.0	0	6.4	12	160	M	M	2		15	160
15	79	49	64	7	1	0	0.00	0.0	0	18.4	31	180	M	M	6		39	170
16	87	62	75	17	0	10	0.00	0.0	0	15.1	28	240	M	M	7		35	240
17	81	54	68	10	0	3	0.58	0.0	0	7.6	18	260	M	M	7	13	24	260
18	81	60	71	13	0	6	T	0.0	0	6.5	20	180	M	M	7	13	24	180
19	75	52	64	6	1	0	0.00	0.0	0	17.8	30	310	M	M	5		38	320
20	68	46	57	-2	8	0	0.00	0.0	0	13.5	24	330	M	M	4		31	290
21	75	46	61	2	4	0	0.00	0.0	0	6.6	14	110	M	M	6		18	140
22	81	50	66	7	0	1	0.00	0.0	0	15.9	29	180	M	M	5		36	180
23	78	62	70	10	0	5	0.00	0.0	0	20.3	33	190	M	M	8		41	180
24	89	65	77	17	0	12	0.00	0.0	0	10.7	26	200	M	M	7		34	200
25	78	63	71	11	0	6	0.00	0.0	0	11.2	22	160	M	M	8	18	26	160
26	88	70	79	19	0	14	0.00	0.0	0	18.1	29	180	M	M	9		36	190
27	72	58	65	4	0	0	1.73	0.0	0	8.9	23	70	M	M	10	138	28	70
28	67	54	61	0	4	0	0.52	0.0	0	6.5	21	310	M	M	8	13	24	320
29	74	53	64	3	1	0	0.00	0.0	0	8.4	23	360	M	M	6	128	28	360
30	72	48	60	-1	5	0	0.00	0.0	0	7.7	15	20	M	M	3		19	30
31	80	51	66	4	0	1	0.00	0.0	0	15.5	31	190	M	M	6		38	200
SM	2317	1608		114	70	2.90		0.0	364.1				M		183			
AV	74.7	51.9								11.7	FASTST		M	M	6		MAX(MPH)	
									MISC ---->	#	38	10					# 46	20

NOTES:
LAST OF SEVERAL OCCURRENCES

COLUMN 17 PEAK WIND IN M.P.H.

PRELIMINARY LOCAL CLIMATOLOGICAL DATA (WS FORM: F-6) , PAGE 2

STATION: DALLAS FORT WORTH
MONTH: MARCH
YEAR: 2018
LATITUDE: 32 54 N
LONGITUDE: 97 2 W

[TEMPERATURE DATA]
AVERAGE MONTHLY: 63.3
DPTR FM NORMAL: 5.7
HIGHEST: 89 ON 24
LOWEST: 37 ON 14

[PRECIPITATION DATA]
TOTAL FOR MONTH: 2.90
DPTR FM NORMAL: -0.59
GRTST 24HR 1.73 ON 27-27

SNOW, ICE PELLETS, HAIL
TOTAL MONTH: 0.0 INCH
GRTST 24HR 0.0
GRTST DEPTH: 0

[NO. OF DAYS WITH]
[WEATHER - DAYS WITH]

SYMBOLS USED IN COLUMN 16
1 = FOG OR MIST
2 = FOG REDUCING VISIBILITY TO 1/4 MILE OR LESS
3 = THUNDER
4 = ICE PELLETS
5 = HAIL
6 = FREEZING RAIN OR DRIZZLE
7 = DUSTSTORM OR SANDSTORM: VSBY 1/2 MILE OR LESS
8 = SMOKE OR HAZE
9 = BLOWING SNOW
X = TORNADO

Figure 21. NWS Forecast Office Report for Dallas-Fort Worth, March 2018. Source: NWS Dallas-Fort Worth (2014).

WFO Monthly/Daily Climate Data

396
CXUS54 KEWX 010910
CF6SAT
PRELIMINARY LOCAL CLIMATOLOGICAL DATA (WS FORM: F-6)

STATION: SAN ANTONIO
MONTH: MARCH
YEAR: 2018
LATITUDE: 29 31 N
LONGITUDE: 98 28 W

TEMPERATURE IN F:							:PCPN:		SNOW:	WIND				:SUNSHINE:		SKY		:PK WND	
1	2	3	4	5	6A	6B	7	8	9 12Z	10 AVG	11 MX	12 2MIN	13	14	15	16	17	18	
DY	MAX	MIN	AVG	DEP	HDD	CDD	WTR	SNW	DPTH	SPD	SPD	DIR	MIN	PSBL	S-S	WX	SPD	DR	
1	75	54	65	6	0	0	T	0.0	0	10.9	29	340	M	M	6		38	350	
2	74	51	63	4	2	0	0.00	0.0	0	7.1	14	130	M	M	4		17	140	
3	72	55	64	5	1	0	0.07	0.0	0	7.8	17	140	M	M	9	18	19	130	
4	80	65	73	14	0	8	0.00	0.0	0	13.3	22	140	M	M	9	1	27	170	
5	82	63	73	13	0	8	T	0.0	0	8.1	20	10	M	M	9		24	10	
6	74	56	65	5	0	0	0.00	0.0	0	9.2	17	50	M	M	7		24	50	
7	68	46	57	-3	8	0	0.00	0.0	0	5.9	14	10	M	M	3		19	10	
8	69	46	58	-2	7	0	0.00	0.0	0	8.9	22	160	M	M	7		25	160	
9	71	52	62	2	3	0	T	0.0	0	11.1	21	200	M	M	9	1	25	190	
10	89	64	77	16	0	12	0.00	0.0	0	8.5	16	170	M	M	6	1	22	190	
11	70	57	64	3	1	0	0.00	0.0	0	11.4	26	20	M	M	6	1	36	10	
12	68	48	58	-3	7	0	0.00	0.0	0	7.9	20	10	M	M	7		26	10	
13	70	47	59	-3	6	0	0.00	0.0	0	5.5	14	70	M	M	7		17	70	
14	70	48	59	-3	6	0	0.00	0.0	0	7.3	15	170	M	M	7		24	130	
15	70	50	60	-2	5	0	T	0.0	0	11.0	22	180	M	M	8	12	26	200	
16	87	62	75	13	0	10	T	0.0	0	6.5	15	160	M	M	8	12	19	50	
17	85	64	75	13	0	10	0.00	0.0	0	9.3	22	140	M	M	8	1	26	140	
18	84	67	76	13	0	11	0.26	T	0	5.2	26	250	M	M	7	1358	32	250	
19	84	59	72	9	0	7	0.00	0.0	0	9.9	22	340	M	M	5	1	29	300	
20	77	52	65	2	0	0	0.00	0.0	0	9.2	23	350	M	M	2		31	10	
21	77	45	61	-2	4	0	0.00	0.0	0	9.7	23	140	M	M	3		27	150	
22	80	52	66	2	0	1	0.00	0.0	0	11.5	25	130	M	M	6		30	130	
23	80	62	71	7	0	6	0.00	0.0	0	13.3	23	140	M	M	9		29	150	
24	80	67	74	10	0	9	0.00	0.0	0	6.1	15	170	M	M	9		19	170	
25	79	68	74	10	0	9	0.00	0.0	0	7.6	21	130	M	M	10	1	25	120	
26	87	68	78	14	0	13	0.00	0.0	0	15.3	28	140	M	M	8	1	39	140	
27	81	62	72	7	0	7	0.18	0.0	0	11.7	20	10	M	M	9	13	26	120	
28	74	60	67	2	0	2	3.51	0.0	0	7.4	25	290	M	M	9	13	30	290	
29	81	55	68	3	0	3	0.00	0.0	0	8.6	16	350	M	M	5	1	23	220	
30	74	56	65	0	0	0	0.00	0.0	0	9.2	17	40	M	M	0		23	50	
31	81	61	71	5	0	6	0.00	0.0	0	12.7	21	130	M	M	7		27	190	
SM	2393	1762			50	122	4.02	T		287.1			M		209				
AV	77.2	56.8								9.3	FASTST		M	M	7	MAX(MPH)			
									MISC ---->	# 29	340					# 39 140			

NOTES:
LAST OF SEVERAL OCCURRENCES

COLUMN 17 PEAK WIND IN M.P.H.

PRELIMINARY LOCAL CLIMATOLOGICAL DATA (WS FORM: F-6) , PAGE 2

STATION: SAN ANTONIO
MONTH: MARCH
YEAR: 2018
LATITUDE: 29 31 N
LONGITUDE: 98 28 W

[TEMPERATURE DATA]

AVERAGE MONTHLY: 67.0
DPTR FM NORMAL: 4.8
HIGHEST: 89 ON 10
LOWEST: 45 ON 21

[NO. OF DAYS WITH]

[PRECIPITATION DATA]

TOTAL FOR MONTH: 4.02
DPTR FM NORMAL: 1.71
GRTST 24HR 3.51 ON 28-28

SNOW, ICE PELLETS, HAIL
TOTAL MONTH: T
GRTST 24HR T ON 18-18
GRTST DEPTH: 0

[WEATHER - DAYS WITH]

SYMBOLS USED IN COLUMN 16

1 = FOG OR MIST
2 = FOG REDUCING VISIBILITY TO 1/4 MILE OR LESS
3 = THUNDER
4 = ICE PELLETS
5 = HAIL
6 = FREEZING RAIN OR DRIZZLE
7 = DUSTSTORM OR SANDSTORM: VSBY 1/2 MILE OR LESS
8 = SMOKE OR HAZE
9 = BLOWING SNOW
X = TORNADO

Figure 22. NWS Forecast Office Report for San Antonio, March 2018. Source: NWS Austin-San Antonio (2014).

D. CASE 4

Case 4 took place from 8–13 February 2019. This case showed arguably the longest and most pronounced CBAR signature, beginning in the ITCZ 1,100 km south of Hawaii, stretching through Ohio. Its length was 7,565 km, its width was 805 km, and its length-width ratio was greater than nine. On 1800 UTC 11 February, when the CBAR was well-developed, the IR imagery showed an abundant amount of moisture at the ITCZ being carried toward Central America, entering at Baja, and pushing through Mexico into Texas and up through Ohio as shown in Figure 23. Figure 24 shows this same moisture signature following the same path for the WV imagery. The IVT plot in Figure 25 mirrors this moisture signature, showing elevated IVT levels along the CBAR path. There once again is a Gulf AR present, with convergence along the Texas Coast. This appears to be another overrunning of cool Pacific moisture over warm Gulf moisture.

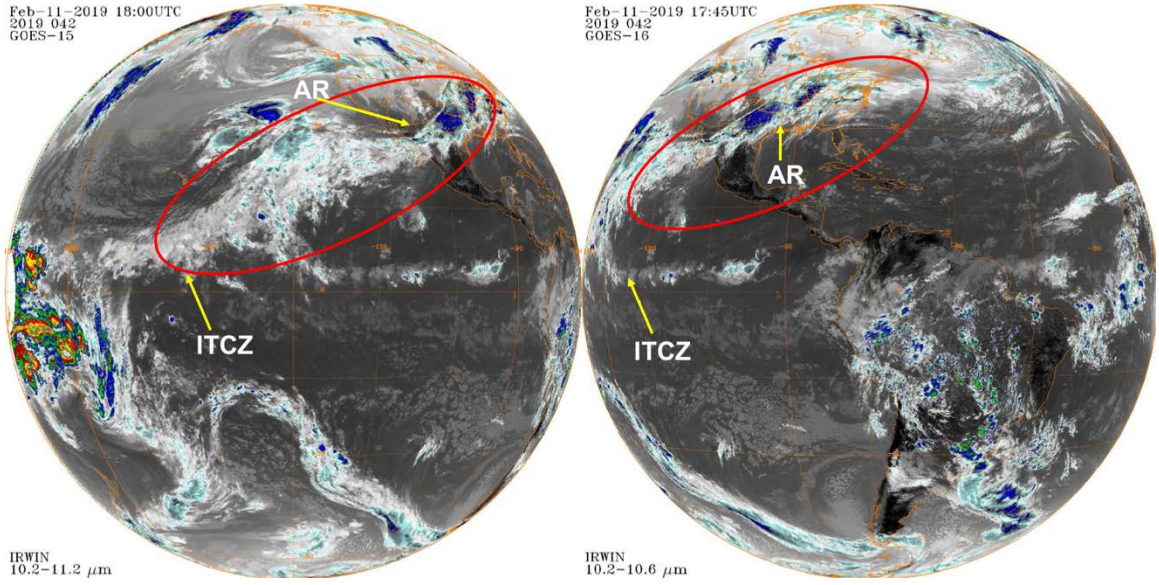

Left: GOES-15 (West) 1800 UTC 11 February 2019; right: GOES-16 (East) 1745 UTC 11 February 2019.

Figure 23. Case 4 GOES IR Imagery. Source: Knapp (2008).

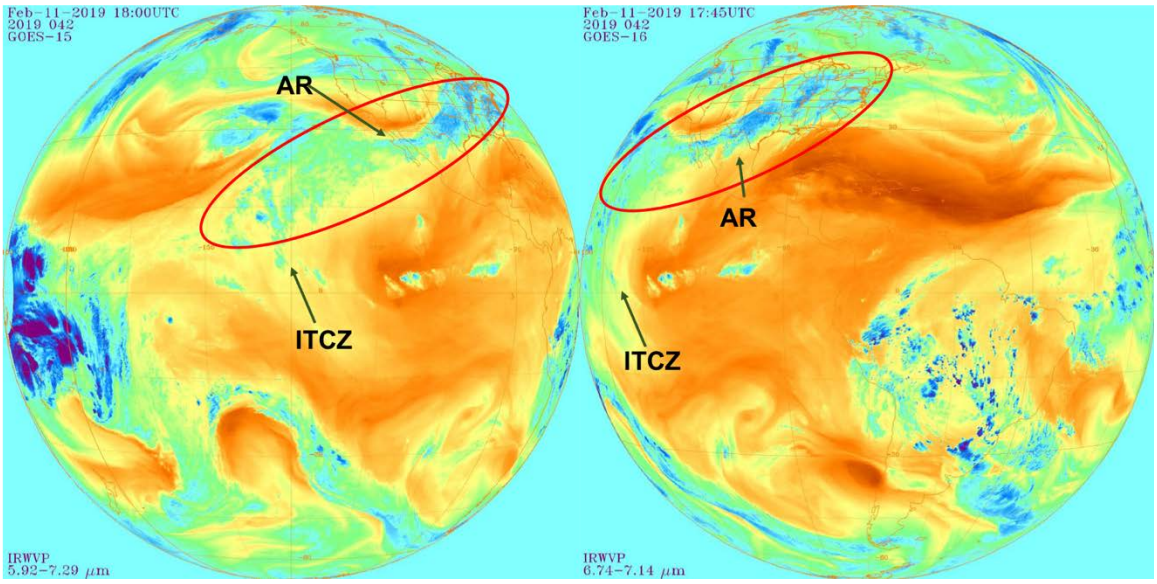

Left: GOES-15 (West) 1800 UTC 11 February 2019; right: GOES-16 (East) 1745 UTC 11 February 2019.

Figure 24. Case 4 GOES WV Imagery. Source: Knapp (2008).

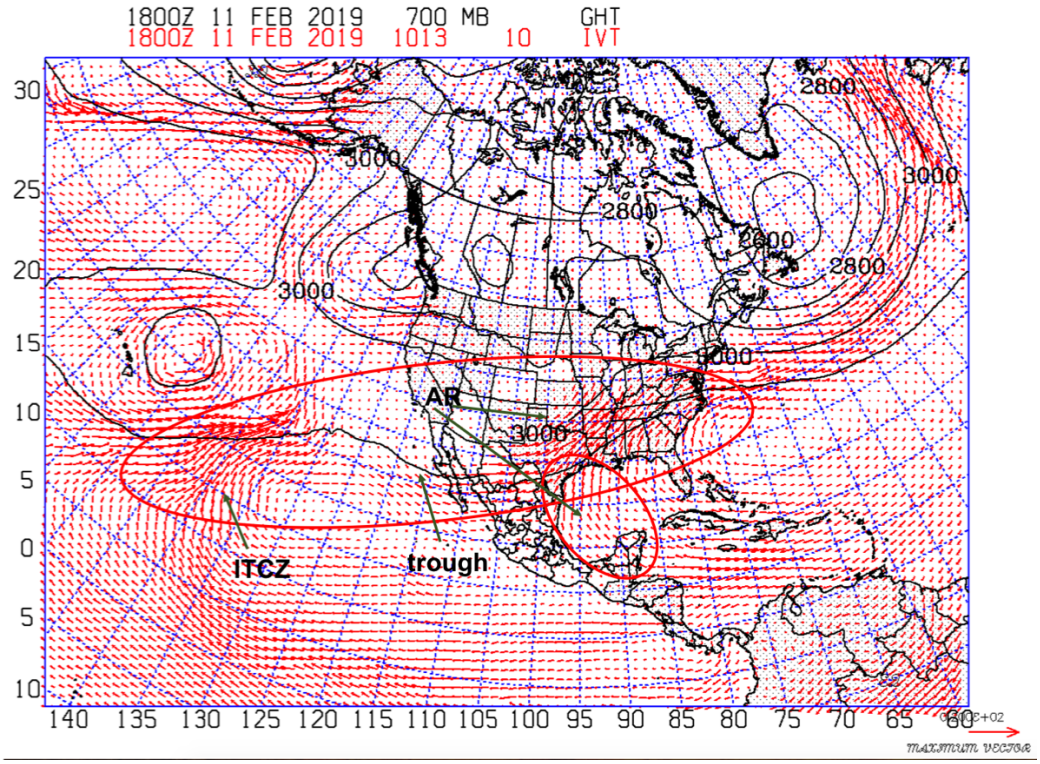

IVT plot for 1800 UTC 11 February 2019. High IVT values begin near a low close to Hawaii and continue through the U.S. and out into the Atlantic.

Figure 25. Case 4 IVT Plot.

This CBAR also follows the 250 mb subtropical jet and the 5,800 m geopotential height contour shown in Figure 26. Strong vertical wind shear does not appear to be present when looking at the 250 mb and 850 mb wind fields except over the Texas Coast shown in Figure 27.

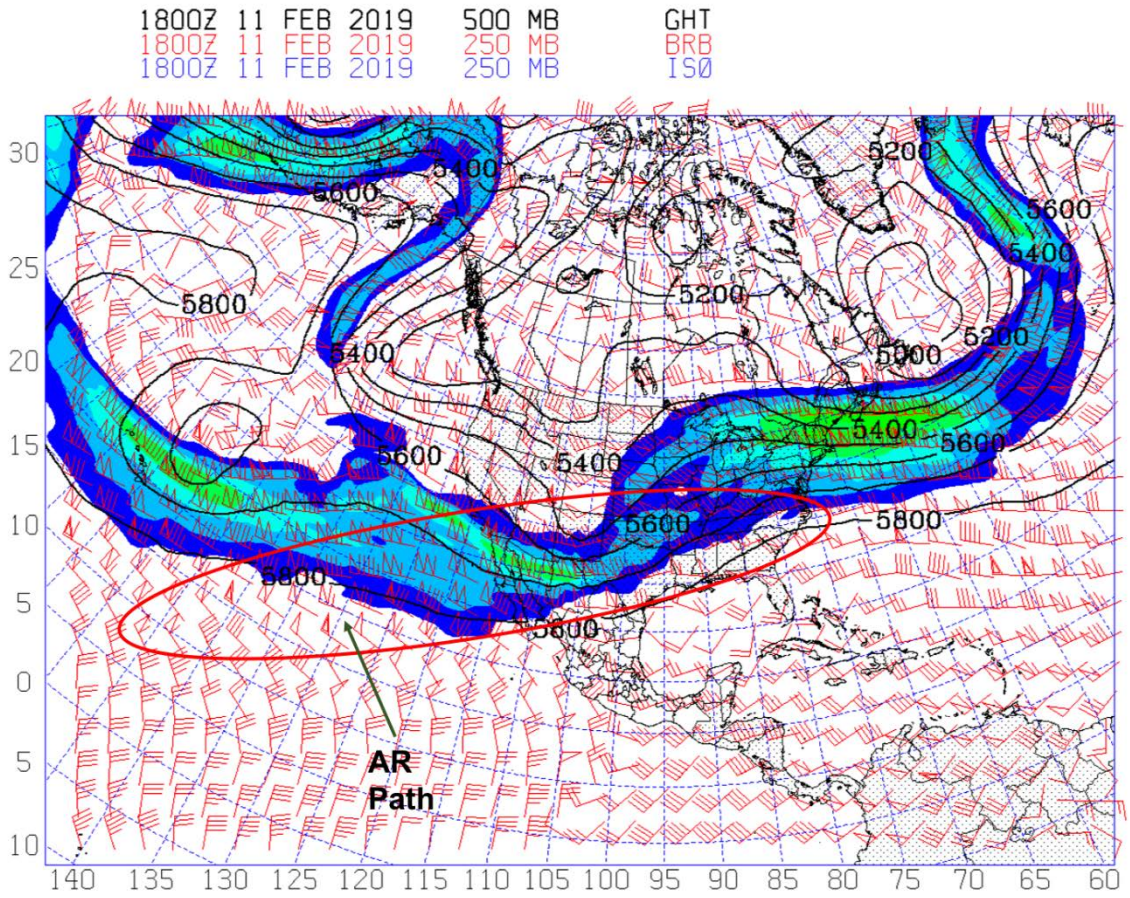

The 500 mb Geopotential Height contours are shown in black, the 250 mb jet stream is shown with the color fill, and the 250 mb wind is shown with red barbs, 1800 UTC 11 February 2019.

Figure 26. Case 4 Upper-Air Chart.

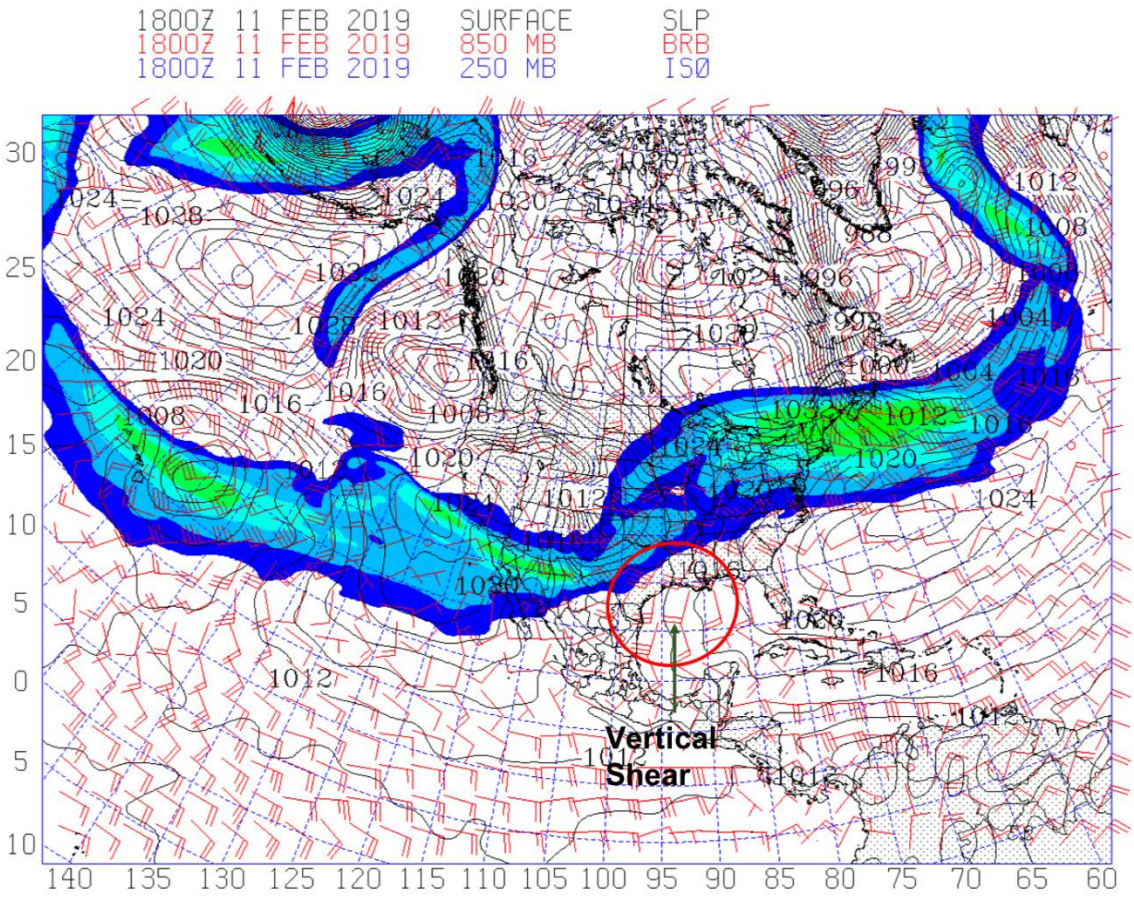

Sea-level pressure is shown in black contours, 850 mb wind with red barbs, and 250 mb jet stream with a color fill, 1800 UTC 11 February 2019.

Figure 27. Case 4 Surface and Upper-Air Chart.

As this appears to be an overrunning event, the stations in Texas reported precipitation as well as adverse effects. Shown in Figure 28, the DFW Forecast Office reported 0.55 in. of precipitation with fog or mist, while Figure 29 shows the SAT Forecast Office reported 0.30 in. of precipitation with fog or mist and ice pellets.

WFO Monthly/Daily Climate Data

```
000
CXUS54 KFWD 201840
CF6DFW
PRELIMINARY LOCAL CLIMATOLOGICAL DATA (WS FORM: F-6)

                                        STATION:   DALLAS FORT WORTH
                                        MONTH:     FEBRUARY
                                        YEAR:      2019
                                        LATITUDE:   32 54 N
                                        LONGITUDE:  97  2 W

  TEMPERATURE IN F:        :PCPN:    SNOW:  WIND       :SUNSHINE: SKY      :PK WND
=================================================================================
1   2   3   4   5  6A  6B    7    8   9   10  11  12  13   14  15   16   17  18
                                     12Z  AVG MX 2MIN
DY MAX MIN AVG DEP HDD CDD  WTR  SNW DPTH SPD SPD DIR MIN PSBL S-S WX    SPD DR
=================================================================================

 1  62  52  57  10   8   0 0.03  0.0    0  7.1 14 160   M    M   8 1      16 160
 2  66  53  60  13   5   0    T  0.0    0  8.1 14 160   M    M   9 18     17 150
 3  72  60  66  18   0   1    T  0.0    0 13.9 26 190   M    M   9 1      34 190
 4  80  58  69  21   0   4 0.00  0.0    0 11.6 18 200   M    M   4 1      22 200
 5  78  60  69  21   0   4 0.00  0.0    0 13.4 26 180   M    M   8 18     30 180
 6  77  68  73  25   0   8    T  0.0    0 15.0 24 170   M    M  10 18     31 180
 7  71  29  50   2  15   0 0.24  0.0    0 19.2 43 270   M    M   8 13     58 250
 8  36  23  30 -18  35   0 0.00  0.0    0 10.7 20  20   M    M   7        27  30
 9  39  34  37 -12  28   0 0.11  0.0    0  7.2 13 140   M    M  10 1      16 130
10  44  35  40  -9  25   0 0.10  0.0    0  5.4 15 150   M    M  10 1      18 150
11  59  44  52   3  13   0 0.34  0.0    0  9.8 21 250   M    M  10 1      26 240
12  57  39  48  -1  17   0 0.00  0.0    0 14.9 38 330   M    M   1        44 330
13  62  35  49   0  16   0 0.00  0.0    0 15.0 31 200   M    M   6        38 200
14  78  50  64  14   1   0 0.00  0.0    0 15.8 31 210   M    M   7        37 210
15  73  36  55   5  10   0 0.00  0.0    0  9.7 24 350   M    M   7 1      28 350
16  42  33  38 -12  27   0 0.01  0.0    0  7.0 20  20   M    M  10 128    23  10
17  53  38  46  -4  19   0    T  0.0    0 12.0 26 350   M    M   8 18     30 350
18  43  32  38 -12  27   0 0.00  0.0    0 12.7 21  30   M    M   9        25  20
19  39  35  37 -14  28   0 0.35  0.0    0  9.1 18  60   M    M  10 138    23  80
20  58  37  48  -3  17   0 0.00  0.0    0  7.8 17 310   M    M   8        21 280
21  52  39  46  -5  19   0 0.01  0.0    0  8.3 18 110   M    M   9 13     24 110
22  49  45  47  -5  18   0 0.08  0.0    0  7.1 23 110   M    M  10 13     29 120
23  69  47  58   6   7   0 0.01  0.0    0 16.6 33 300   M    M   7 1278   42 300
24  59  36  48  -4  17   0 0.00  0.0    0  9.0 20 330   M    M   1        25 320
25  65  37  51  -1  14   0 0.00  0.0    0  9.7 22 140   M    M   4        27 150
26  64  48  56   3   9   0    T  0.0    0  8.8 14 120   M    M   9 12     17 140
27  62  31  47  -6  18   0 0.01  0.0    0 10.8 23 340   M    M  10 12     29 340
28  37  29  33 -20  32   0    T  0.0    0 11.0 20 350   M    M   9 168    23 340
=================================================================================
SM 1646 1163       425  17  1.29     0.0 306.7          M      218
=================================================================================
AV 58.8 41.5                            11.0 FASTST   M    M   8    MAX(MPH)
                                  MISC ---->  # 43 270              # 58  250
=================================================================================
NOTES:
# LAST OF SEVERAL OCCURRENCES

COLUMN 17 PEAK WIND IN M.P.H.

PRELIMINARY LOCAL CLIMATOLOGICAL DATA (WS FORM: F-6) , PAGE 2

                                        STATION:  DALLAS FORT WORTH
                                        MONTH:    FEBRUARY
                                        YEAR:     2019
                                        LATITUDE:   32 54 N
                                        LONGITUDE:  97  2 W

[TEMPERATURE DATA]      [PRECIPITATION DATA]       SYMBOLS USED IN COLUMN 16

AVERAGE MONTHLY: 50.2   TOTAL FOR MONTH:   1.29    1 = FOG OR MIST
DPTR FM NORMAL:   0.3   DPTR FM NORMAL:   -1.37    2 = FOG REDUCING VISIBILITY
HIGHEST:     80 ON  4   GRTST 24HR  0.35 ON 19-19      TO 1/4 MILE OR LESS
LOWEST:      23 ON  8                              3 = THUNDER
                        SNOW, ICE PELLETS, HAIL    4 = ICE PELLETS
                        TOTAL MONTH:    0.0 INCH   5 = HAIL
                        GRTST 24HR      0.0        6 = FREEZING RAIN OR DRIZZLE
                        GRTST DEPTH:    0          7 = DUSTSTORM OR SANDSTORM:
                                                       VSBY 1/2 MILE OR LESS
                                                   8 = SMOKE OR HAZE
[NO. OF DAYS WITH]      [WEATHER - DAYS WITH]      9 = BLOWING SNOW
                                                   X = TORNADO
```

Figure 28. NWS Forecast Office Report for Dallas-Fort Worth, February 2019. Source: NWS Dallas-Fort Worth (2014).

WFO Monthly/Daily Climate Data

```
000
CXUS54 KEWX 251445
CF6SAT
PRELIMINARY LOCAL CLIMATOLOGICAL DATA (WS FORM: F-6)

                                        STATION:   SAN ANTONIO
                                        MONTH:     FEBRUARY
                                        YEAR:      2019
                                        LATITUDE:   29 31 N
                                        LONGITUDE:  98 28 W

  TEMPERATURE IN F:        :PCPN:    SNOW:  WIND      :SUNSHINE: SKY     :PK WND
==============================================================================
1   2   3   4   5  6A  6B    7    8   9   10  11  12  13   14  15   16   17  18
                                     12Z  AVG MX 2MIN
DY MAX MIN AVG DEP HDD CDD  WTR  SNW DPTH SPD SPD DIR MIN PSBL S-S WX    SPD DR
==============================================================================

 1  67  57  62   9   3   0    T  0.0    0  4.8 12 100   M    M  10        14  80
 2  65  59  62   9   3   0    T  0.0    0  5.9 14 120   M    M  10 12     16 130
 3  75  62  69  16   0   4 0.01  0.0    0  7.0 15 180   M    M   8 1      20 220
 4  72  64  68  14   0   3    T  0.0    0  5.9 12 140   M    M  10 12     14 180
 5  76  66  71  17   0   6 0.01  0.0    0  7.9 16 150   M    M   9 128    20 170
 6  76  67  72  18   0   7    T  0.0    0  9.5 22 130   M    M  10 128    26 130
 7  70  43  57   3   8   0    T  0.0    0 12.9 25 130   M    M  10 1      31 130
 8  43  37  40 -14  25   0    T    T    0 12.2 23  10   M    M  10 4      33  20
 9  40  34  37 -17  28   0 0.19  0.0    0  7.3 13  40   M    M  10 1      16  40
10  51  38  45 -10  20   0 0.10  0.0    0  4.4 10 100   M    M  10 1      12 100
11  60  50  55   0  10   0 0.01  0.0    0  4.4 16  80   M    M  10 1      21  80
12  66  41  54  -1  11   0 0.00  0.0    0  8.3 21 340   M    M   4        25 340
13  65  32  49  -6  16   0 0.00  0.0    0  8.1 18 160   M    M   5        25 160
14  70  50  60   5   5   0 0.00  0.0    0  6.8 20 210   M    M   7        26 220
15  86  46  66  10   0   1 0.00  0.0    0  5.8 15 200   M    M   7        19 190
16  65  51  58   2   7   0 0.00  0.0    0  7.5 16  10   M    M   7 1      22  40
17  71  50  61   5   4   0    T  0.0    0 11.0 20  10   M    M   8 1      25  10
18  63  44  54  -2  11   0 0.00  0.0    0 11.8 21  60   M    M   8        26  60
19  47  42  45 -11  20   0 0.07  0.0    0 10.0 15 360   M    M  10 1      22 340
20  68  36  52  -5  13   0    T  0.0    0  4.1 14 290   M    M   5        22 360
21  58  47  53  -4  12   0 0.00  0.0    0  7.0 14  80   M    M   9        18  70
22  65  51  58   1   7   0 0.01  0.0    0  4.8 14 110   M    M  10 12     17  50
23  75  51  63   6   2   0 0.03  0.0    0  9.3 24 310   M    M   8 1      32 310
24  66  47  57  -1   8   0 0.00  0.0    0  8.3 17  10   M    M   3        22 360
25  67  47  57  -1   8   0 0.00  0.0    0  9.3 20 140   M    M   6        24 150
26  73  56  65   7   0   0 0.03  0.0    0  5.3 14 120   M    M   8 12     17 120
27  79  61  70  12   0   5    T  0.0    0  4.3 15 140   M    M   7 12     17 140
28  68  46  57  -1   8   0 0.01  0.0    0  9.2 21  10   M    M  10 1      25  10
==============================================================================
SM 1847 1375       229  26  0.47    T    213.1          M      229
==============================================================================
AV 66.0 49.1                              7.6 FASTST   M    M   8    MAX(MPH)
                                  MISC ----->  # 25 130              # 33   20
==============================================================================
NOTES:
# LAST OF SEVERAL OCCURRENCES

COLUMN 17 PEAK WIND IN M.P.H.

PRELIMINARY LOCAL CLIMATOLOGICAL DATA (WS FORM: F-6) , PAGE 2

                                        STATION:  SAN ANTONIO
                                        MONTH:    FEBRUARY
                                        YEAR:     2019
                                        LATITUDE:   29 31 N
                                        LONGITUDE:  98 28 W

[TEMPERATURE DATA]      [PRECIPITATION DATA]       SYMBOLS USED IN COLUMN 16

AVERAGE MONTHLY: 57.5   TOTAL FOR MONTH:   0.47    1 = FOG OR MIST
DPTR FM NORMAL:   1.9   DPTR FM NORMAL:   -1.32    2 = FOG REDUCING VISIBILITY
HIGHEST:     86 ON 15   GRTST 24HR  0.19 ON  9- 9      TO 1/4 MILE OR LESS
LOWEST:      32 ON 13                              3 = THUNDER
                        SNOW, ICE PELLETS, HAIL    4 = ICE PELLETS
                        TOTAL MONTH:    T          5 = HAIL
                        GRTST 24HR    T  ON  8- 8  6 = FREEZING RAIN OR DRIZZLE
                        GRTST DEPTH:   0           7 = DUSTSTORM OR SANDSTORM:
                                                       VSBY 1/2 MILE OR LESS
                                                   8 = SMOKE OR HAZE
[NO. OF DAYS WITH]      [WEATHER - DAYS WITH]      9 = BLOWING SNOW
                                                   X = TORNADO
```

Figure 29. NWS Forecast Office Report for San Antonio, February 2019. Source: NWS Austin-San Antonio (2014).

E. CASE STUDY SUMMARY

All four cases show ARs emerging from a convergent boundary, namely the ITCZ. These CBARs travel from the ITCZ into Mexico, penetrate through the south-central U.S. into Texas, and propagate out of the eastern U.S. All cases exceed the standard length-width ratio of two, and all seem to follow the subtropical jet stream pattern. In contrast to events such as the Pineapple Express and Maya Express AR events, these case studies appear to suggest a convergence of two ARs. Each case shows a moisture source from the Gulf (possibly the Maya Express AR) which converges with the Pacific CBAR. This is likely why fog and mist are observed in all cases. Vertical wind shear appears in Cases 1 and 3, which may be why Case 1 had a report of freezing rain and Case 3 had a report of thunderstorms. The next chapter will examine the evolution of each case and analyze their effects on weather.

IV. RESULTS

These four case studies were chosen as examples of systems that may exhibit characteristics of CBARs that are different from the traditional AR systems. In each case, the AR originates from the ITCZ and propagates as an AR coherently over time, and they each have a length longer than its width.

The following results will show that CBARs tend to validate the proposed hypotheses: 1) CBARs form as a result of an associated convergent boundary (in this study, the ITCZ); 2) CBARs form and evolve independent of extratropical cyclones; and 3) CBARs have a significant impact on inland weather.

A. CASE 1

Figure 30 shows the GOES IR imagery at specific times in the evolution of the CBAR. At the onset at 0600 UTC 12 February 2015, a new moisture source is originating from the ITCZ at 18°N-120°W. This is also evident in the IVT plot for that time, which shows a swath of IVT stretching to 38°N-77°W, as seen in Figure 31. The total column integrated water content (TQV) is also shown in Figure 31. Higher TQV values can be seen where the IVT is elevated, confirming the satellite imagery. By 1800 UTC, this moisture is being pulled up through Baja into northern Mexico. By 1145 UTC 23 February, the Pacific moisture tap is weak, but the IVT at 1200 UTC continues through the southwestern U.S. into Texas. By 1745 UTC 25 February, the moisture tap from the Pacific is cut off, and the transport has moved inland between 33–36°N and 94–75°W.

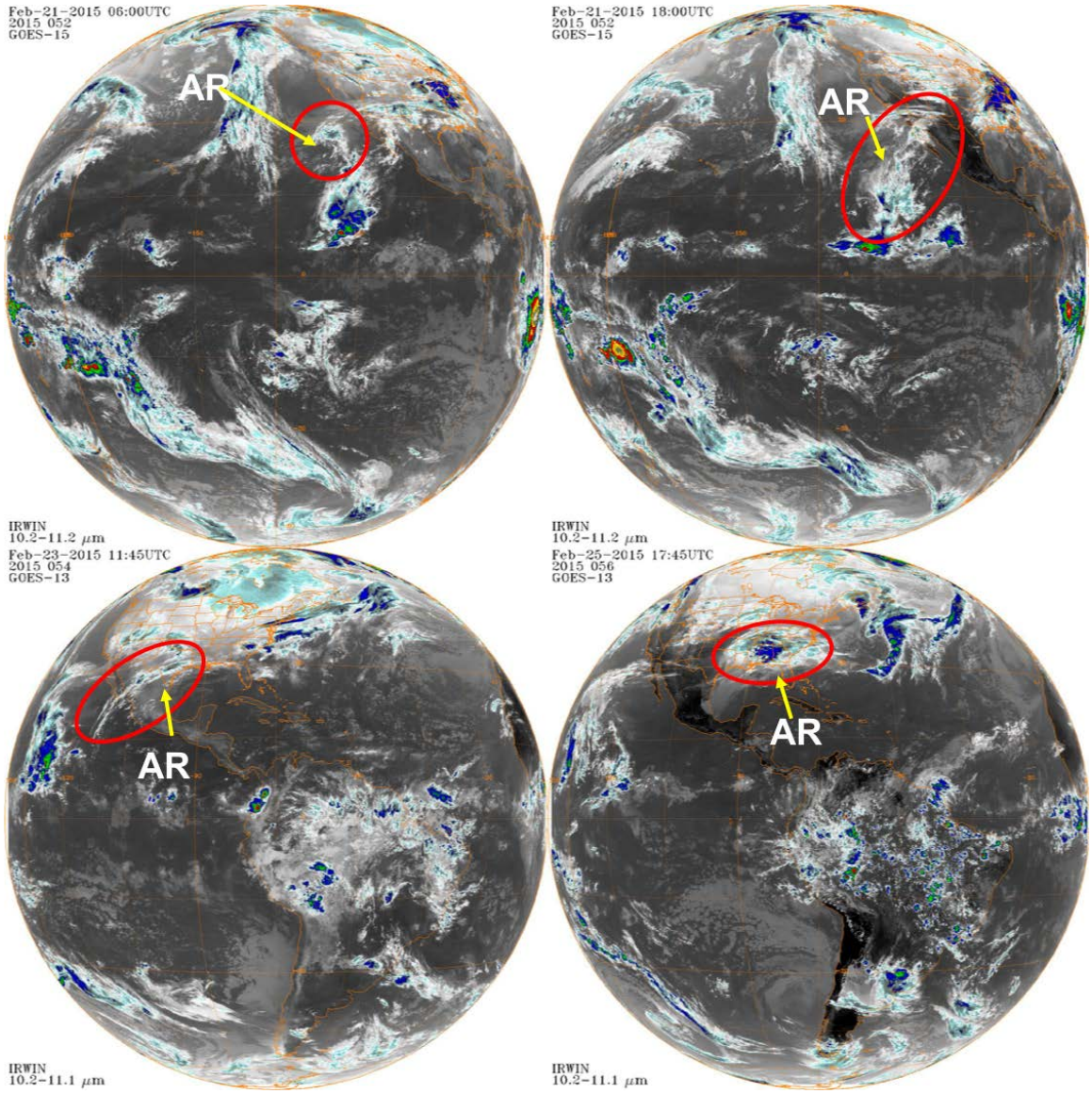

Upper-left: 0600 UTC 21 February 2015; upper-right: 1800 UTC 21 February 2015; lower-left: 1145 UTC 23 February 2015; lower-right: 1745 UTC 25 February 2015.

Figure 30. Case 1 CBAR Satellite Evolution. Source: Knapp (2008).

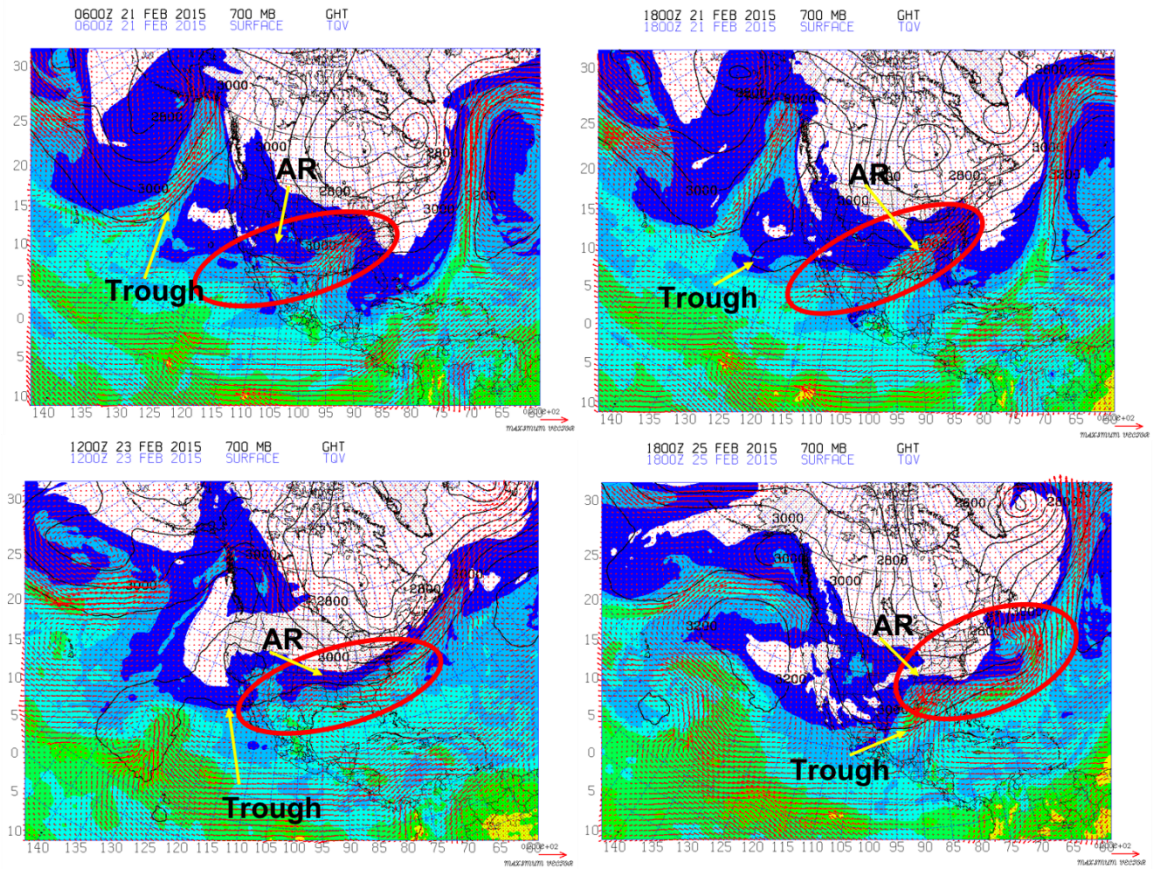

IVT is shown with red barbs, the 700 mb GPT is shown with black contours, and TQV is shown with a color fill. Upper-left: 0600 UTC 21 February 2015; upper-right: 1800 UTC 21 February 2015; lower-left: 1200 UTC 23 February 2015; lower-right: 1800 UTC 25 February 2015.

Figure 31. Case 1 CBAR IVT Evolution.

Of note, the water vapor transport moves in a coherent fashion throughout the case period, typical of an AR. This case emerged from a convergent boundary, as moisture was transported from the surface to the upper troposphere by way of convection in the ITCZ. Once the moisture reached the 500 mb pressure level, a weak trough seen in the upper-left panel of Figure 32 provided a means for the moisture to couple to the subtropical jet, carrying the moisture along the 5,800 m contour on the 500 mb GPT surface. Since this transport's origin was from a convergent boundary, this AR is classified as a CBAR, making landfall first over the Baja Peninsula. Due to this characteristic, these CBARs are labeled as "Baja Express."

Figure 32 contains an analysis of the 250 mb jet stream and 500 mb GPT which shows the possible path of this CBAR. The trough at 500 mb, located between 125–130°W, provides a tap into the ITCZ moisture, which then follows the path of the 5,800 m GPT line. Throughout the time period, as the 5,800 m line propagates and evolves, the CBAR tends to follow its path through the AR life cycle. This 5,800 m line corresponds with the southern portion of the 250 mb jet stream.

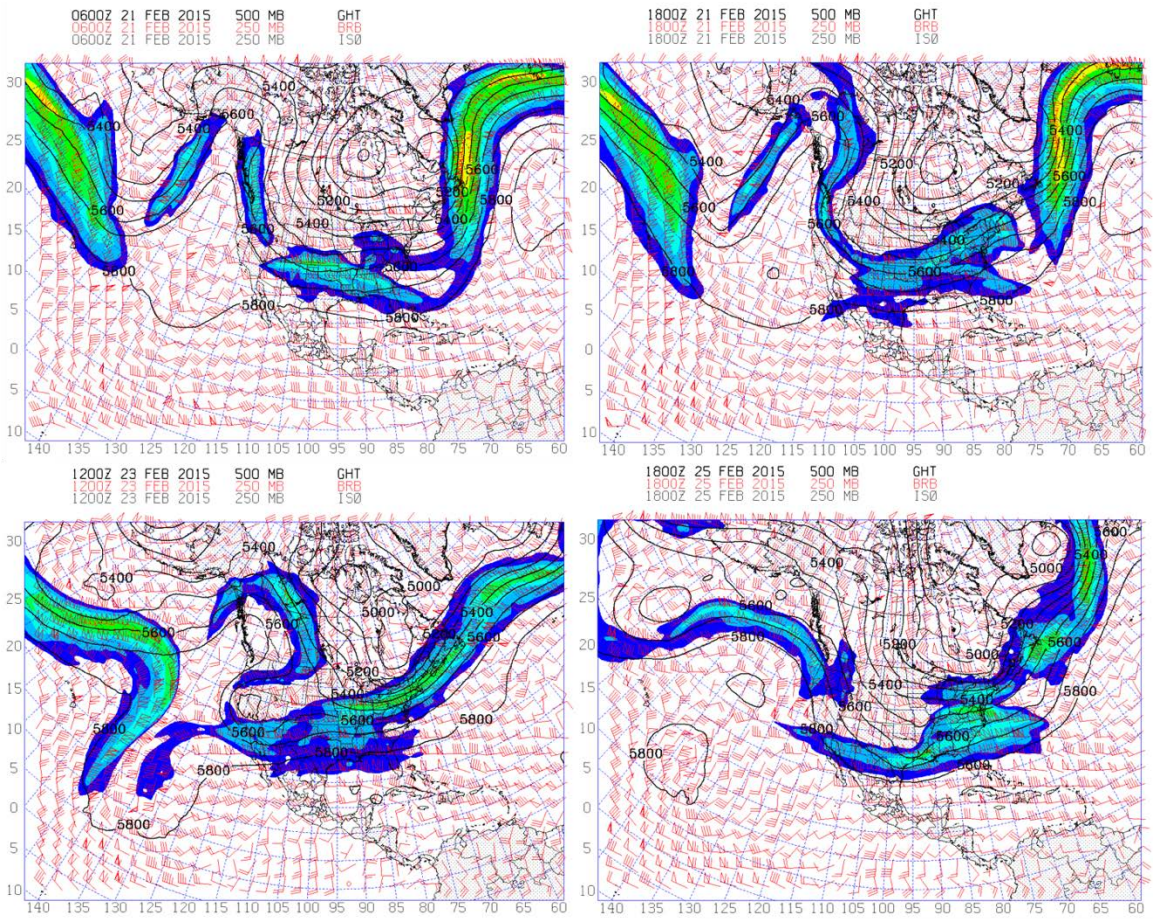

The 500 mb GPT is shown in black contours, the 250 mb wind is shown with red barbs, and the 250 mb jet stream is shown with a color fill. Upper-left: 0600 UTC 21 February 2015; upper-right: 1800 UTC 21 February 2015; lower-left: 1200 UTC 23 February 2015; lower-right: 1800 UTC 25 February 2015.

Figure 32. Case 1 CBAR Upper-Air Evolution.

Temperature at 850 mb was analyzed to look for fronts along the CBAR path, shown in Figure 33. During the onset of the CBAR, a strong temperature gradient does not exist at the CBAR's origin of 18°N-120°W at 0600 UTC 21 February. A frontal boundary does exist in North Texas at this point, where a previous system is moving through. By 1800 UTC 21 February, the Baja Express begins moving through Baja and into northern Mexico, and the 850 mb temperature plot still shows no evidence of a low-level thermal gradient along this path. This lack of a low-level thermal gradient shows that the CBAR is primarily an upper-level feature. However, by 1200 UTC 23 February, a cold front is moving through Texas. The CBAR path from the IVT plot and GOES IR imagery shows the CBAR pushing across the western boundary of the front which is oriented north-south. Further east over Texas, the CBAR and the cold front suggest a coupling to the low-level baroclinic structure. By 1800 UTC 25 February, the CBAR has moved through the southern U.S. and stretches from 33–36°N and 94–75°W. The Pacific moisture tap has terminated at this point, and the frontal boundary has passed through Texas. Though studies suggest that ARs are associated with extratropical cyclones, this CBAR appears to have formed independently. However, the CBAR then coupled with a cyclone after reaching Texas. For this event, the onset of the CBAR at 0600 UTC 21 February is primarily an upper-level feature, as the moisture couples with the 250 mb jet stream. It doesn't couple with the lower-level cyclone until 1200 UTC 23 February, as it follows a frontal boundary through Texas. Although it becomes a part of the frontal pattern midway through its lifecycle, the front exists alone after the CBAR terminates at 1800 UTC 25 February. It is also evident that the 700 mb pattern has weakened over the ITCZ, providing little to no moisture into northern Mexico and the southwestern U.S., as seen in Figure 31.

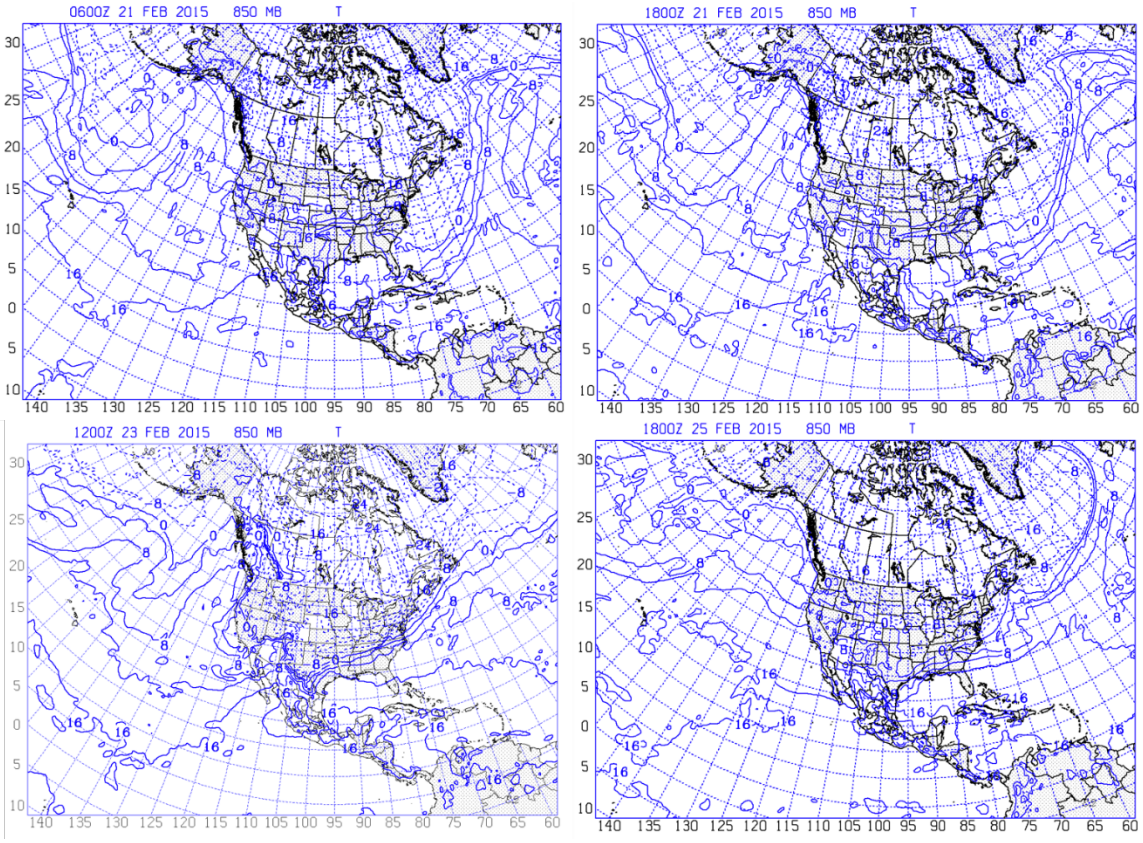

Close contours indicate a front. Upper-left: 0600 UTC 21 February 2015; upper-right: 1800 UTC 21 February 2015; lower-left: 1200 UTC 23 February 2015; lower-right: 1800 UTC 25 February 2015.

Figure 33. Case 1 CBAR 850 mb Temperature Evolution.

The CBAR signature is evident in the vertical cross sections taken at different points along the CBAR at 1200 UTC 22 February in Figure 34, when the CBAR was well defined. In order to identify the CBAR structure, the cross sections show the mixing ratio (QV), potential temperature θ (THE), and cross cross-section wind (XXW). ARs are typically characterized by mixing ratio values of 0.005 kg kg^{-1} (5 g kg^{-1}). Over the Eastern Pacific near the ITCZ as shown on the upper-left panel of Figure 34, QV values of 0.005 kg kg^{-1} are associated with a strong southwesterly flow of greater than 10 m s^{-1}, as seen near the center of that panel between 600–700 mb (note that the negative sign in the XXW plot denotes a change in wind direction, not a decrease in wind speed). Values as high as 0.015 kg kg^{-1} are seen near the surface. As the CBAR travels over Baja shown in the upper-center panel of Figure 34, the surface mixing ratio values drop slightly, but the 0.005 kg

kg^{-1} value still reaches up to the 650 mb level. The CBAR is evident where the QV values correspond with a fast flow of greater than 15 m s^{-1} between 600–750 mb. However, as the CBAR moves more inland over Texas, the 0.005 kg kg^{-1} value drops to the 700 mb level, and the CBAR still has a fast flow of greater than 15 m s^{-1}. Of interesting note, there appears to be a second signature of high-value QV along the coastline, seen in the lower-left panel. The IVT plot in Figure 31 shows elevated moisture flux coming from the Gulf of Mexico, typical of a Maya Express. The lower-left panel of the cross section in Figure 34 indicates that there may be an overrunning of the Baja Express over the Maya express, and a possible convergence of the two ARs. This phenomenon has not been mentioned in previous studies. As the CBAR continues to the East Coast, it is much weaker in terms of the QV. However, a stronger flow of greater than 25 m s^{-1} is evident near 700 mb. A 0.005 kg kg^{-1} and greater QV value is still evident, though it only goes up just above 800 mb.

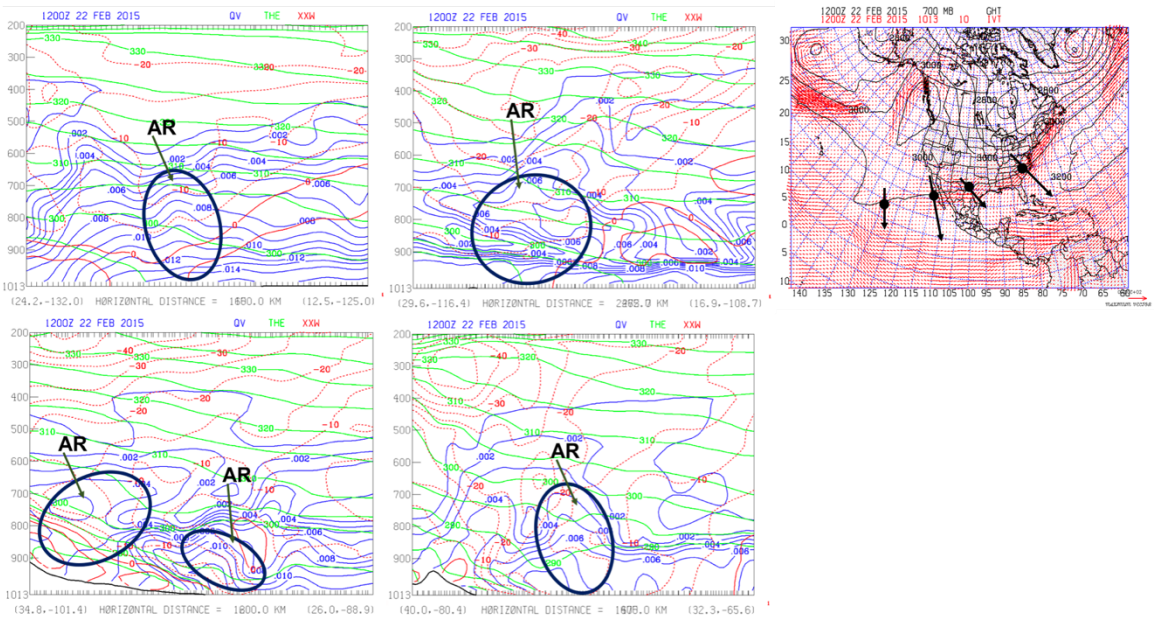

1200 UTC 22 February 2015. QV is shown with blue contours, THE is shown with green contours, and XXW is shown with red contours. The black arrows show the positions of the North-to-South cross-sections taken for this case. The black dots show the center of where the cross-section was taken. Upper-left: Eastern Pacific; upper-center: Baja; upper-right: IVT; lower-left: Texas; lower-right: East Coast.

Figure 34. Case 1 CBAR Vertical Cross Section.

ARs, according to the AMS *Glossary of Meteorology* (2019), are typically associated with low-level jet streams. This CBAR emerges from the ITCZ, where no identifiable low-level jet stream exists. Once this CBAR moves over land, a weak low-level jet stream is apparent through the rest of its path. Even so, it follows the upper-level flow pattern, regardless of the lower-level coupling. This may explain how the Baja Express CBAR can propagate and penetrate further inland compared to the Pineapple Express and Maya Express ARs.

Potential temperature contours do not show any strong frontal boundary near the ITCZ, where the CBAR originates. A weak frontal boundary begins to form as the CBAR moves over Baja. Once in Texas and along the East Coast, a weak frontal boundary is more evident, with its associated low-level jet.

The vertical cross section analysis shows that this type of AR emerges from a deep pool of moisture over the Eastern Pacific. A weak wind maximum extends down to 700 mb, initiating the CBAR in the ITCZ from an upper-level trough. For Case 1, once the CBAR moves inland, it appears to be associated with a weak frontal boundary and its associated low-level jet stream, consistent with the AMS definition (AMS, 2019). This association with the front and jet may be why the CBAR is able to extend so far inland. However, this CBAR still appears to exist and propagate independently, as the front still exists after the CBAR terminates.

Other evidence that this CBAR is unlike a typical AR is shown in the parcel trajectory along certain points of the CBAR path, marked by black dots. Figure 35 shows the higher-level trajectories at 700 mb that end at 1800 UTC 23 February. The trajectories begin from four specific points along the AR and are traced back to the previous 48 hours in order to identify where the parcel originated from 48 hours prior and how it traveled. The first trajectory was taken at the tip of Baja, 22°27'N-109°47'W. This trajectory traced back to central Mexico. The 2nd trajectory began at the Mexico/Texas border, 28°23'N-104°49'W, and traced back to the eastern Pacific near 20°N and 115°W. A third trajectory was taken in Texas at 29°33'N-98°39'W, which also traced back to the eastern Pacific near 22°N-118°W. The fourth trajectory was taken at the Florida/Alabama border, 30°29'N-

87°28'W, and also traced back to the eastern Pacific near 113°N-18°W. The trajectory along all points shows the parcel coming from the Pacific near the ITCZ, which corresponds with the GOES IR imagery and IVT path. The QV analysis shows the 0.005 kg kg^{-1} line reaching up to 650 mb. However, the 850 mb trajectories ending at the same points are shown in Figure 36 and verify the possible convergence of the Baja Express CBAR and the Maya Express AR. From origin to the Big Bend area, 28°N-104°49'W, the trajectory at 850 mb is from the Pacific, with the Baja trajectory remaining stationary and the Big Bend trajectory beginning near 23°N-115°W. However, for points further east in Texas, the trajectory is from the Gulf, tracing back to 23°N-90°W, showing a convergence of moisture transports at lower levels. The fact that a Pacific transport continues to the East Coast at 700 mb and a Gulf transport occurs at lower levels indicates that overrunning is occurring over Texas.

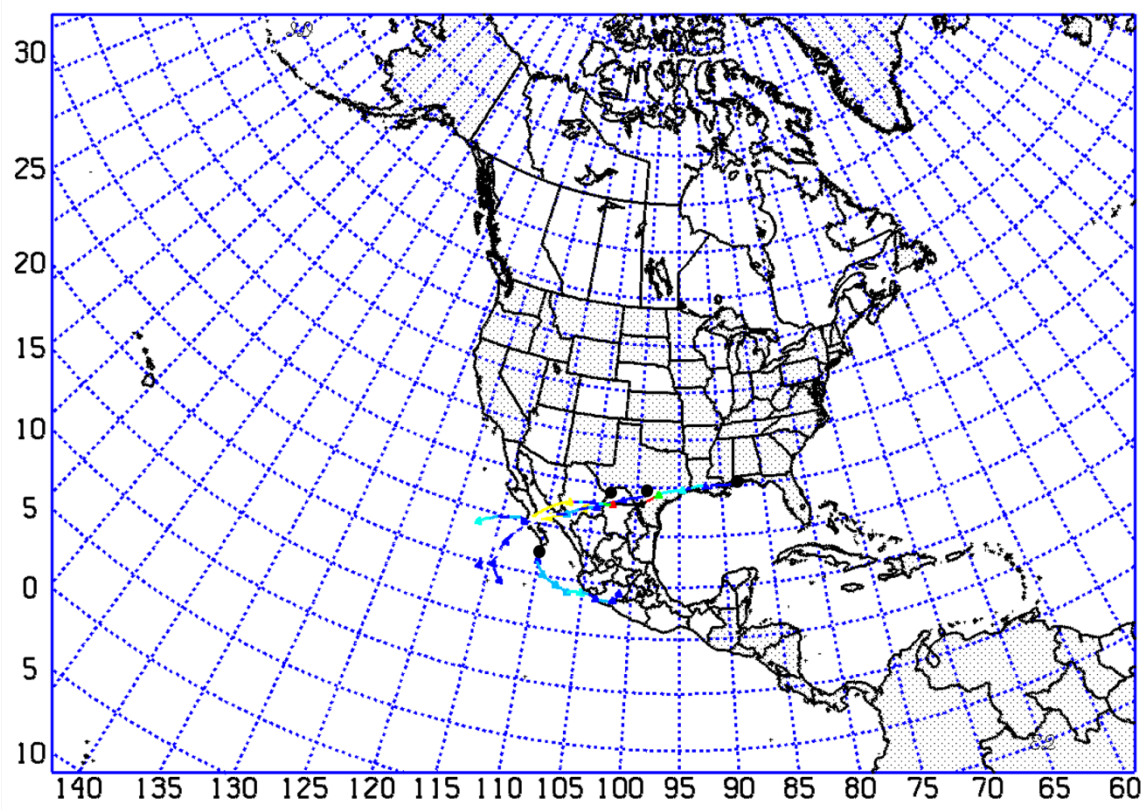

Figure 35. 700 mb Parcel Trajectory.

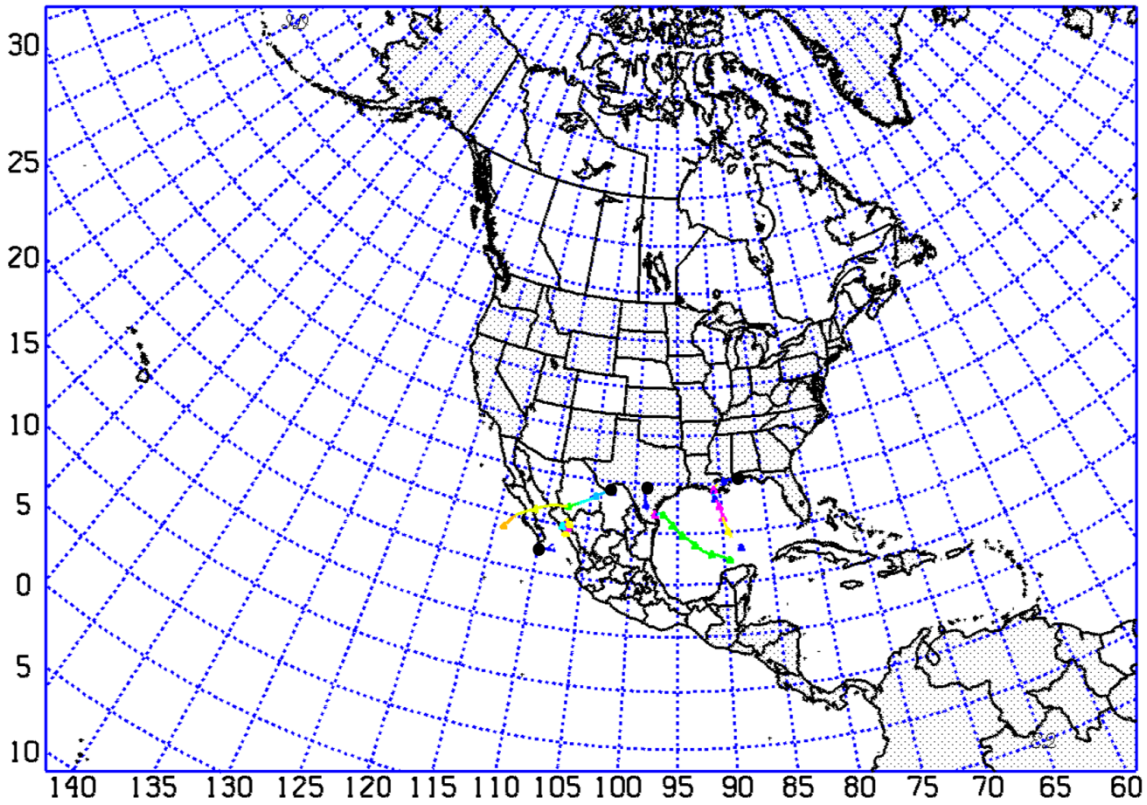

Figure 36. 850 mb Parcel Trajectory.

Figure 37 shows the moisture budget for this Baja Express event. This data was taken from a box centered around Texas in order to show the source of the moisture influx/outflux and determine the degree that precipitation is being fueled by Pacific moisture. This also indicates that several moisture transports may be converging. For this case, a slight majority of the moisture inflow is from the west (the Pacific), as confirmed by the satellite imagery and the IVT plot. However, a comparable amount is coming in from the south (Gulf of Mexico), as evident in the IVT plot, revealing a second key moisture source for this event. This indicates separate AR systems converging in Texas, which may be the primary means of precipitation. For Case 1, the total moisture flux exceeds precipitation due to the time lag between the instantaneous moisture flux and the accumulated precipitation over the past 6 hours. Precipitation for Case 1 was reported as fog and mist with freezing rain, consistent with light precipitation and overrunning, as the Pacific moisture from the west flows over the Gulf moisture from the south. This is also

evident from the trajectories, as moisture at 700 mb primarily came from the eastern Pacific as seen in Figure 35.

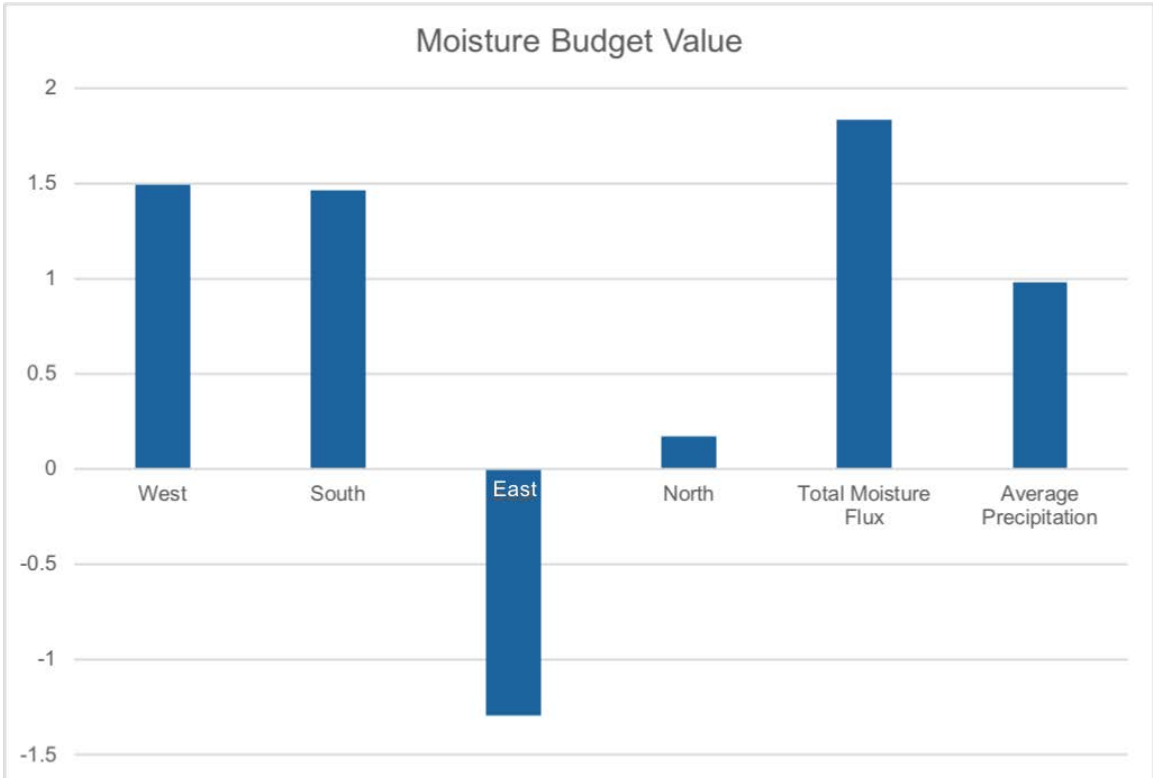

Figure 37. Moisture Budget for Case 1 in Texas.

Due to the effects of converging AR systems, it is evident that CBARs will aid in producing adverse weather effects along their path as seen in the lower-left panel of Figure 34. Case 1 exhibited fog and drizzle in Texas by both SAT and DFW, and due to frontal passage, freezing rain was reported by DFW, shown in Figure 7. Thunder was also noted in the DFW report, possibly due to the convergence along the Texas Gulf Coast.

B. CASE 2

Figure 38 shows the evolution of the January 2017 CBAR. Case 2 originates near the same area as Case 1. GOES IR imagery suggests the CBAR propagating through Baja and out toward the East Coast throughout the time period. The IR imagery shows a very defined Pacific flow. However, in Figure 39, the IVT plot shows a weaker Pacific flow and

a stronger Gulf flow. TQV is also shown in Figure 39. Higher TQV values can be seen where the IVT is elevated, confirming the satellite imagery. In the upper-left panel of Figure 39, there does not appear to be an AR at 1800 UTC 15 January, though the upper-left panel of Figure 38 shows an abundant amount of moisture in the ITCZ. The AR begins to develop at 0000 UTC 17 January as a 700 mb trough deepens just behind it, seen in the upper-right panel of Figure 39. By 1200 UTC 18 January, shown in the lower-left panel, the AR is well defined, and the GOES IR imagery shows the AR extending through Texas into Arkansas in the lower-left panel of Figure 38. The Pacific moisture tap begins to diminish at 1200 UTC 19 January, though the satellite imagery shows a strong AR signature, seen in the lower-right panels of Figures 38 and 39. The lower panels of Figure 39 also show moisture coming up from the Gulf of Mexico interacting with the moisture coming from the Pacific.

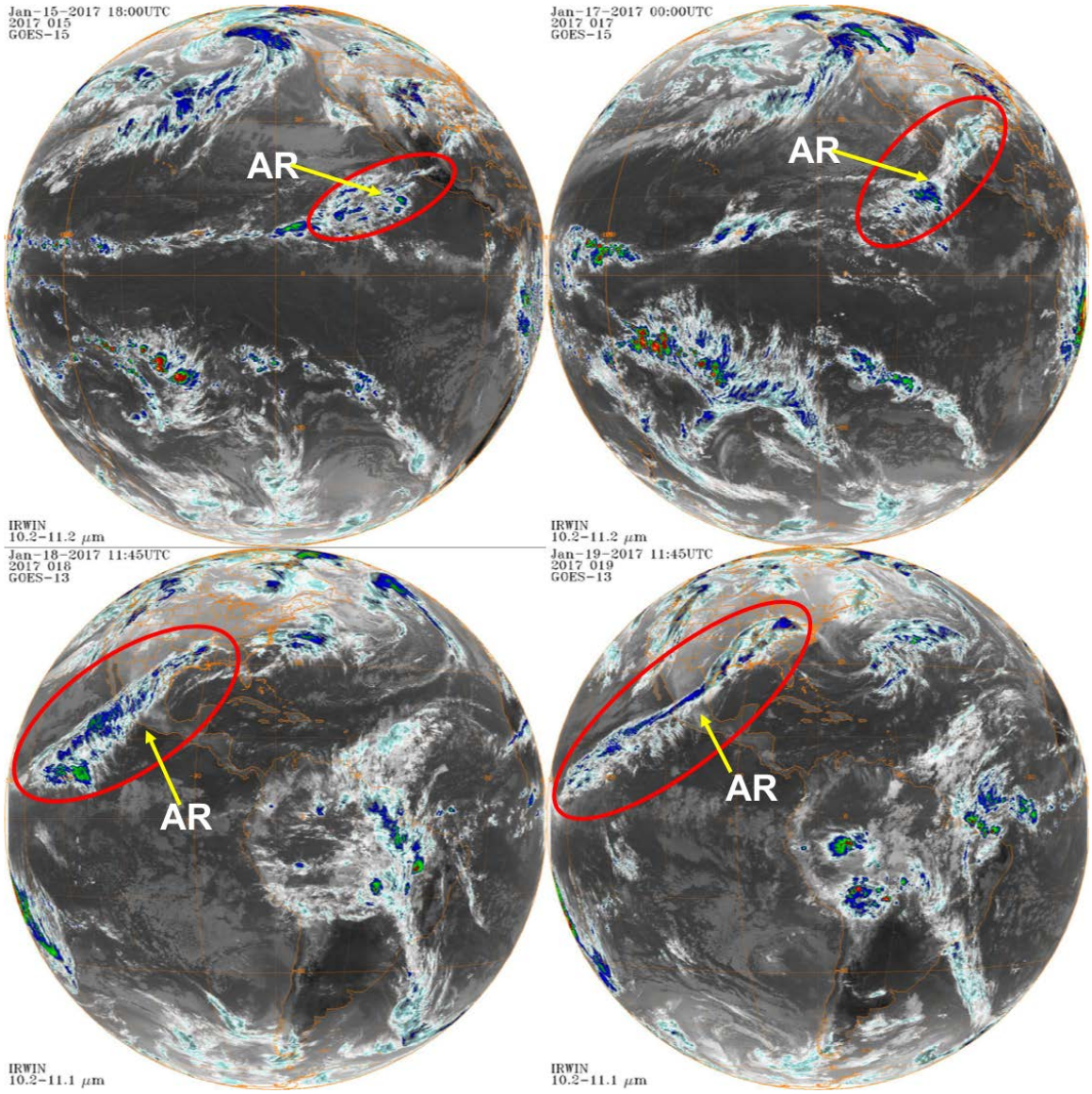

Upper-left: 1800 UTC 15 January 2017; upper-right: 0000 UTC 17 January 2017; lower-left: 1145 UTC 18 January 2017; lower-right: 1145 UTC 19 January 2017.

Figure 38. Case 2 CBAR Satellite Evolution. Source: Knapp (2008).

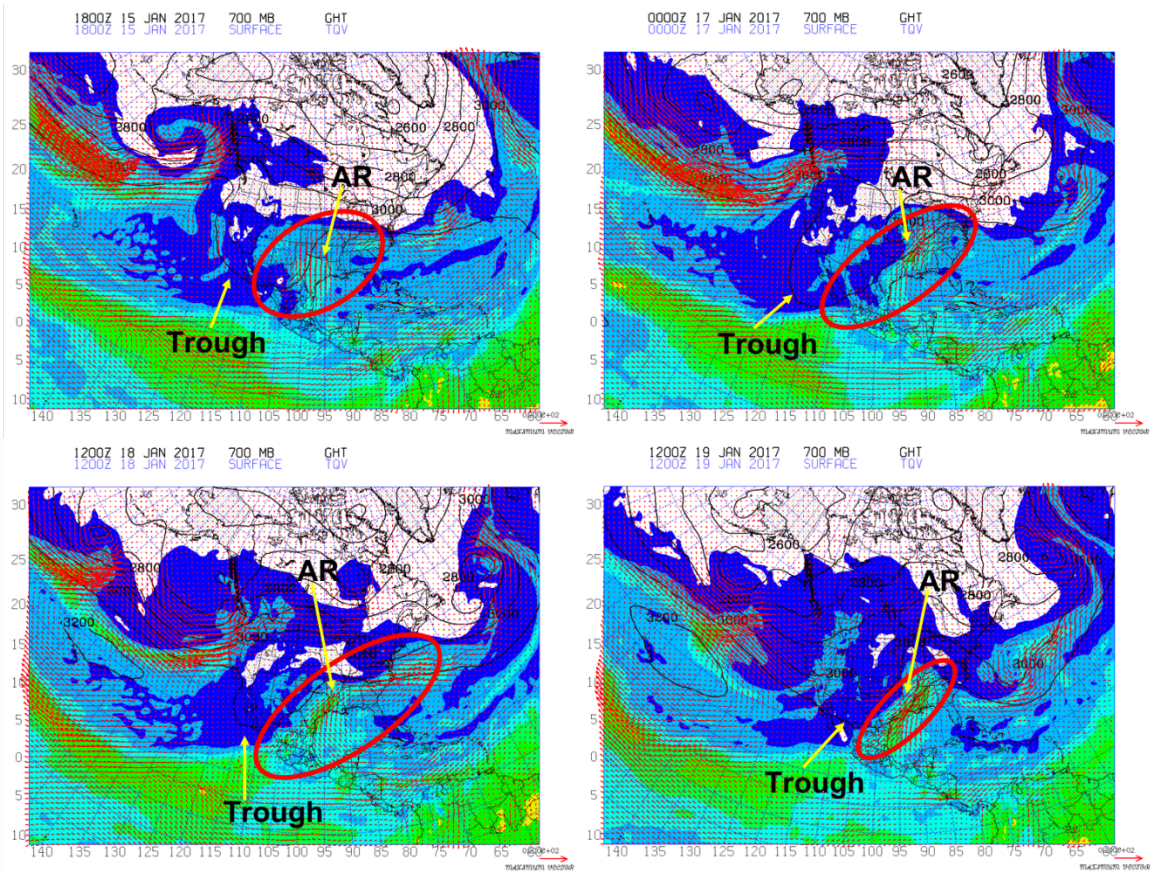

IVT is shown with red barbs, the 700 mb GPT is shown with black contours, and TQV is shown with a color fill. Upper-left: 1800 UTC 15 January 2017; upper-right: 0000 UTC 17 January 2017; lower-left: 1200 UTC 18 January 2017; lower-right: 1200 UTC 19 January 2017.

Figure 39. Case 2 CBAR IVT Evolution.

As in Case 1, the GOES imagery shows this CBAR moving in a coherent fashion as suggested by Zhu and Newell (1994), with no evidence of lower level baroclinic structure. However, the signature in Case 2 is more defined than in Case 1.

Figure 40 shows the 500 mb GPT and 250 mb jet stream plot, where the CBAR originates just south of the 5,800 m line. The upper-level jet does exist at 1800 UTC 15 January. However, by 0000 UTC 17 January, the 5,800 m line dips south and the 250 mb jet stream forms west of Baja, where the CBAR is becoming well-formed. The transport once again follows the 5800 m GPT line just south of the 250 mb jet throughout its life cycle, showing the emergence of the CBAR from Pacific moisture through Texas and on

toward the East Coast.

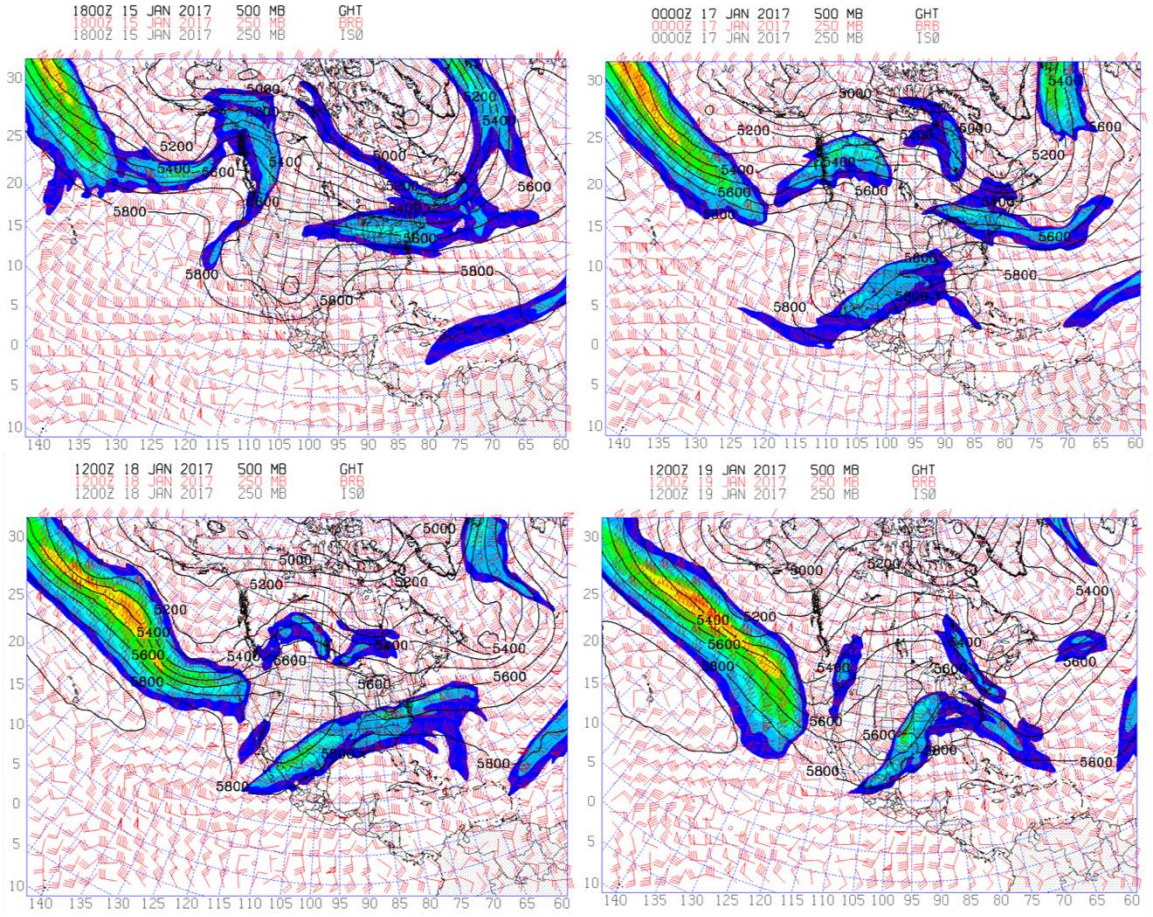

The 500 mb GPT is shown in black contours, the 250 mb wind is shown with red barbs, and the 250 mb jet stream is shown with a color fill. Upper-left: 1800 UTC 15 January 2017; upper-right: 0000 UTC 17 January 2017; lower-left: 1200 UTC 18 January 2017; lower-right: 1200 UTC 19 January 2017.

Figure 40. Case 2 CBAR Upper-Air Evolution.

Figure 41 shows a weak front over the eastern Pacific near the CBAR origin in the upper panels of the 850 mb temperature plot. Though the thermal gradient is weak, it is more defined than in Case 1. This may help isolate the moisture plume as cool dry air pushes south with the trough seen in the 700 mb GPT surface in Figure 39. The cross-sections in Figure 42 confirm this structure. This front is evident up until 1200 UTC 18 January in which it is washed out by 1200 UTC 19 January. The CBAR continues at this point, even though the front does not. On 15 January, it is clear that even with this

boundary, the moisture is being pulled in from the ITCZ, allowing this AR to be classified as a CBAR from the start. The CBAR continues even as the boundary terminates.

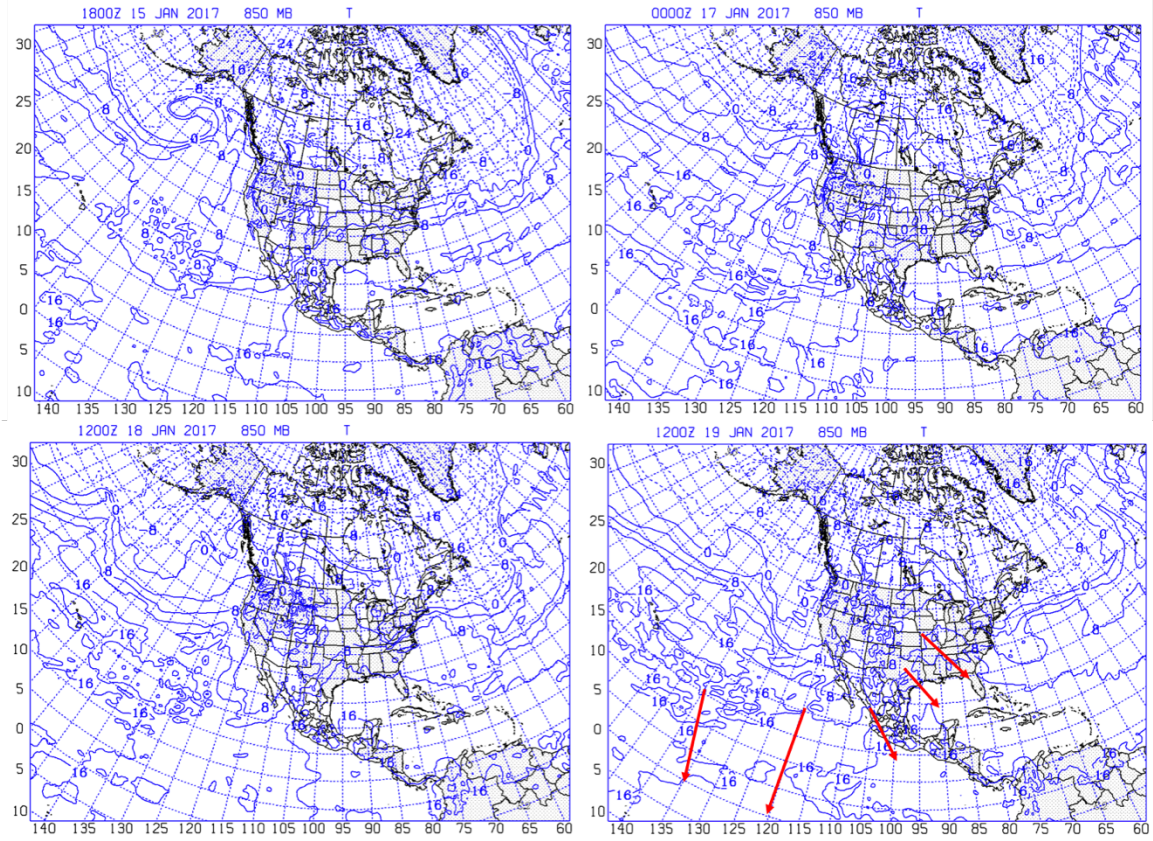

Close contours indicate a front. The red arrows show the positions of the North-to-South cross-sections taken for this case. Upper-left: 1800 UTC 15 January 2017; upper-right: 0000 UTC 17 January 2017; lower-left: 1200 UTC 18 January 2017; lower-right: 1200 UTC 19 January 2017;

Figure 41. Case 2 CBAR 850 mb Temperature Evolution.

Further frontal analysis is done with the potential temperature plots on the vertical cross sections in Figure 42. The vertical cross sections were plotted for 1200 UTC 19 January along the path of the CBAR, corresponding to the lower right panel of Figure 38. This cross-section corresponds to the time in which the IR imagery showed a very well-defined CBAR stretching from the ITCZ to the U.S. East Coast, shown in the lower-right panel of Figure 38. The IVT at this time is not as well defined, but the IR imagery shows a clear CBAR also shown by the high TQV values in the lower-right panel of Figure 39.

Though the potential temperature surface at the origin in the Eastern Pacific and over Baja does not show a strong frontal boundary. This indicates that this moisture is coming from the ITCZ in the upper levels and is independent of an extratropical cyclone. However, when the CBAR is over Texas and over the southeastern U.S. as shown in the lower-left and right panels, respectively, a shallow frontal boundary (850-900 mb vertical extent) is evident, along with a defined low-level jet stream. Though an extratropical cyclone appears to be involved further inland, this Baja Express event is pulling moisture from the convergent boundary first, then extending along the 5,800 m GPT line just south of the 250 mb jet stream before it interacts with any major system.

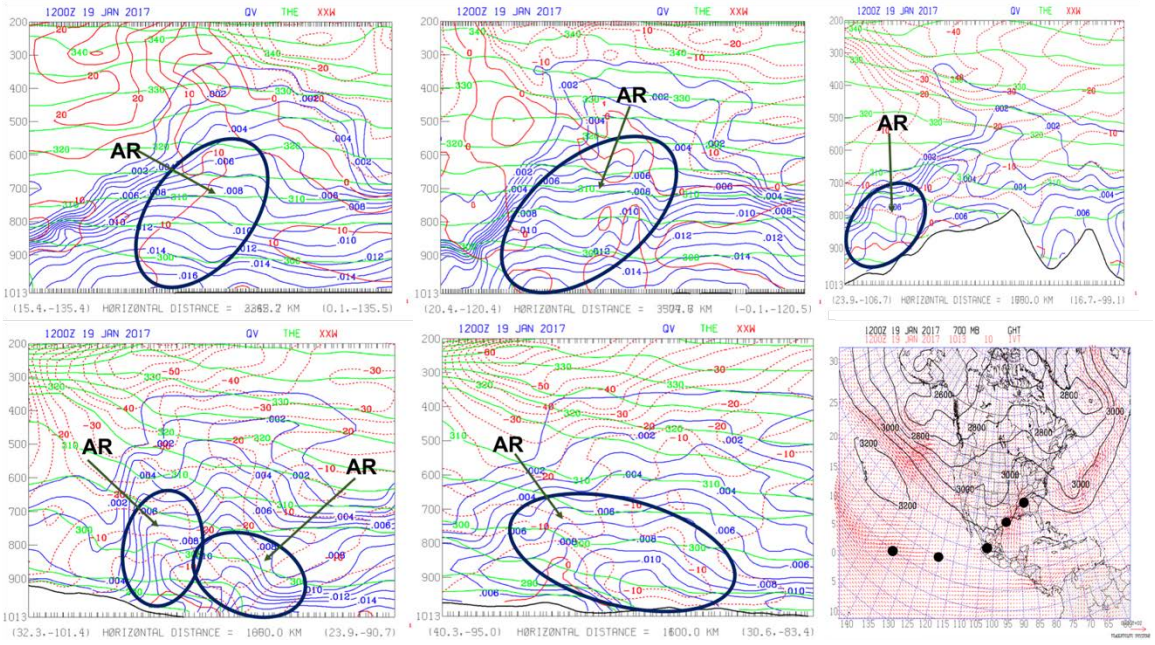

1200 UTC 19 January 2017. QV is shown with blue contours, THE is shown with green contours, and XXW is shown with red contours. The black arrows show the positions of the North-to-South cross-sections taken for this case. The black dots show the center of where the cross-section was taken. Upper-left: origin in East Pacific; upper-center: eastern Pacific; upper-right: western Mexico; lower left: Texas Gulf Coast; lower-center: southeastern U.S.; lower-right: IVT.

Figure 42. Case 2 CBAR Vertical Cross Section.

An analysis of QV shows a clear CBAR signature. Near its origin and over the Eastern Pacific in the upper-left and upper-center panels of Figure 42, the 0.005 kg kg^{-1}

contour extends up to near 550 mb. Over western Mexico shown in the upper-right panel of Figure 42, the signature is distorted but still evident, with the 0.005 kg kg^{-1} contour reaching up to 650 mb. As in Case 1, when the CBAR is over the Texas Gulf Coast, there appears to be an overrunning of the Baja Express with the Maya Express with high QV still reaching up to 600 mb, shown in the lower-left panel. Once the CBAR reaches the southeast US, the 0.005 kg kg^{-1} contour is still at 650 mb, and the signature suggests that the CBAR continues, seen in the lower-center panel. This QV analysis shows that regardless of penetration over land, the moisture transport is continuous from the ITCZ through Mexico and out toward the U.S. East Coast with high QV values consistently up to 650 mb (higher near the origin). It also verifies that two AR systems may be converging near the Texas Gulf Coast in the lower-left panel, also shown in the IVT pot in the lower-right panel.

Hedstrom (2014) noted that ARs appear to be associated with the WCB of extratropical cyclones, where strong wind and abundant water vapor exist at low latitudes. For Case 2, there does not appear to be a significant thermal gradient or low-level jet stream involved with this Baja Express event when it originates over the eastern Pacific, further suggesting that CBARs may be independent of extratropical cyclones.

Parcel trajectory for Case 2 is not included due to the complex nature of this particular system. The parcel trajectories in both the 850 mb level and the 700 mb level showed no consistent flow pattern, which makes it difficult to gather any useful information regarding the moisture source from the trajectories.

The moisture budget in Figure 43 shows the majority of the moisture for this case coming from the south. Consistent with Case 1, the total moisture flux exceeds the amount of precipitation. Consistent with the GOES imagery and IVT plot, moisture is coming in from the west, though the amount is less than from the south. Total moisture flux and average precipitation were higher in this case, but precipitation was still limited to fog and mist as reported by DFW and SAT in Figures 14 and 15, respectively, again leading to the conclusion that this is also overrunning of the Baja Express over the Maya Express, as the Pacific moisture once again converges with the Gulf moisture as seen in the IVT plots in Figure 39.

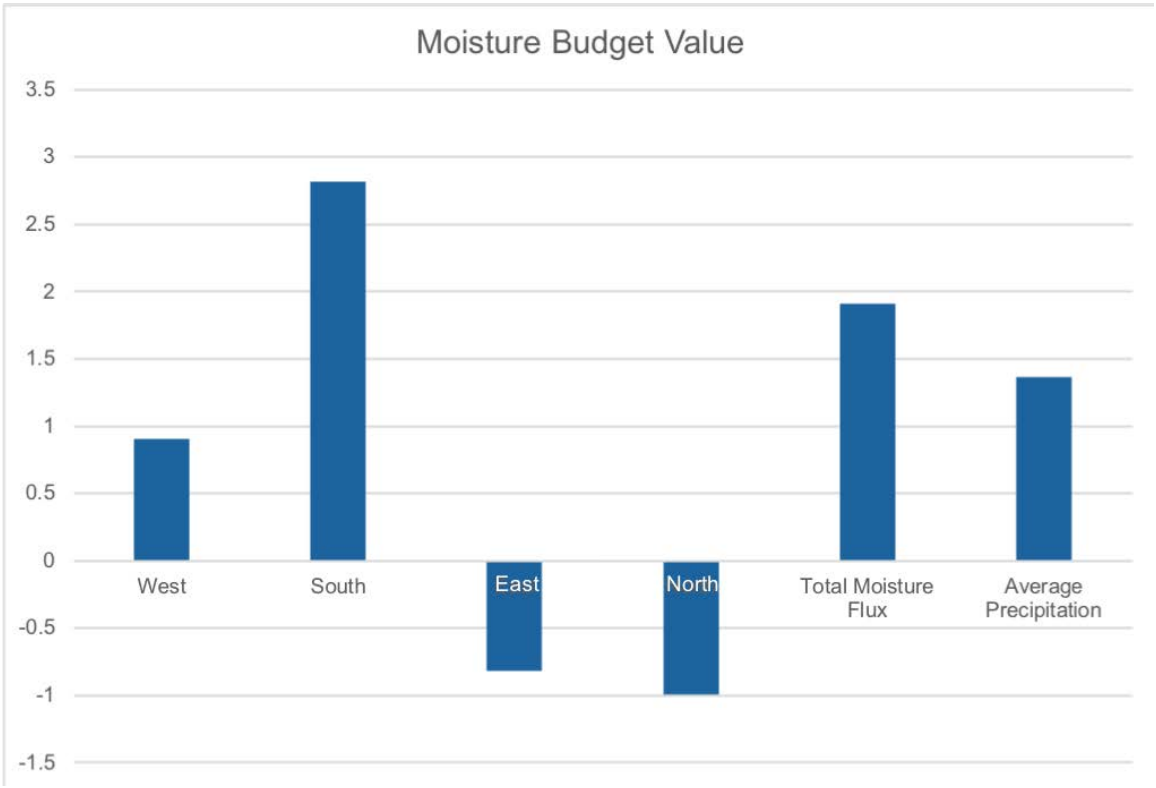

Figure 43. Moisture Budget for Case 2 in Texas.

As with Case 1, this Baja Express event produced precipitation deep inland in Texas. The lower-left panel of the cross-section in Figure 42 shows the CBAR structure in Texas, which is associated with a weak thermal gradient and defined low-level jet. As the moisture from the Pacific is above the moisture from the Gulf, precipitation was light and mostly in the form of fog and drizzle as reported by both DFW and SAT in Figures 14 and 15, respectively. This is contrary to the freezing rain and thunder in Case 1. However, as with Case 1, this Baja Express event produced fog and light drizzle.

C. CASE 3

In Case 3, though CBAR evolution was similar to the previous cases in the beginning, the result revealed a substantial difference. Figure 44 shows the CBAR entering Baja on 1800 UTC 25 March 2018 in the upper-left panel. As with the previous cases, this moisture transport begins with a tap from the ITCZ, though further west than Cases 1 and 2. The upper-right panel of Figure 45 shows that by 1200 UTC 26 March, the IVT signature

marked by the red circle in the image has increased and is much stronger than at 1800 UTC 25 March. Figure 45 also shows the TQV for Case 3. Higher TQV indicate the path of the increased IVT values in the red circle on the image. The TQV gets higher as the CBAR evolves, consistent with the satellite imagery along the CBAR path. The upper-right panel of Figure 45 shows the convergence of two systems is clear in North Texas. The Baja Express is receiving moisture from the ITCZ, and the head of the CBAR is near Illinois. There does not appear to be any low-level circulation or low-pressure system evident. However, a strong Maya Express is seen over Texas coming from the Gulf of Mexico at 1200 UTC 26 March in the upper-left panel of Figure 45, which may be a part of the low-pressure system west of Florida. Convergence is strong in North Texas and through Missouri. This pattern continues into 2345 UTC and 0000 UTC 27 March as seen in the lower-left panel of Figures 44 and 45. A trough at 700 mb is seen over the Eastern Pacific at 1800 UTC 25 March as seen in the upper-left panel of Figure 45, initiating the CBAR. This trough deepens at 1200 UTC 26 March and 0000 UTC 27 March as the CBAR evolves. The Baja Express is still receiving a light moisture tap from the Pacific at 0000 UTC 27 March, suggesting that the CBAR continues to receive moisture from the ITCZ due to the deepening of the 700 mb trough. The convergence has moved northeastward through Indiana and up to Wisconsin. However, by 0545 UTC 29 March, the Baja Express event appears to be eroded into the Maya Express, and the Pacific moisture tap has ceased, as seen in the lower-right panel of Figure 44. The IVT plot in the lower-right panel of Figure 45 shows moisture continuing to come from the Gulf of Mexico at 0600 UTC 29 March and moving out to the U.S. East Coast. The 700 mb trough has moved east, and a ridge has built in over the eastern Pacific, shutting off the Pacific moisture tap.

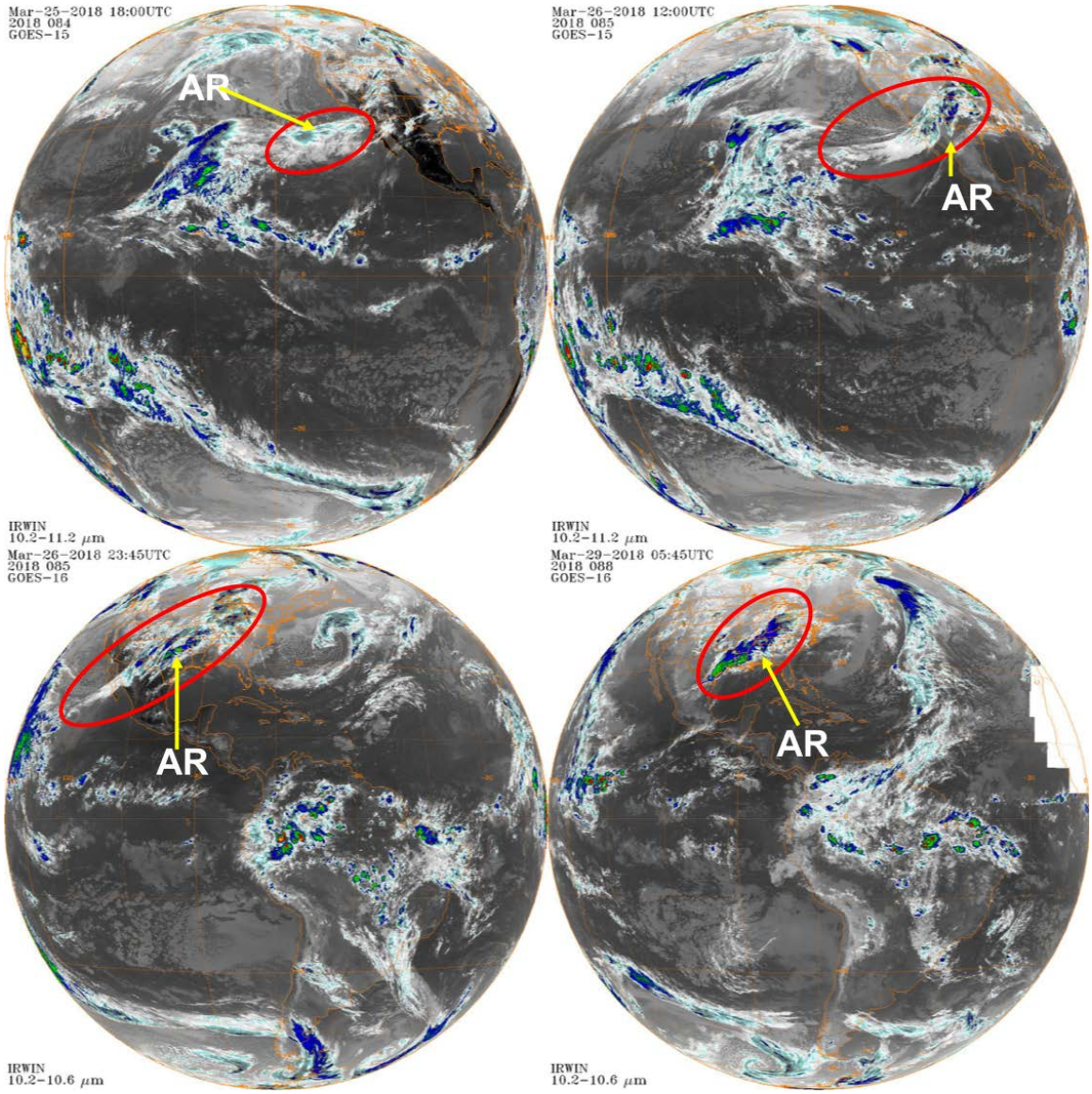

Upper-left: 1800 UTC 25 March 2018; upper-right: 1200 UTC 26 March 2018; lower-left: 2345 UTC 26 March 2018; lower-right: 0545 UTC 29 March 2018.

Figure 44. Case 3 CBAR Satellite Evolution. Source: Knapp (2008).

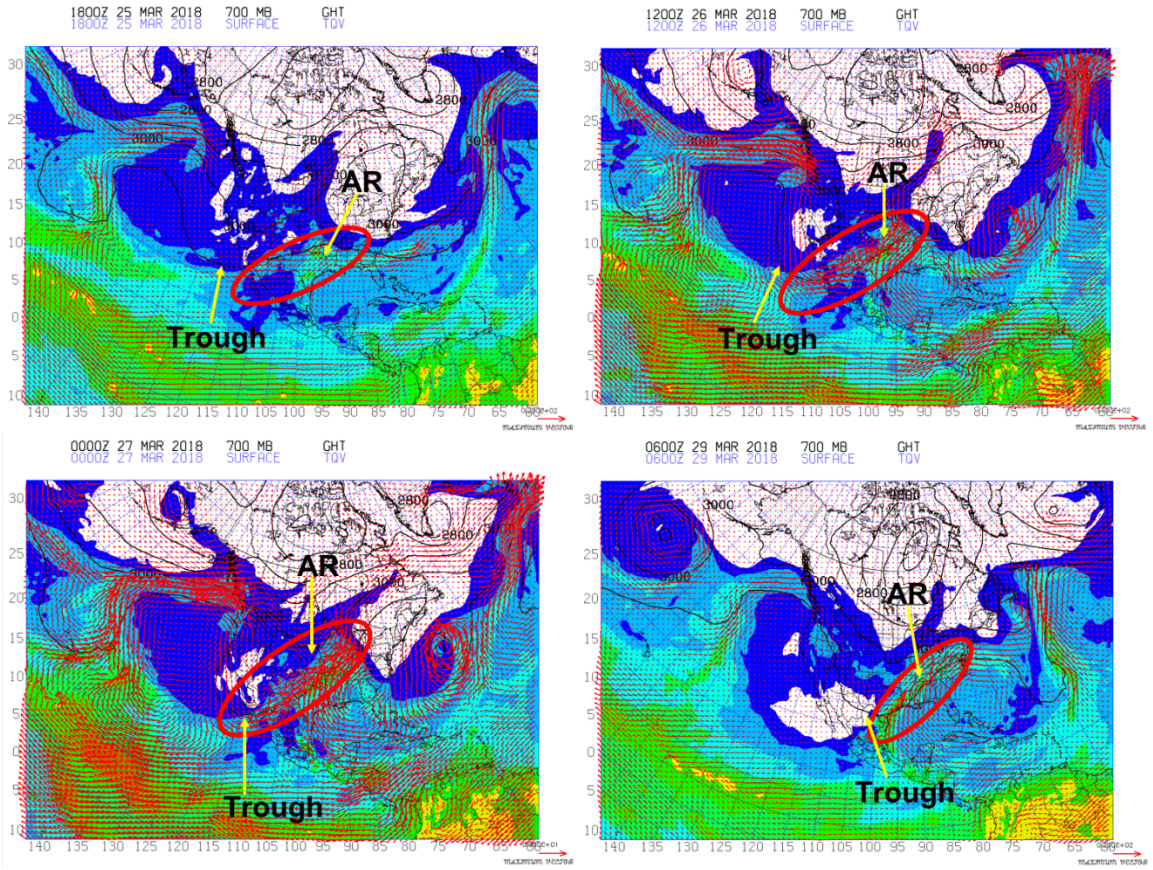

IVT is shown with red barbs, the 700 mb GPT is shown with black contours, and TQV is shown with a color fill. Upper-left: 1800 UTC 25 March 2018; upper-right: 1200 UTC 26 March 2018; lower-left: 0000 UTC 27 March 2018; lower-right: 0600 UTC 29 March 2018.

Figure 45. Case 3 CBAR IVT Evolution.

As with Cases 1 and 2, the CBAR follows the 5,800 m GPT line at 500 mb, which is just south of the 250 mb jet stream, seen in Figure 46. Though the Pacific moisture tap appears dormant at 0600 UTC 29 March in the lower-right panel, the jet stream and the 5,800 m GPT line is still over the East Pacific. As seen in the upper-left panel of Figure 45, a trough at 700 mb initiates the CBAR, and this trough deepens throughout the CBAR's evolution. However, a ridge has strengthened over the East Pacific at 700 mb, seen in the lower-right panel of Figure 45, cutting off the Pacific moisture tap. By 0600 UTC 29 March, the trough is pulling in moisture from the Gulf of Mexico as the system moves east. As with the previous two cases, the CBAR structure evolves in a coherent fashion throughout the time period.

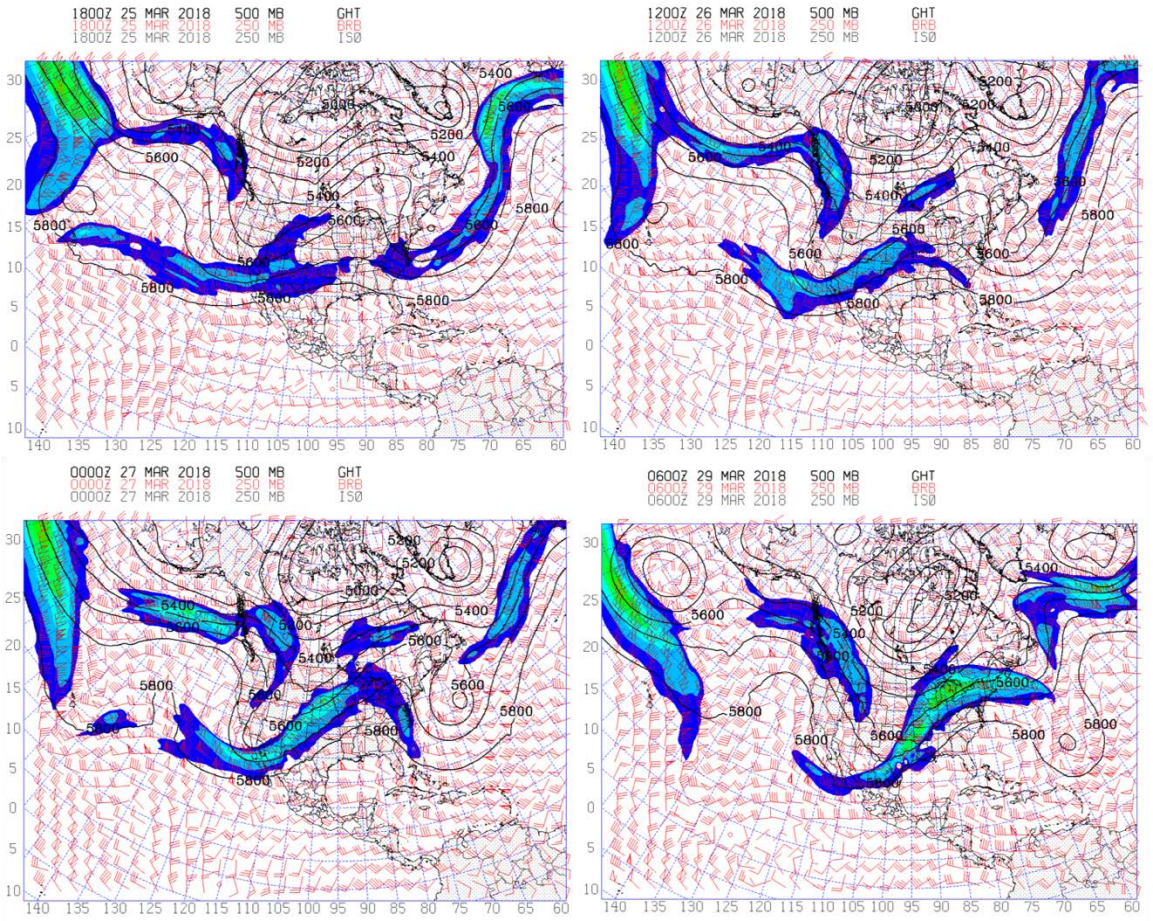

The 500 mb GPT is shown in black contours, the 250 mb wind is shown with red barbs, and the 250 mb jet stream is shown with a color fill. Upper-left: 1800 UTC 25 March 2018; upper-right: 1200 UTC 26 March 2018; lower-left: 0000 UTC 27 March 2018; lower-right: 0600 UTC 29 March 2018.

Figure 46. Case 3 CBAR Upper-Air Evolution.

The 850 mb temperature plot shows a front over the eastern Pacific at the CBAR's origin, shown in the upper-left panel of Figure 47, and the satellite imagery in Figure 44 shows moisture that may be related to this thermal gradient. As the front pushes down to Baja, it aids in tapping the ITCZ moisture to the west to initiate this CBAR. The CBAR appears to be coupled to the surface front east of the mountains in Mexico at 1200 UTC 26 March, consistent with the IVT in the upper-right panel of Figure 45. The 850 mb front appears to follow the 500 mb pattern until it decouples at 0600 UTC 29 March, shown in the lower-right panels of Figures 44–47. This indicates that this Baja Express event

originated with the help of a thermal gradient in the East Pacific in conjunction with the trough at 700 mb to tap the ITCZ moisture which initiated the event.

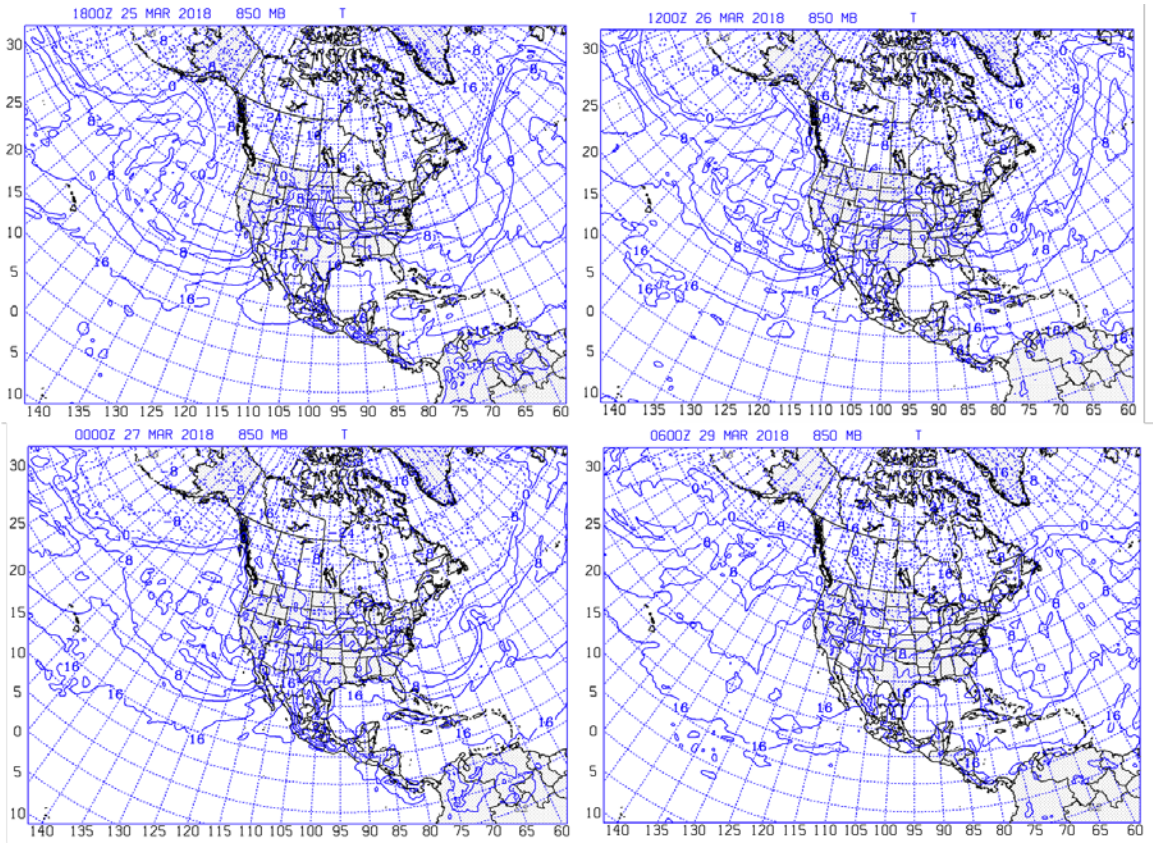

Close contours indicate a front. Upper-left: 1800 UTC 25 March 2018; upper-right: 1200 UTC 26 March 2018; lower-left: 0000 UTC 27 March 2018; lower-right: 0600 UTC 29 March 2018.

Figure 47. Case 3 CBAR 850 mb Temperature Evolution.

Potential temperature analysis shows evidence of a weak front at the onset of the CBAR in the upper-left panel of Figure 48. This front is located over the eastern Pacific, where the moisture and wind near 700 mb appear to indicate the start of this CBAR, where IVT values are high. The front does get stronger along the CBAR path further east along the Baja coast. The front appears strongest over the southeastern U.S. and East Coast, shown in the lower-left and center panels, where a more classic front and associated low-level jet stream are established. Though it appears that the 850 mb front is ahead of the

CBAR at first and behind it later on, the potential temperature contours show that the CBAR remains ahead of the front along its path. The cross-flow wind values in Figure 48 also show evidence of a low-level jet stream, also indicating an extratropical system.

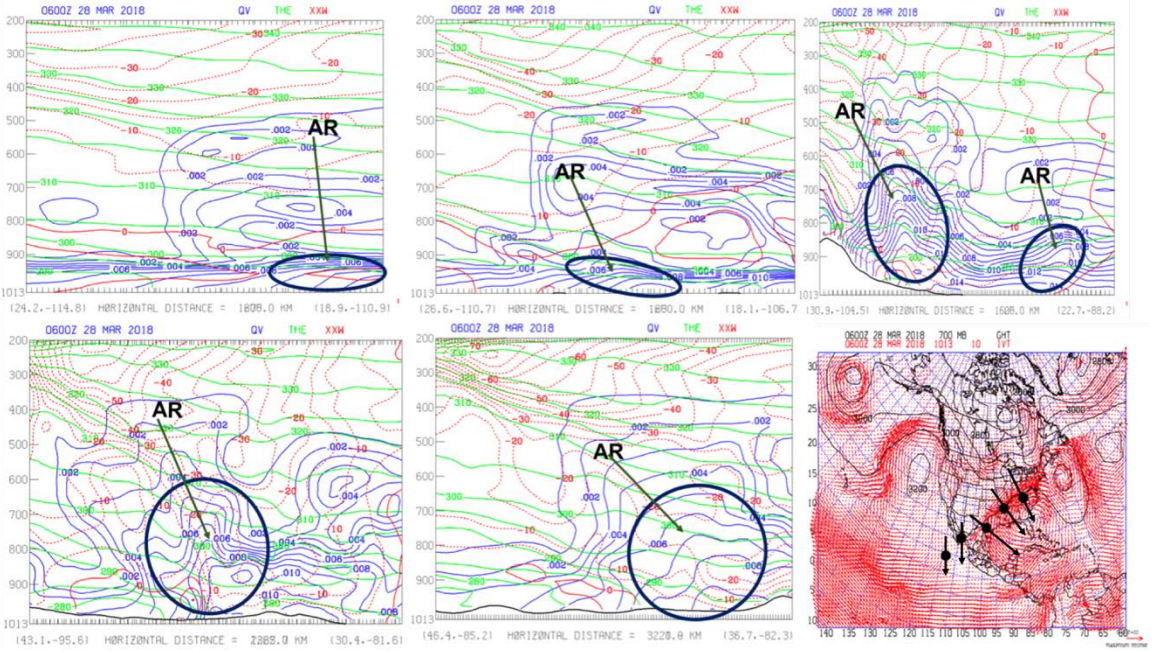

0600 UTC 28 March 2018. QV is shown with blue contours, THE is shown with green contours, and XXW is shown with red contours. The black arrows show the positions of the North-to-South cross-sections taken for this case. The black dots show the center of where the cross-section was taken. Upper-left: eastern Pacific; upper-center: West Mexico; upper-right: Texas; lower-left: southeastern U.S.; lower-center: East Coast; lower-right: IVT.

Figure 48. Case 3 CBAR Vertical Cross Section.

The QV signature shows values of 0.005 kg kg^{-1} and greater at 950 mb and lower at origin in the eastern Pacific as seen in the upper-left panel of Figure 48. However, the AR signature appears over Texas and continues to the U.S. East Coast, with 0.005 kg kg^{-1} values around 650 mb, shown in the upper-right, lower-left, and lower-center panels. There is also a strong signature of two AR systems converging as seen in the upper-right and lower-left panels. As these two systems near 850 mb and at a higher elevation near 700 mb, this looks to not be an overrunning event. This is likely why the Texas NWS reported

thunderstorms and a large amount of rainfall during this event from both DFW and SAT, seen in Figures 21 and 22, respectively.

Unlike the previous cases, the six 700 mb parcel trajectories in Figure 49 show parcel transport from the Gulf into Texas and further north at higher levels as seen by the trajectories that end at 0600 UTC 28 March. As with Case 1, these trajectories are taken at a starting point and traced back 48 hours. Six trajectories were taken and are marked with a black dot on the figure. The first trajectory was taken at the tip of Baja near the rear of the CBAR, 22°57'N-109°26'W, which appears to curve back toward Mexico. The second trajectory began near the Texas/Mexico border at 28°39'N-103°24'W, tracing back to west of Baja near 28°N-120°W. A third trajectory was taken in Texas at 30°03'N-98°07'W, which traced back to the Yucatan Peninsula near 17°N-90°W. The fourth trajectory began in northeast Arkansas at 35°37'N-90°05'W and traced back to the eastern Pacific south of Mexico near 13°N-97°W. The fifth trajectory began in eastern Illinois at 41°14'N-87°48'W and traced back to the eastern Pacific near 22°N-118°W. A sixth trajectory was taken near the head of the CBAR in Maine at 44°32'N-70°24'W, actually tracing back to the Atlantic near 40°N-57°W. All trajectories were taken along the CBAR path. Figure 50 shows the trajectories at the 850 mb level with each trajectory beginning at the same point as those in Figure 49. Though the parcel trajectories do not show a continuous flow pattern, the plots show parcel propagation from the Pacific penetrating deep into the U.S. for the western points. The trajectory taken in Texas at 30°03'N-98°07'W traces back to the Gulf of Mexico near 20°N-85°W, showing that moisture at both 850 mb and 700 mb in Texas both come from the Gulf of Mexico, while trajectories taken west of Texas come from Pacific moisture sources. This proves the convergence of moisture sources at lower and upper levels, which is responsible for the heavy rain and thunderstorms in Texas. Though the Baja Express may appear to be associated with an extratropical cyclone toward the end of its life cycle, this moisture still originates from the Pacific and travels through Baja into Northern Mexico and through the U.S.

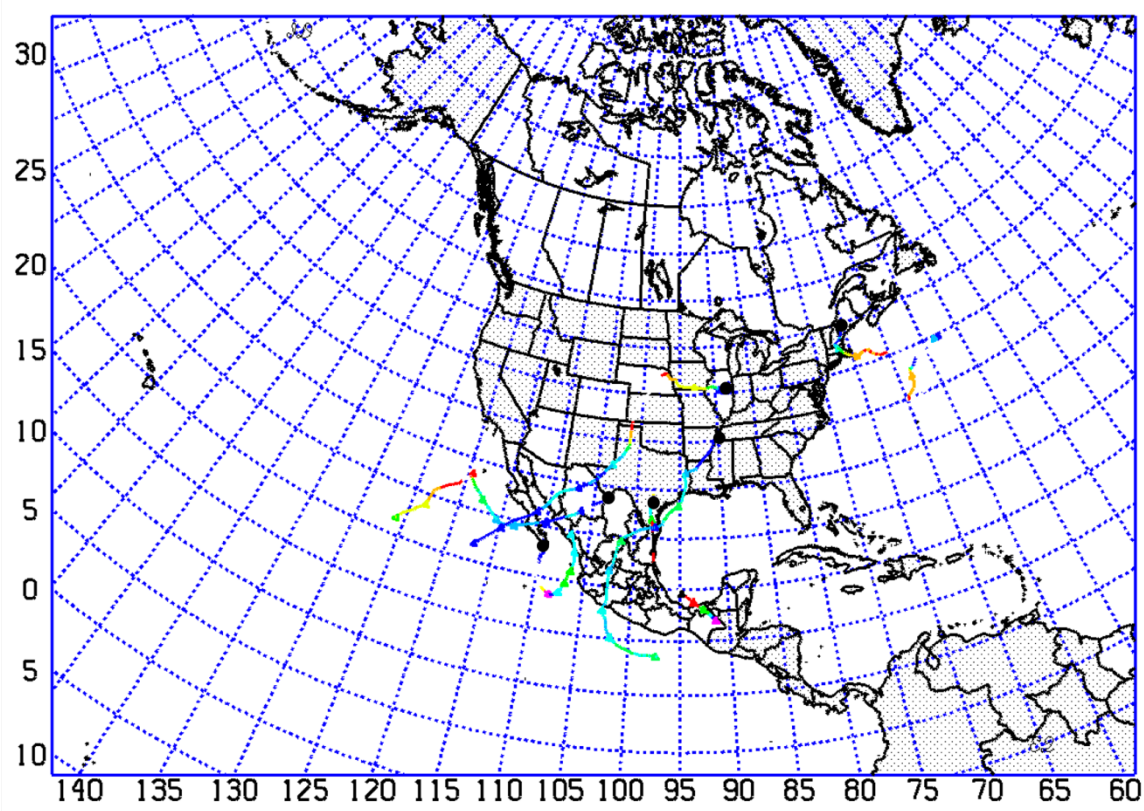

Figure 49. 700 mb Parcel Trajectory.

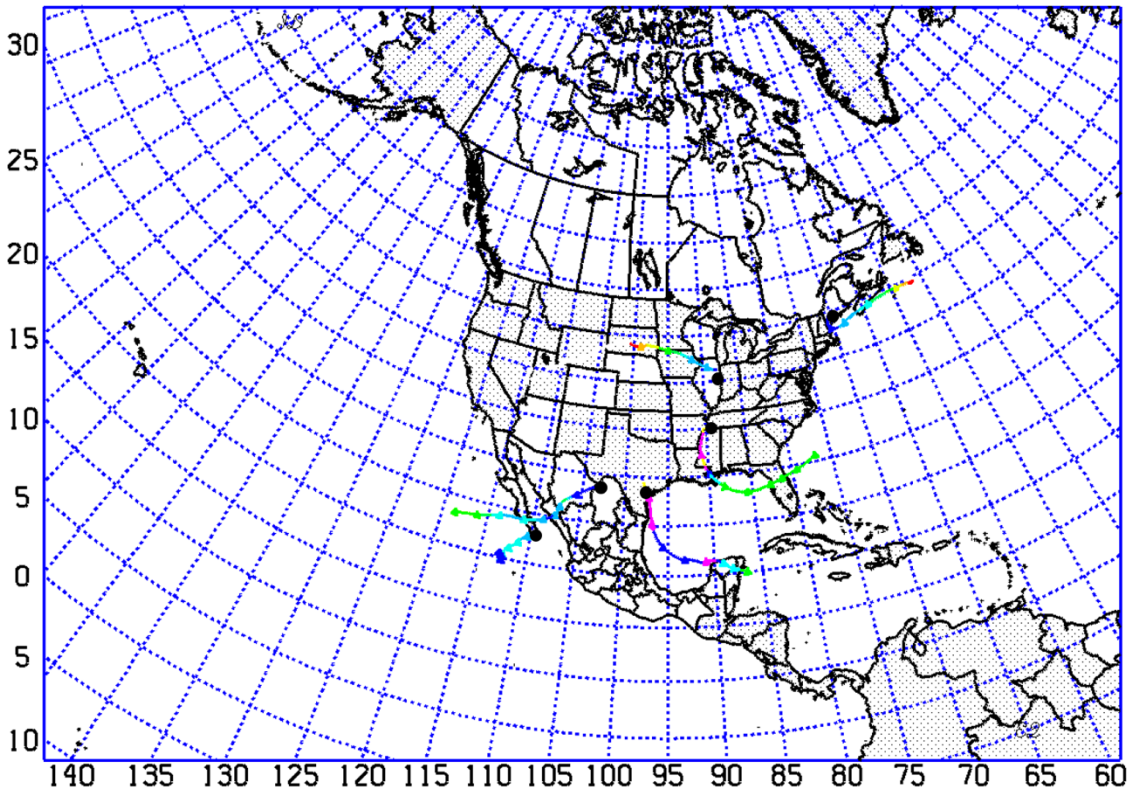

Figure 50. 850 mb Parcel Trajectory.

Figure 51 shows that the majority of the moisture influx came from the south, with a much less amount coming from the west. As with the other two cases, the total moisture flux exceeds the average precipitation. Satellite imagery and the IVT plot, Figures 44 and 45, respectively, shows moisture initially coming from the ITCZ, seen in the upper-left panels. However, by 0600 UTC 29 March as seen in the lower-right panels of Figures 44 and 45, the Pacific moisture gets cut off. The trough at 700 mb moves over Texas at this point, drawing moisture up from the Gulf of Mexico, while a ridge build over the eastern Pacific, allowing that moisture to be confined to the ITCZ. The system looks to be primarily extratropical with moisture influx from the Maya Express in the Gulf of Mexico. The convergence of the two systems in Texas is likely the reason for the thunderstorms and heavy rain that were reported.

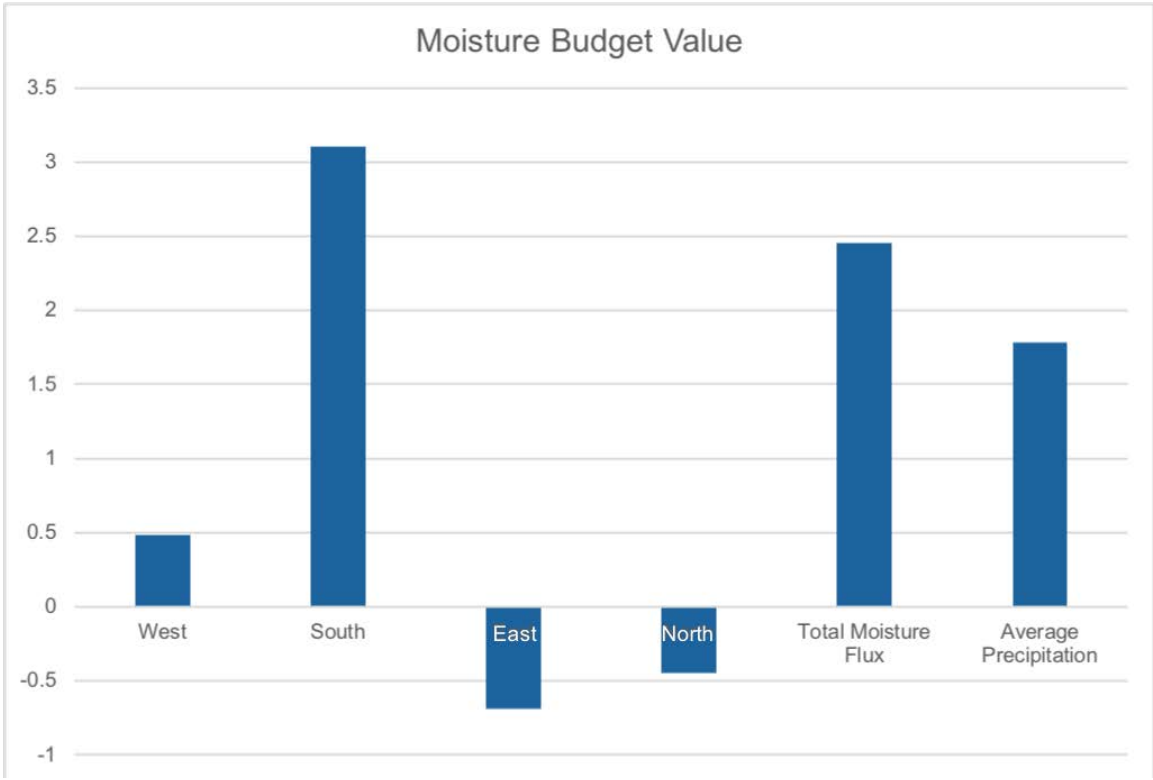

Figure 51. Moisture Budget for Case 3 in Texas.

Both DFW and SAT reported heavy rain and thunderstorms as shown in Figures 21 and 22, respectively. This weather was preceded by fog and mist. The resulting thunderstorm and heavy rain event were due to the convergence of Pacific moisture and Gulf moisture at low and mid-levels (850 mb and 700 mb), seen in the trajectories in figures 49 and 50. The upper-right panel of the cross-section in Figure 48 shows the AR systems converging in Texas near the center of the panel. This is unique in the fact that other Baja Express events are an overrunning of the CBAR over the Maya Express AR.

D. CASE 4

Figure 52 shows the Case 4 CBAR well-defined in the IR imagery throughout the time period. At 1200 UTC 08 February 2019 in the upper-left panel, there is an abundant amount of moisture in the ITCZ just east of Hawaii propagating toward Baja. There appears to be an extratropical cyclone off the coast of northern California. The IVT plot also shows a cyclone north of where the ITCZ moisture is, with a complete cyclonic transport around

the low, shown in Figure 53 in the upper-left panel. Figure 53 also shows the TQV for Case 4. TQV values increase throughout the evolution of this CBAR and are consistent with the satellite signature. One may assume that the moisture transport is a result of moisture being pulled into the WCB of the cyclones. However, the CBAR appears to be south of the extratropical cyclone which may have initiated the event, and the ITCZ moisture appears to be moving with (but not part of) the southern end of the cyclone west of northern California. By 1200 UTC 10 February in the upper-right panel, the moisture has moved east of the low near Hawaii, and the low up north is further northeast of this transport. The ITCZ moisture is extending toward Baja at this point. The low north of Hawaii may be aiding in the transport, but the IVT and GOES imagery show that this moisture is a separate entity, originating from the ITCZ and following the upper-level pattern. At 1745 UTC 11 February in the lower-left panel of Figure 52, the Baja Express CBAR stretches from the ITCZ up to the US East Coast possibly coupled with the AR in the Midwest, arguably making this the longest CBAR of the cases. The low around Hawaii still exists. However, as seen in the lower-left panel of Figure 53, a trough at 700 mb has deepened, and moisture continues to come from the East Pacific. The plot shows high levels of IVT along the path through the East Coast. Though initially it appears that there are no associated extratropical cyclones from the IVT plot, the 850 mb temperature plots in Figure 55 and the cross-sections in Figure 56 show thermal gradients along the CBAR path along with associated low-level jet streams. The thermal gradient likely began the moisture tap from the ITCZ, and as the moisture reached the upper troposphere, the CBAR extended along the 5,800 m contour following the 250 mb jet stream, shown in Figure 54. By 2345 UTC 12 February, as seen in the lower-right panel of Figure 52, the Pacific moisture tap is cut off and the CBAR is pushing through the East Coast. A low-pressure system has developed over the Great Lakes, and it appears that some of the moisture is now pulled into this cyclone and is a part of the WCB. However, from the GOES imagery and the IVT plot, the CBAR appears to push past this cyclone and continue out into the Atlantic, apart from this low-pressure system. As such, this Baja Express occurrence emerges from the ITCZ. Though it may be initiated by the low north of Hawaii, it extends into the central U.S. and out to the eastern seaboard in a coherent fashion throughout the case study.

Of note, a trough at 700 mb is evident at the onset of the CBAR as seen in the upper-left panel of Figure 53. This trough deepens over the East Pacific as the CBAR becomes more defined, as in the upper-right and lower-left panels. However, the 700 mb trough moves east by 0000 UTC 13 February, and a ridge has built over the East Pacific. As with the other cases, the Pacific moisture tap is cut off when a ridge at 700 mb builds over the East Pacific.

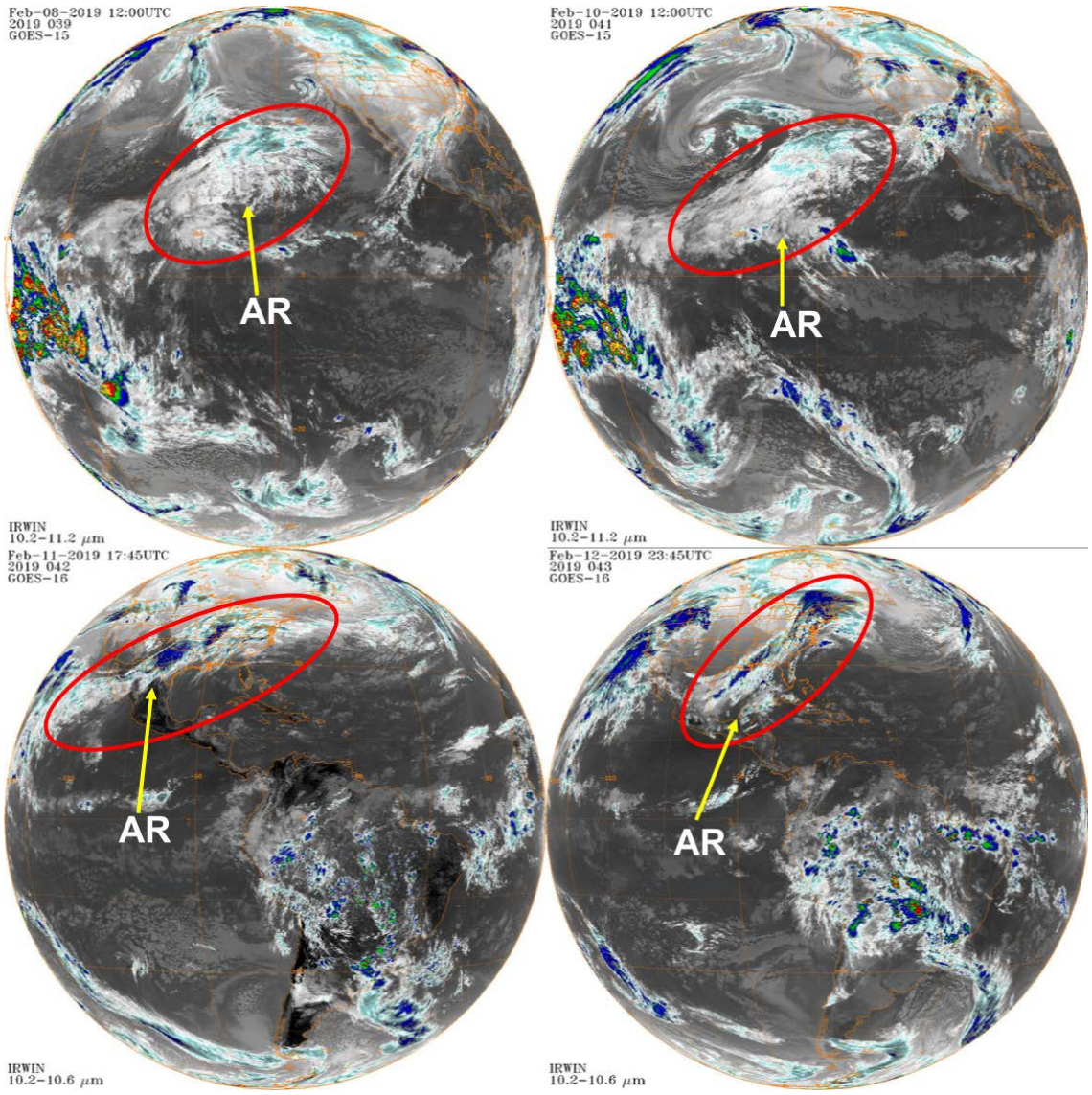

Upper-left: 1200 UTC 08 February 2019; upper-right: 1200 UTC 10 February 2019; lower-left: 1745 UTC 11 February 2019; lower-right: 2345 UTC 12 February 2019.

Figure 52. Case 4 CBAR Satellite Evolution. Source: Knapp (2008).

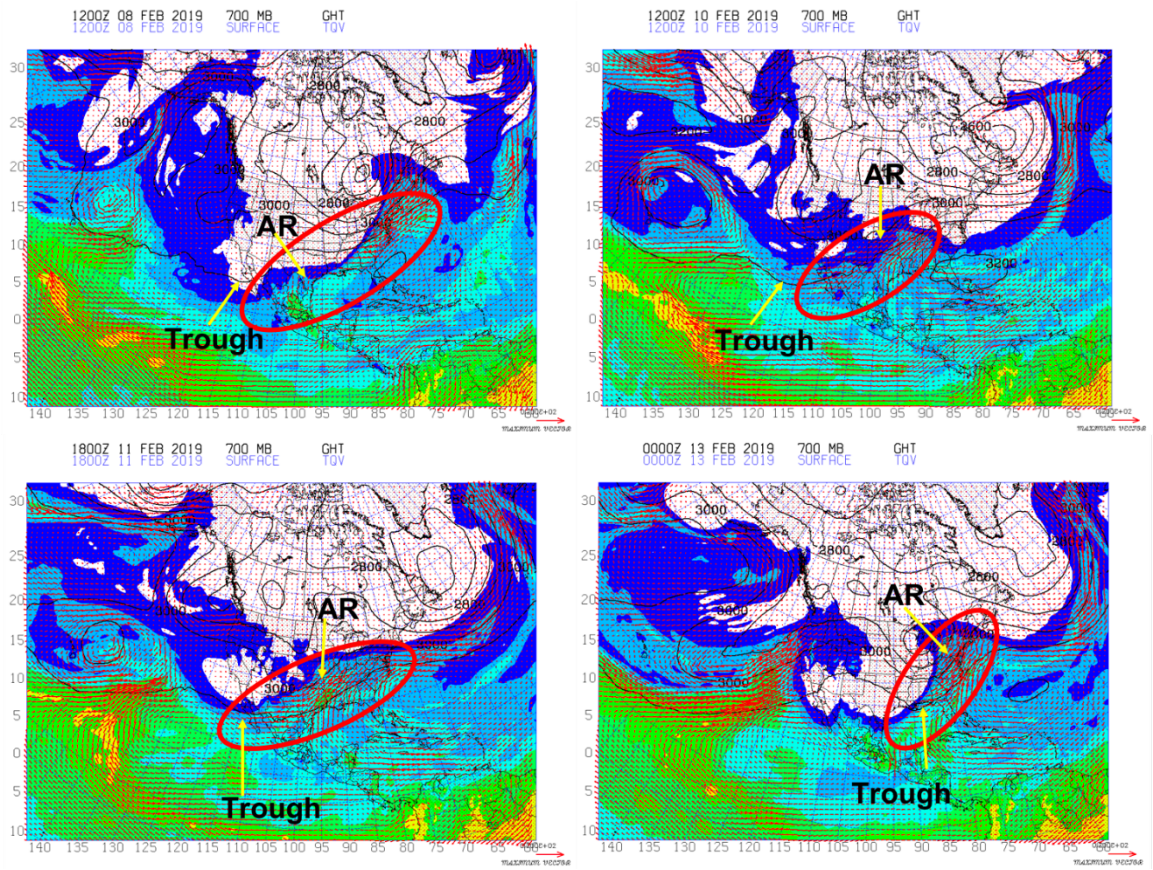

IVT is shown with red barbs, the 700 mb GPT is shown with black contours, and TQV is shown with a color fill. Upper-left: 1200 UTC 08 February 2019; upper-right: 1200 UTC 10 February 2019; lower-left: 1800 UTC 11 February 2019; lower-right: 0000 UTC 13 February 2019.

Figure 53. Case 4 CBAR IVT Evolution.

The jet stream aloft defines this CBAR as in the three previous cases. In Case 4, the jet stream is just above the 5,800 m line, shown in Figure 54. The upper-level pattern mirrors the CBAR path throughout the time period. At 1200 UTC 8 February in the upper-left panel, there is a trough at 500 mb west of Baja near 25°N and 115°W, and the CBAR forms and follows the jet here, apart from a low-pressure system. This position is also consistent with the trough at 700 mb seen in the upper-left panel of Figure 53. By 1200 UTC 10 February in the upper-right panel, an upper-level low has formed over northern California and stays in place through 11 February but is gone at 0000 UTC 13 February. The CBAR is still formed and is evolving with the 500 mb trough east of the Rocky Mountains and not from the trough over northern California, as shown in the lower-left and

right panels. The low-pressure over the Great Lakes is present on 13 February, but the CBAR still follows the jet and 5,800 m line, indicating that this event (and the others) form prior to the low-pressure system and deviated from the WCB, but propagated along the upper-level jet and the 5,800 m line at 500 mb instead.

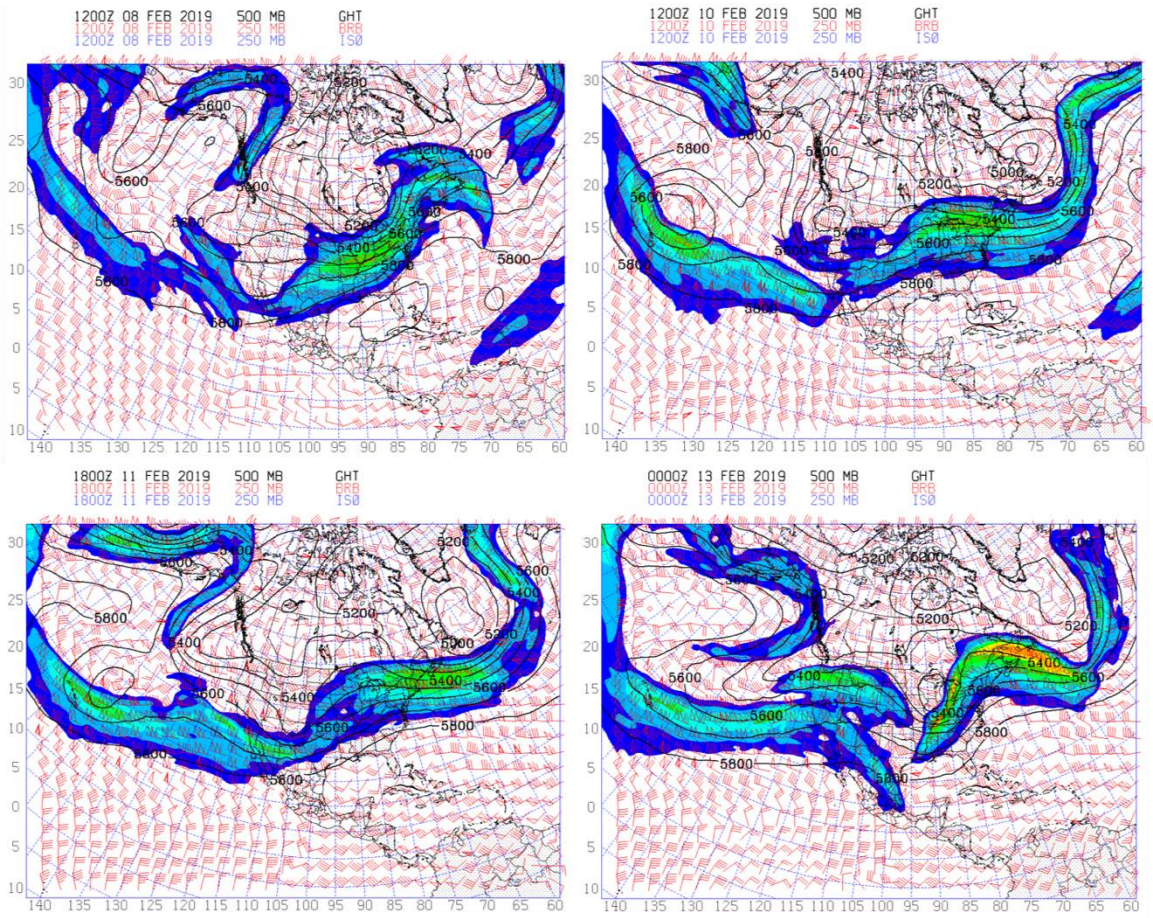

The 500 mb GPT is shown in black contours, the 250 mb wind is shown with red barbs, and the 250 mb jet stream is shown with a color fill. Upper-left: 1200 UTC 08 February 2019; upper-right: 1200 UTC 10 February 2019; lower-left: 1800 UTC 11 February 2019; lower-right: 0000 UTC 13 February 2019.

Figure 54. Case 4 CBAR Upper-Air Evolution.

Figure 55 shows the 850 mb temperature plot, where a fairly weak front exists west of Baja and a stronger front along the East Coast at 1200 UTC 8 February in the upper-left panel. At this point, the CBAR is just forming east of Hawaii. The front on the East Coast

is another system moving through the US, not related to the CBAR in question. By 1200 UTC 10 February in the upper-right panel, the front is stronger and better formed west of Baja into northern Mexico. At 1800 UTC 11 February, when the CBAR is well established, the front is weaker outside of Baja but is stronger in Colorado and Kansas due to the low developing in the Great Lakes region north of the CBAR path, as seen in the lower-left panel. A strong boundary still exists near Ohio where the head of the CBAR is located. Though the head of the CBAR seems to follow the boundary toward the Atlantic, the body and tail of the CBAR are well intact and appear to not be associated with a frontal boundary on the back end. This confirms that at certain points, this event becomes associated with a low-pressure system, but formed independently and follows the upper-level pattern whereas it only follows the lower-level pattern part of the time.

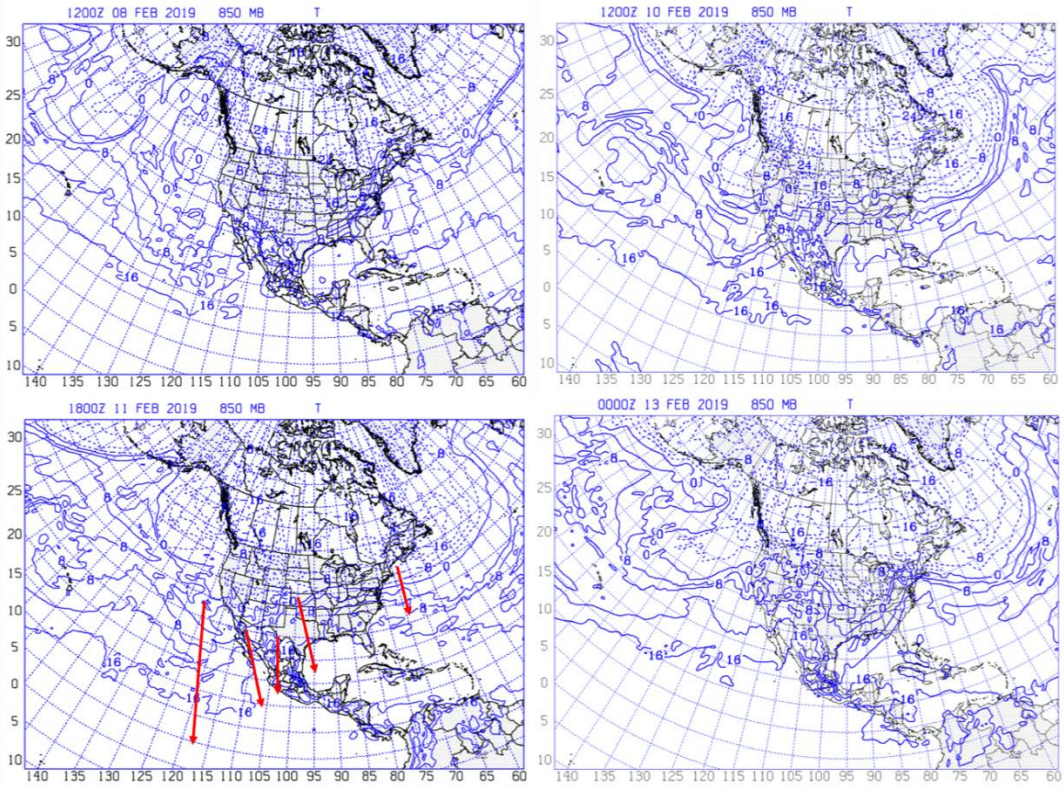

Close contours indicate a front. The red arrows show the positions of the North-to-South cross-sections taken for this case. Upper-left: 1200 UTC 08 February 2019; upper-right: 1200 UTC 10 February 2019; lower-left: 1800 UTC 11 February 2019; lower-right: 0000 UTC 13 February 2019.

Figure 55. Case 4 CBAR 850 mb Temperature Evolution.

Cross-sections were taken along the CBAR path for 1800 UTC 11 February, when the CBAR was well-defined. The cross section near the CBAR origin in the upper-left panel of Figure 56 is taken through the frontal boundary associated with the low near Hawaii. Low-level jets are present in the cross-flow wind field. As with the other cases, the 0.005 kg kg^{-1} IVT contour is around 600 mb. However, there appears to be convergence in this area, indicative of the ITCZ. The IVT plot in the upper-left panel of Figure 53 shows this convergence just southeast of the low. Over the Gulf of California as seen in the upper-center panel of Figure 56, low-level jets and the front are weaker. There does appear to be two AR systems, but the GOES imagery and IVT plots do not reflect this. The 0.005 kg kg^{-1} contour is around 700 mb at this point. As the CBAR extends over the mountains of Mexico shown in the upper-right panel, the low-level jet stream is not visible in the cross-section perpendicular flow plot, and the frontal boundary is more in the upper level, around 500600 mb. The 0.005 kg kg^{-1} contour has dropped to around 700 mb. As is common with all the cases, convergence is seen over the Texas Gulf Coast and is visible in the QV plots in the lower-left panel. Gulf moisture is indicated by the AR marked on the right of the panel where higher QV values are in the lower troposphere around 850 mb, and the Pacific moisture is the AR to the left where higher QV values extend up to 650 mb. This convergence is consistent with the IVT plot. The 0.005 kg kg^{-1} contour is around 600 mb, and the Maya Express event is infringing along the Gulf Coast. This appears to be a typical overrunning event. As the CBAR extends to the East Coast, the high QV values, shown in the lower-center panel, continue to be at 700 mb, and the front along the East Coast is forming, though no low-level jet stream appears at this point.

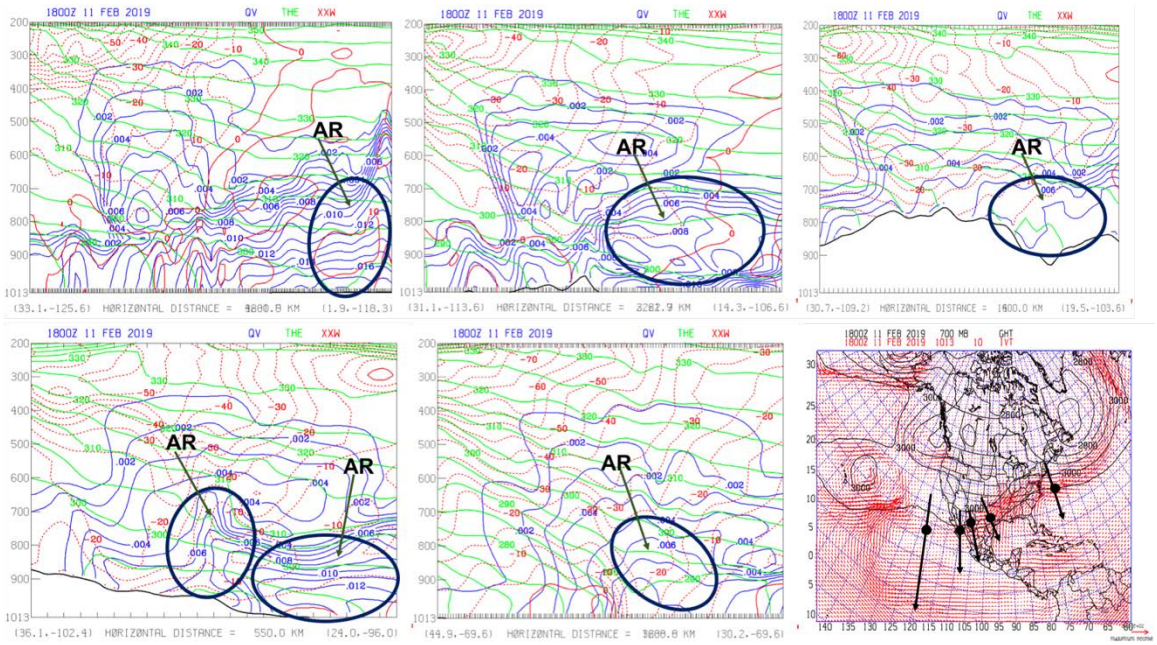

QV is shown with blue contours, THE is shown with green contours, and XXW is shown with red contours for 1800 UTC 11 February 2019. The black arrows show the positions of the North-to-South cross-sections taken for this case. The black dots show the center of where the cross-section was taken. Upper-left: eastern Pacific; upper-center: Gulf of California; upper-right: West Mexico; lower-left: Texas; lower-center: East Coast; lower-right: IVT.

Figure 56. Case 4 CBAR Vertical Cross Section.

Trajectories are taken at 1800 UTC 11 February at six locations along the CBAR path with the endings marked by black dots. Figure 57 shows the general trajectories at 700 mb are clearly from the Pacific, and from near the same source. The first trajectory was taken further east in the Pacific at 20°54'N-130°48'W, tracing back to 27°N-133°W. The second trajectory was taken in Baja at 27°15'N-115°24'W, and it traced back to the eastern Pacific near 24°N-138°W. The third trajectory was taken in Western Mexico at 27°16'N-110°54'W, also tracing back to the eastern Pacific near 20°N-112°W. A fourth trajectory was taken in Texas at 31°23'N-99°00'W, tracing back to the Gulf of California at 25°N-110°W. The fifth trajectory began in western Kentucky at 37°30'N-89°05'W and again traced back to the eastern Pacific near 20°N-120°W. A sixth trajectory was taken in New York at 42°30'N-78°12'W, tracing back to Nevada near 35°N-155°W. All six trajectories at 700 mb traced back to or near the eastern Pacific along the CBAR path. The 850 mb

trajectory shows where parcels going into Texas are from the Pacific near 20°N-155°W, but the converging paths of two different air masses is evident into Texas from the Gulf near 30°N-88°W in Figure 58. This is where the overrunning of the Baja Express CBAR and the Maya Express AR occurs.

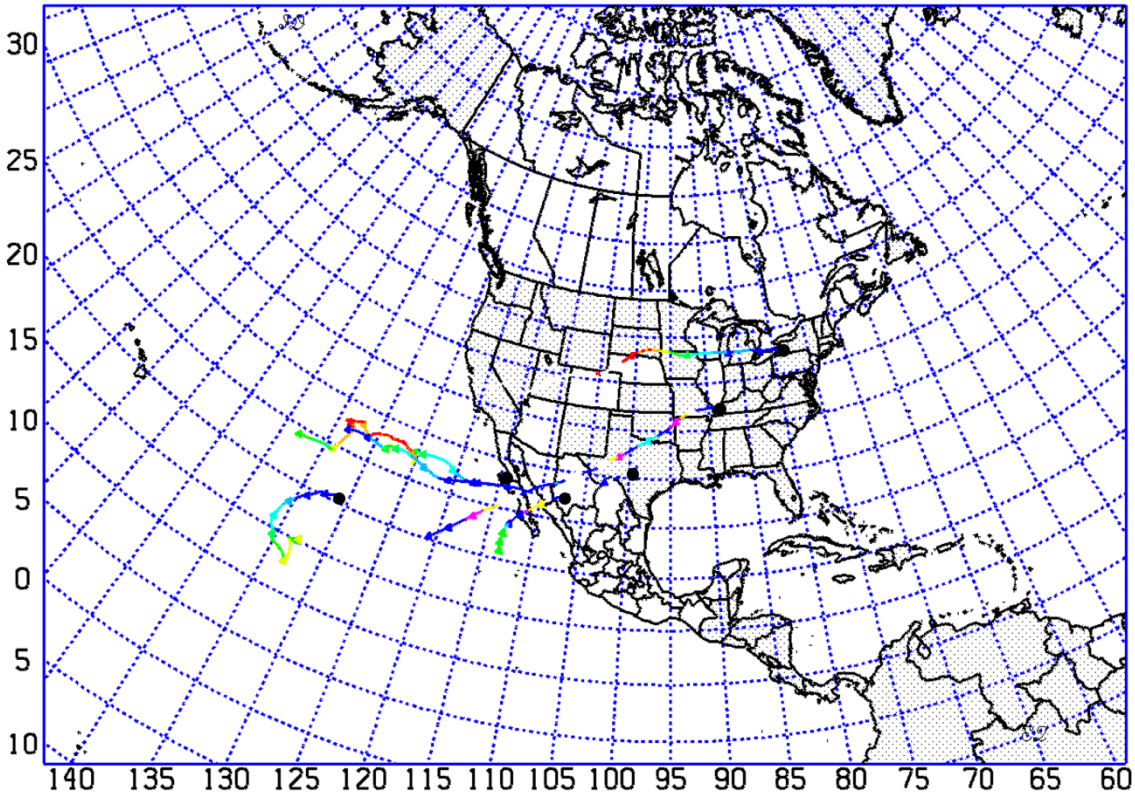

Figure 57. 700 mb Parcel Trajectory.

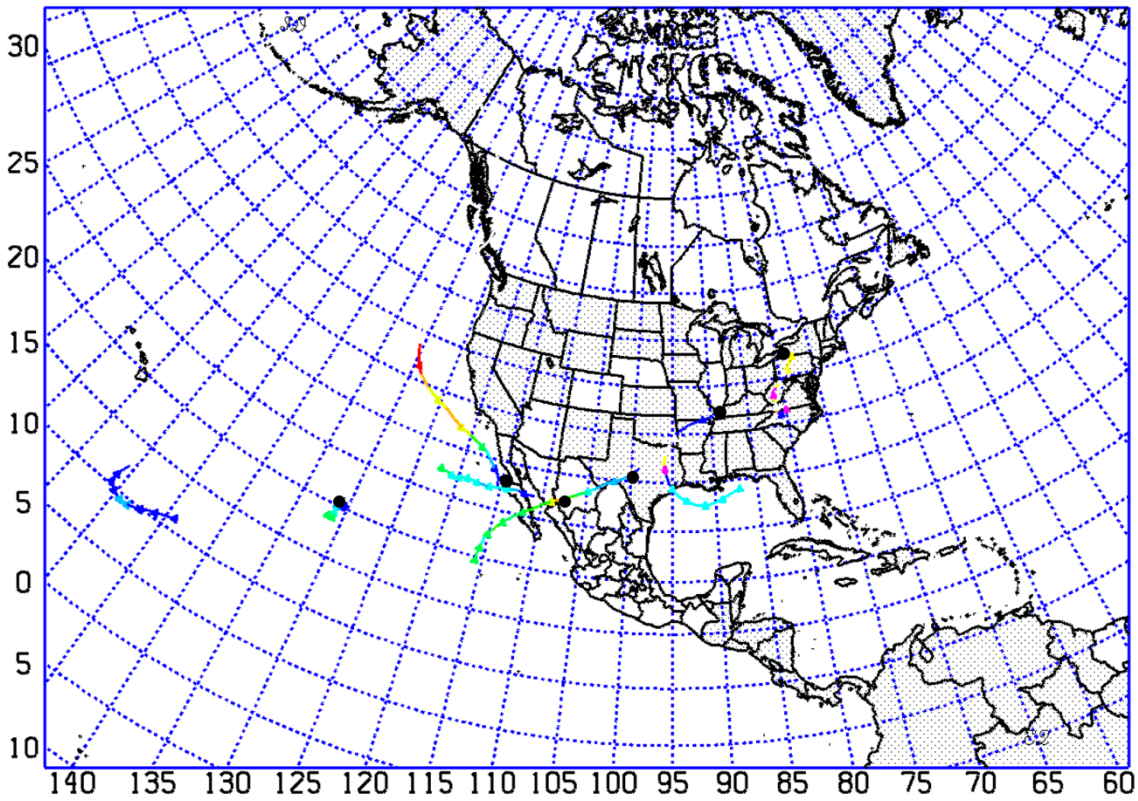

Figure 58. 850 mb Parcel Trajectory.

Case 4 shows a much stronger moisture inflow from the west compared to the other cases, as seen in Figure 59. However, the transport is more equal from the west and the south. The value is still slightly higher from the south, but the strong western inflow proves that there is likely a CBAR coming in from the Pacific into Texas interacting with the AR from the south. As with the other cases, precipitation for Case 4 is fog or mist as reported from both DFW and SAT in Figures 28 and 29, respectively. This is consistent with an overrunning of the Baja Express over the Maya Express as the Pacific moisture at 700 mb along the CBAR path comes from the eastern pacific as seen in Figure 57 whereas the lower level moisture east of Texas comes from the Gulf of Mexico at lower levels seen in Figure 58. The lower-left panel of the cross-section in Figure 56 shows the QV convergence in Texas where higher QV values are in the lower troposphere around 850 mb, and the Pacific moisture is the AR to the left where higher QV values extend up to 650 mb.

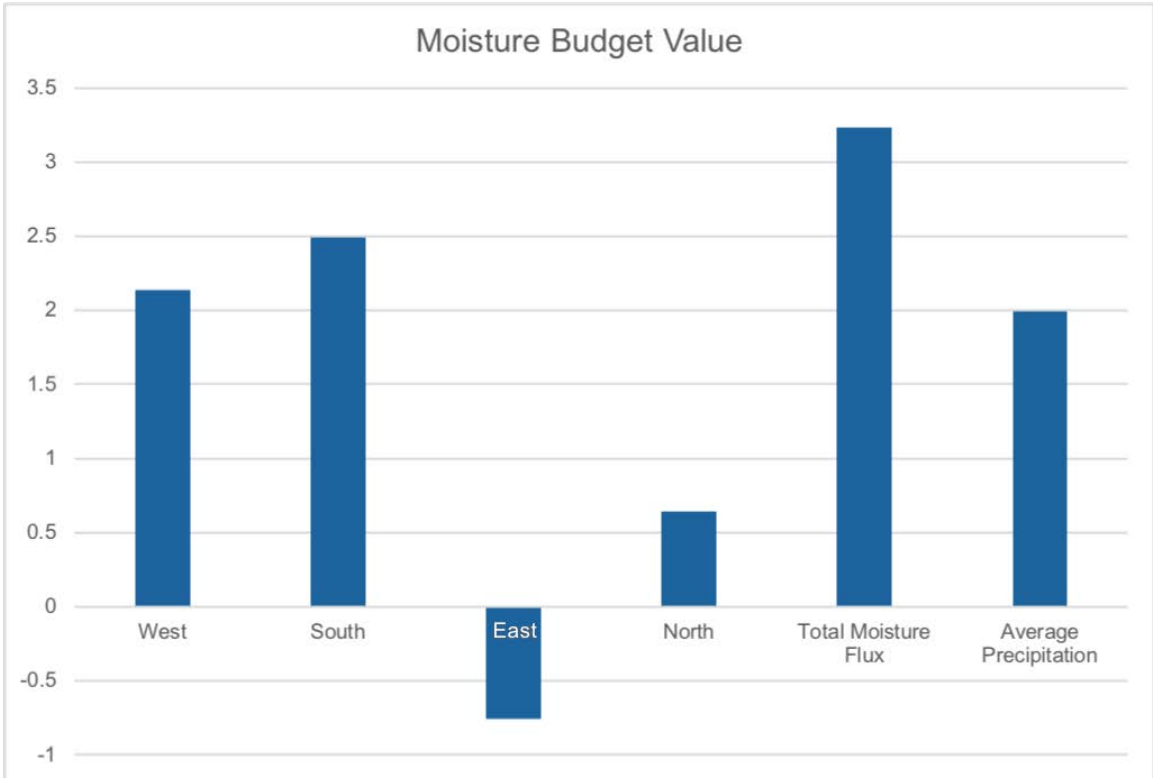

Figure 59. Moisture Budget for Case 4 in Texas.

A result of this overrunning event in Texas was around half an inch of precipitation in northern Texas along with fog and mist. This is typical with all cases, including what was observed prior to the severe weather in Case 3.

In summary, as the CBAR pulls moisture in from the ITCZ, it is transported initially by the low-pressure system near Hawaii and propagates into Baja and through Mexico, reaching into Texas and stretching out to the East Coast. Though several systems appear to be involved, the CBAR continues to propagate possibly by way of these systems but receiving moisture from the ITCZ. In other words, this CBAR event isn't necessarily a part of the extratropical cyclones, but its propagation may be aided by those systems.

E. SUMMARY

Each case used the methods in Chapter II to analyze CBARs and to show that they are different from the typical AR. This research shows that CBARs originate from the ITCZ moisture pool. The CBAR then couples to the upper level jet stream. At that point, they

may evolve independently of other systems, though they may interact with extratropical systems. Table 1 is a summary table of certain key elements for all four cases, including the primary source region of the moisture, the QV height at the point of convergence for the Pacific CBAR and Gulf of Mexico AR, average precipitation, and the adverse weather reported by the NWS offices in DFW and SAT. The final section summarizes the findings of this study and shows how the four cases validate the proposed hypotheses. That section also highlights additional research that may be done to further the scientific study of CBARs.

Table 1. Case Study Summary Table

Case #:	Primary Source Region	QV Height at Point of Convergence	Average Precipitation	Adverse Weather Reported by NWS
1	Nearly equal from Pacific and Gulf of Mexico (Figure 37)	Baja Express (Pacific CBAR): 700 mb Maya Express (Gulf AR): 800 mb (Figure 34, lower left)	1 inch (Figure 37)	DFW: Fog or mist; thunder; ice pellets; freezing rain SAT: Fog or mist; freezing rain or drizzle; smoke or haze (Figures 7 and 8)
2	Gulf of Mexico (Figure 43)	Baja Express: 600 mb Maya Express: 750 mb (Figure 42, lower left)	1.3 inches (Figure 43)	DFW: Fog or mist; fog reducing visibility to 0.25 miles or less SAT: Fog or mist; thunder (Figures 14 and 15)
3	Gulf of Mexico (Figure 51)	Baja Express: 700 mb Maya Express: 775 mb (Figure 48, upper right)	1.75 inches (Figure 51)	DFW: Fog or mist; fog reducing visibility to 0.25 miles or less; thunder; smoke or haze SAT: Fog or mist; thunder (Figures 21 and 22)

Case #:	Primary Source Region	QV Height at Point of Convergence	Average Precipitation	Adverse Weather Reported by NWS
4	Gulf of Mexico (though only slightly higher than Pacific) (Figure 59)	Baja Express: 625 mb Maya Express: 775 (Figure 56, lower left)	2 inches (Figure 59)	DFW: Fog or mist SAT: Fog or mist; ice pellets (Figures 28 and 29)

THIS PAGE INTENTIONALLY LEFT BLANK

V. CONCLUSION

Four cases of similar ARs were analyzed to define a new type of AR labeled in this study as convergent boundary atmospheric river, or CBAR. Three hypotheses were proposed: 1) CBARs form as a result of an associated convergent boundary (in this study, the ITCZ); 2) CBARs form and evolve independent of extratropical cyclones; and 3) CBARs have a significant impact on inland weather.

For each case, GOES IR imagery showed moisture convergence at the ITCZ. This moisture began to take a filamentary form from the ITCZ, propagating northeastward into Baja. Since each case formed as a part of a convergent boundary, they are classified as CBARs. As each case made landfall in Baja, the events are referred to as Baja Express events. Cases 1 and 3 did not have any visible fronts at the CBAR origin, as shown in the 850 mb temperature plots. However, Cases 2 and 4 had a weak front near the origin, and their moisture was being fed by the ITCZ. This indicates that this is a CBAR event that formed as a result of the convergent boundary and not an extratropical cyclone. However, all four case studies revealed a trough at the 700 mb level. The trough was weak at the onset, but likely the reason moisture was pulled up from the ITCZ. The 700 mb trough may be the key initiator for all four CBARs. As the CBARs propagated, the 700 mb trough deepened. One the trough flattened, and a ridge began building over the eastern Pacific, the Pacific moisture tap was cut off. This analysis of these four cases validates that 1) the CBARs form as a result of the associated convergent boundary, and 2) these formations are independent of the nearby extratropical cyclones.

Once formed, the 700 mb trough deepened, and all four cases evolved along the 5,800 m contour on the 500 mb GPT chart. This corresponds to the flow pattern of the 250 mb jet stream. The THE plots in Cases 1 and 2 do not show evidence of a frontal boundary at the origin or during propagation through Texas. A frontal boundary is evident once these CBARs enter Texas. However, the propagation throughout the event remains consistent with the 5,800 m contour and 250 mb jet stream. The THE plots for Cases 3 and 4 show evidence of a frontal boundary near the CBAR origin. Case 4 shows consistent propagation with the upper-level pattern throughout, though its transport may be aided by extratropical

cyclones along its path. This may be due to the deepening of the trough at 700 mb. Though the CBAR in Case 3 originally emerged from the ITCZ, it converged with the AR from the Gulf of Mexico and became a part of that system, following the associated extratropical cyclone. The 700 mb trough moved inland and a ridge built in over the eastern Pacific, cutting off the Pacific moisture tap to the system. The data for cases 1, 2, and 4 validates that 2) CBARs evolve independently of extratropical cyclones, though one may be present along the CBAR path.

Though not initially hypothesized, this research shows that much of the precipitation is likely dynamically forced due to overrunning of one system over another. The Baja Express CBARs propagated inland from the Pacific and converged with the Maya Express ARs from the Gulf of Mexico as shown by the moisture budget inflow, parcel trajectories, and IVT. Cases 1, 2, and 4 exhibited fog or mist with light drizzle, precipitation normally associated with overrunning. This corresponds to the idea that the Baja Express CBAR overruns the Maya Express AR in those cases. In Case 3, the two systems converged at both the 700 mb level and the 850 mb level, indicating a solid convergence, not an overrunning event. As a result, heavy rain and thunderstorms were reported at the convergence point in Texas. All four cases exhibited adverse weather conditions, which validates that 3) CBARs have a significant impact on inland weather.

Deep inland penetration of an AR system is likely the result of a CBAR in the upper troposphere, which has not been deeply studied. The goal of this study was to examine the properties and effects of CBAR events in order to address a gap in the study of ARs and to study the effects of these events in order to improve AR forecasts. Though this research proves the four aforementioned hypotheses, this phenomenon known as CBAR warrants a more in-depth analysis. Future study may examine the effects on inland hydrology, the dynamics and forecasting of dense fog events associated with CBARs, CBAR propagation and why they follow the upper air pattern regardless of nearby extratropical cyclones, the effects of climate and anomalies on CBAR events, and inland drought or flood conditions related to the absence or presence of CBARs.

LIST OF REFERENCES

AMS, cited 2019: Atmospheric River. *Glossary of Meteorology*. [Available online at http://glossary.ametsoc.org/wiki/Atmospheric_river.]

Dacre, H.F., P.A. Clark, O. Martinez-Alvarado, M.A. Stringer, and D.A. Lavers, 2015: How do atmospheric rivers form? *Bull. Amer. Meteor. Soc.*, 1243–1255, doi:10.1175/BAMS-D-14-00031.1.

Guan, B. and D.E. Waliser, 2015: Detection of atmospheric rivers: Evaluation and application of an algorithm for global studies. *J. Geophys. Res. Atmos.*, **120**, 12,514-12,535, doi:10.1002/2015JD024257.

Guan, B. and D.E. Waliser, 2017: Atmospheric rivers in 20-year weather and climate simulations: a multimodel, global evaluation. *J. Geophys Res Atmos.*, **122**, 5556–5581, doi:10.1002/2016JD026174.

Hedstrom, S.L., 2014: Atmospheric rivers and the forcing of extreme precipitation in the Midwest U.S. M.S. thesis, Department of Meteorology, Naval Postgraduate School, 46 pp.

Knapp, K. R., 2008: Scientific data stewardship of international satellite cloud climatology Project B1 global geostationary observations. *Journal of Applied Remote Sensing*, **2**, 023548, doi:10.1117/1.3043461.

NCEI (2019). Climate Forecast System. Accessed 06 September 2019, https://www.ncdc.noaa.gov/data-access/model-data/model-datasets/climate-forecast-system-version2-cfsv2.

Newell, R.E., N.E. Newell, Y. Zhu, and C. Scott, 1992: Tropospheric rivers? – A pilot study. *Geophysical Research Letters*, **12**, 2401–2404.

Nuss, W. and S. Drake, 1990: *VISUAL Meteorological Diagnostic and Display Program*, Naval Postgraduate School Department of Meteorology, 51 pp.

NWS Austin/San Antonio, 2014: San Antonio International Airport preliminary monthly climate data (updated frequently). National Weather Service Austin/San Antonio Forecast Office, accessed 18 October 2019, https://w2.weather.gov/climate/index.php?wfo=ewx.

NWS Dallas/Fort Worth, 2014: Dallas/Fort Worth International Airport preliminary monthly climate data (updated frequently). National Weather Service Fort Worth Forecast Office accessed 18 October 2019, https://w2.weather.gov/climate/index.php?wfo=fwd.

Paltan, H., D. Waliser, W.H. Lim, B. Guan, D. Yamazaki, R. Pant, and S. Dadson, 2017: Global floods and water availability driven by atmospheric rivers. *Geophysical Research Letters*, **44**, 10,387-10,395, doi:10.1002/2017GL074882.

Payne, A.E., and G. Magnusdottir, 2016: Persistent landfalling atmospheric rivers over the West Coast of North America. *J. Geophys Res. Atmos.*, **121**, 13,287-13,300, doi:10.1002/2016JD025549.

Ralph, F.M., M. Dettinger, D. Lavers, I.V. Gorodetskaya, A. Martin, M. Viale, A.B. White, N. Oakley, J. Rutz, J.R. Spackman, H. Wernli, and J. Cordeira, 2017: Atmospheric rivers emerge as a global science and applications focus. *Bull. Amer. Meteor. Soc.*, 1969–1973, doi:10.1175/BAMS-D-16-0262.1.

Rutz, J.J., W.J. Steenburgh, and F.M. Ralph, 2015: The inland penetration of atmospheric rivers over western North America: A Lagrangian analysis. *Mon. Wea. Rev.*, **143**, 1924–1944, doi:10.1175/MWR-D-14-00288.1.

Zhou, Y., H. Kim, and B. Guan, 2018: Life cycle of atmospheric rivers: Identification and climatological characteristics. *J. Geophys. Res. Atmos.*, **123**, 1–11, doi:10.1029/2018JD029180.

Zhu, Y. and R.E. Newell, 1994: Atmospheric rivers and bombs. *Geophysical Research Letters*, **21**, 1999–2002.

Zhu, Y. and R.E. Newell, 1998: A proposed algorithm for moisture fluxes from atmospheric rivers. *Mon. Wea. Rev.*, **126**, 725–735.

INITIAL DISTRIBUTION LIST

1. Defense Technical Information Center
   Ft. Belvoir, Virginia

2. Dudley Knox Library
   Naval Postgraduate School
   Monterey, California